Master Thesis

Submitted within the UNIGIS MSc. programme
at the Department of Geoinformatics - Z_GIS
University of Salzburg, Austria
Under the provisions of UNIGIS India framework

Analysis of Land Use Land Cover Change in Greater Cairo Region: 1984-2016

by

Ahmed Omar Shehata Omar

GIS_104409

A thesis submitted in partial fulfillment of the requirements of
the degree of
Master of Science (Geographical Information Science & Systems) – MSc (GISc)

Advisor (s):

Dr. Shahnawaz

Cairo-Egypt, 18-11-2017

Science Pledge

By my signature below, I certify that my thesis is entirely the result of my own work. I have cited all sources I have used in my thesis and I have always indicated their origin.

Cairo-Egypt, 18-11-2017 Ahmed Omar

Acknowledgements

I would like to thank my thesis advisor **Dr. Shahnawaz** for his great academic and moral support especially in the most difficult times. As I cannot but appreciate the constructive suggestions, criticisms and encouragement. He consistently allowed this thesis to be my own work, also steered me in the right the direction whenever he thought I needed it.

Abstract

The Greater Cairo Region (GCR) is one of the most intensively populated areas in the world, one of the fastest growing mega cities in the world. This place an ever increasing need for urban development to accommodate such population growth in both residential complexes and work facilities. Since 1980th, rapid population growth and urbanization have become issues in big cities in developing countries like Greater Cairo. As a consequence of explosive growth, the living conditions of Greater Cairo deteriorate (Cairo, Giza, and Qalyubia). Development trends of the last twenty years have increased general wealth and modernization, at a time of a high rate of population growth, thus creating an increased demand for land combined with environmental degradation. This informal increase had a lot of bad effects. Egypt had been tried to solve all population problems and infrastructure through planning schemes for Greater Cairo region. Relatively it is essential to discuss these problems in order to manage and control the urban growth of Greater Cairo region.

The main objective of the present study to highlight and analyze the exchange between the land cover components at Greater Cairo with focusing on urban area and agricultural land between 1984, 1992, 2000, 2008 and 2016 using Landsat satellite data. And detected land cover changes by using remote sensing and GIS. Results showed that urban area of Greater Cairo was 244.6 km^2 in 1984 and increased to 921.2 km^2 in 2016. The cut-off from agricultural lands was 20.3 km^2 between 2000 and 2016**,** whereas urbanization into the neighboring desert was estimated at 674.6 km^2 for the same period. The direction of urban sprawl was mainly controlled by regional topography. Urban sprawl was attributed mainly to accelerated population growth.

Table of Contents

Science Pledge 1

Acknowledgments ……..……... 2

Abstract ……..…… 3

Table of Contents ……..……. 4

List of Tables ……..……... 6

List of Figures ……..……..... 7

List of Maps ……..……..……. 8

Chapter1 Introduction ……..……. 10

1.1 Background ……..……. 10

1.2 Urban growth definition ……..…… 10

1.4 Causes of Urban Growth ……..…… 11

1.4 Population Growth in Greater Cairo ……..…….. 14

1.5 Literature Review ……..……..… 15

1.6 Statement of the problem ……..……..… 17

1.7 Research Aims ……..……..…… 17

1.8 Research Objectives ……..……..…….. 18

1.9 Study Area ……..……..……. 18

Chapter2 Methodology ……..……..…….. 20

2.1 Introduction ……..……..……. 20

2.2 Software used ……..……. 20

2.3 Data Collection ……..…….. 22

2.4 Landsat Satellite Images ……..…….. 22

2.4.1 Characteristics of Landsat 5 TM ……..…….. 23

2.4.2 Characteristics of Landsat 7 ETM+ ……..……. 27

2.4.3 Characteristics of Landsat 8 (OLI) …… 29

2.5 Image Pre-processing …… 31

2.5.1 Geometric Correction …… 31

2.5.2 Radiometric Correction …… 38

2.5.3 Image Enhancement …… 46

2.5.4 Image masking …… 46

2.6 Image Processing …… 48

2.6.1 Image Classification …… 49

2.6.2 Supervised Classification …… 49

2.6.3 Accuracy Assessment …… 56

2.7 Change Detection …… 61

2.7.1 Introduction …… 61

2.7.2 Change Detection Method Selection …… 62

2.7.2.1 Change detection using write function memory insertion …… 62

2.7.2.2 Image Algebra change detection (Band differencing or band ratioing) …… 62

2.7.2.3 Multi-date change detection using a binary mask applied to date 2 …… 63

2.7.2.4 Multi-date change detection using ancillary data source as date 1 …… 63

2.7.2.5 Image regression …… 64

2.7.2.6 Manual, on screen digitising of change …… 64

2.7.2.7 Post-classification comparison change detection …… 64

2.7.3 Change detection using Post-classification Comparison …… 65

Chapter3 Data Analysis and Results …… 66

3.1 Detecting urban growth in Greater Cairo Region …… 66

3.2 Land Use/Cover Classification Maps …… 72

3.3 Land Use/Cover Change Detection …… 83

3.3.1 Transition Matrix …….……..…….. 89

Chapter4 Conclusions ……..…..…..……..……..…….…. 91

4. Conclusions ……..……...……..…..…… 91

References ……..……..……...……...…….. 93

List of Tables

Table1: Details of the Images Used in the Study ……..... 23

Table2: Landsat (5 TM, 7 ETM+, 8 OLI) sensors and their characteristics …..…….……..... 29

Table3: Image to image registration information of Landsat TM 84 to Landsat 8 OLI …..... 32

Table4: Image to image registration information of Landsat TM 92 to Landsat 8 OLI …..... 34

Table5: Image to image registration information of Landsat TM 2000 to Landsat 8 OLI 35

Table6: Image to image registration information of Landsat ETM 2008 to Landsat 8 OLI… 36

Table7: Image Classification Schema and training samples…….……..... 51

Table8: Band combination to identify land cover type …….……..... 51

Table9: Error Matrix for the classified satellite image 1984. ……...…..... 58

Table10: Accuracy Totals for the classified satellite image 1984. ……..…..... 59

Table11: Error Matrix for the classified satellite image 1992. ……..……...…..... 59

Table12: Accuracy Totals for the classified satellite image 1992. ……..…..... 59

Table13: Error Matrix for the classified satellite image 2000. ……..……..... 59

Table14: Accuracy Totals for the classified satellite image 2000. ……..…..... 60

Table15: Error Matrix for the classified satellite image 2008. ……....…..... 60

Table16: Accuracy Totals for the classified satellite image 2008. ……..…..... 60

Table17: Error Matrix for the classified satellite image 2016. ……..……..... 60

Table18: Accuracy Totals for the classified satellite image 2016. ……..……..... 61

Table19: Land Use/Cover Categories in Greater Cairo (1984) ……..……..... 72

Table20: Land Use/Cover Categories in Greater Cairo (1992) ……..……..... 74

Table21: Land Use/Cover Categories in Greater Cairo (2000) ……..……..... 76

Table22: Land Use/Cover Categories in Greater Cairo (2008) ……..……..... 78

Table23: Land Use/Cover Categories in Greater Cairo (2016) ……..…….…. 80

Table24: Characteristics of Land Use/Cover change in Greater Cairo (1984-1992) …..…. 82

Table25: Characteristics of Land Use/Cover change in Greater Cairo (1992-2000) …..... 84

Table26: Characteristics of Land Use/Cover change in Greater Cairo (2000-2008) …..... 84

Table27: Characteristics of Land Use/Cover change in Greater Cairo (2008-2016) ……... 86

Table28: Land Cover Changes: Transition Matrix of year 1984 to 1992 …..…..……..... 89

Table29: Land Cover Changes: Transition Matrix of year 1992 to 2000 …..…..……..... 89

Table30: Land Cover Changes: Transition Matrix of year 2000 to 2008 …..…..……..... 90

Table31: Land Cover Changes: Transition Matrix of year 2008 to 2016 …..…..……..... 90

List of Figures

Figure1: Flow Chart Depicting the Change Detection Methodology …..……..… 21

Figure2: Showing two Landsat 7 ETM+ 2008 images taken in the same month.....… 27

Figure2-1: Showing Landsat 7 ETM+ 2008 image before and after apply filling gaps .....… 28

Figure3: Image to image registration (Landsat 1984 – Landsat 2016) in Envi ……..…..… 33

Figure4: Comparison between the registered image LS 1984 and the base image LS 2016 33

Figure5: Image to image registration (Landsat 1992 – Landsat 2016) in Envi ……....…. 34

Figure6: Comparison between the registered image LS 1992 and the base image LS 2016 35

Figure7: Image to image registration (Landsat 2000 – Landsat 2016) in Envi ……..…. 35

Figure8: Comparison between the registered image LS 2000 and the base image LS 2016 36

Figure9: Image to image registration (Landsat 2008 – Landsat 2016) in Envi ……..…. 37

Figure10: Comparison between the registered image LS 2008 and the base image LS 2016 ……. 37

Figure11: Landsat TM 1984 before and after execution Post FLAASH Band Math Equation 41

Figure12: Landsat TM 1984 image before and after radiometric and atmospheric correction…..... 41

Figure13: Landsat TM 1992 before and after execution Post FLAASH Band Math Equation ……. 42

Figure14: Landsat TM 1992 image before and after radiometric and atmospheric correction……. 42

Figure15: Landsat TM 2000 before and after execution Post FLAASH Band Math Equation 43

Figure16: Landsat TM 2000 image before and after radiometric and atmospheric correction…..... 43

Figure17: Landsat ETM 2008 before and after execution Post FLAASH Band Math Equation ……. 44

Figure18: Landsat ETM 2008 image before and after radiometric and atmospheric correction….. 44

Figure19: Landsat 8 2016 before and after execution Post FLAASH Band Math Equation 45

Figure20: Landsat 8 2016 image before and after radiometric and atmospheric correction …..... 45

Figure21: Landsat 5 TM and Landsat 7 ETM+ for Greater Cairo Region after masking ….. 47

Figure22: Landsat 8 (OLI) 2016 for Greater Cairo Region after masking …….. 48

Figure23: Showing the location of the training areas on Landsat TM 1984...…...……. 52

Figure24: Showing the location of the training areas on Landsat TM 1992...…...……. 52

Figure25: Showing the location of the training areas on Landsat TM 2000...…...……. 53

Figure26: Showing the location of the training areas on Landsat ETM 2008...…...……. 53

Figure27: Showing the location of the training areas on Landsat OLI 2016 …...……. 54

Figure28: Showing Urban Growth in 1984, 1992, 2000, 2008 and 2016 ……..……. 67

Figure29: Distribution of Built-up areas Growth from 1984 to 2016 ……..…….. 72

Figure30: Chart of Land Use/Cover change in Greater Cairo (1984-1992) ……..…….. 74

Figure31: Chart of Land Use/Cover change in Greater Cairo (1992-2000) ……..…. 76

Figure32: Chart of Land Use/Cover change in Greater Cairo (2000-2008) ……..…….. 78

Figure33: Chart of Land Use/Cover change in Greater Cairo (2008-2016) ……..…. 80

List of Maps

Map1: Egypt Map Showing the Location of study area ……..... 18

Map2: Map Showing the Cities and urban Communities in Greater Cairo Region …..... 19

Map3: Landsat Thematic Mapper (TM) 1984 for Greater Cairo Region ……..……..… 24

Map4: Landsat Thematic Mapper (TM) 1992 for Greater Cairo Region ……..……..… 25

Map5: Landsat Thematic Mapper (TM) 2000 for Greater Cairo Region ……..……..... 26

Map6: Landsat 7 ETM+ 2008 for Greater Cairo Region ……..... 28

Map7: Landsat 8 OLI 2016 for Greater Cairo Region ……..... 30

Map8: Landsat TM and ETM+ Classification ……..……..……..... 55

Map9: Landsat 8 OLI 2016 Classification ……..……..……..... 56

Map10: Showing Urban Growth of Greater Cairo Region 1984 - 1992 ….……..…… 68

Map11: Showing Urban Growth of Greater Cairo Region 1992 - 2000 ….……..…… 69

Map12: Showing Urban Growth of Greater Cairo Region 2000 - 2008 ….……..…… 70

Map13: Showing Urban Growth of Greater Cairo Region 2008 - 2016 ….……..…… 71

Map14: Greater Cairo Region Land Use Land Cover 1984 …… 73

Map15: Greater Cairo Region Land Use Land Cover 1992 …… 75

Map16: Greater Cairo Region Land Use Land Cover 2000 …… 77

Map17: Greater Cairo Region Land Use Land Cover 2008 …… 79

Map18: Greater Cairo Region Land Use Land Cover 2016 …… 81

Map19: Change Detection Map showing Changes between 1984 and 1992 ……..…… 83

Map20: Change Detection Map showing Changes between 1992 and 2000 ……..…… 85

Map21: Change Detection Map showing Changes between 2000 and 2008 ……..…… 87

Map22: Change Detection Map showing Changes between 2008 and 2016 ……..…… 88

Chapter-1

1. Introduction

1.1 Background

Recent studies indicate that our world is undergoing the largest wave of urban growth in history (United Nations Fund for Population Activities). One hundred years ago, two out of every ten people lived in an urban area, this number is expected to grow to reach six out of ten in 2030, and seven out of ten in 2050 (World Health Organization). The world's urban residents began to increase significantly since the 1950s and it is expected to almost double, increasing from approximately 3.4 thousands of million in 2009 to 6.4 thousands of million in 2050 (World Health Organization). Consequently, this massive increase in urban population makes governments, policy makers, and civil society organizations face challenges in resources reallocation to overcome the problems that will arise in the future, to achieve a sustainable development of urban areas and to preserve cultural heritage from urban settlements being formed around areas of high legacy.

1.2 Urban growth definition

There are many tangled terms used in the context of urban studies such as urban development, urban growth, and urbanization. It is instructive in this introduction to draw a clear and firm distinction among these terms. Clark (1982) defined urban development as the process of emergence of a world dominated by cities and urban values and the main processes of urban development are urban growth and urbanization. Urban growth is a spatial and demographic process and refers to the increased importance of towns and cities as concentrations of population within a particular economy or society, while Urbanization is a spatial and social process which refers to the change of behavior and social relationships which occur in society as a result of people living in towns and cities (Clark 1982). Urban growth is defined as the rate at which the population of an urban area increases. This result

from urbanization which is the movement of people from rural areas to urban areas. Urban growth may lead to an increase in economic development of a country. Urban growth is also referred as the expansion of a metropolitan or suburban area into the surrounding environment. It can be considered as an indicator of the state of a country's economic condition as the effect of urban growth directly impacts the country's economic development. The more the urban area grows the more employment it generates and in this way economic growth also takes place. With the rise in urbanization, a number of events like rapid population growth because of natural increase, migration from rural areas to urban areas, classification of rural areas as towns because of the changing demographic character of rural areas have also resulted in increased pressure on all existing utilities.

1.3 Causes of Urban Growth

The first and foremost reason of urban growth is increase in urban population. Rapid growth of urban areas is the result of two population growth factors: (1) natural increase in population, and (2) migration to urban areas. Natural population growth results from excess of births over deaths. Migration is defined as the long-term relocation of an individual, household or group to a new location outside the community of origin. In the recent time, the movement of people from rural to urban areas within the country (internal migration) is most significant. Although very insignificant comparing the movement of people within the country; international migration is also increasing. International migration includes labor migration, refugees and undocumented migrants. Both internal and international migrations contribute to urban growth.

Internal migration is often explained in terms of either push factors conditions in the place of origin which is perceived by migrants as detrimental to their wellbeing or economic security, and pull factors the circumstances in new places that attract individuals to move there.

Examples of push factors include high unemployment and political persecution; examples of pull factors include job opportunities or better living facilities. Typically, a pull factor initiates migration that can be sustained by push and other factors that facilitate or make possible the change. For example, a farmer in rural area whose land has become unproductive because of drought (push factor) may decide to move to a nearby city where he perceives more job opportunities and possibilities for a better lifestyle (pull factor).

In general, cities are perceived as places where one could have a better life; because of better opportunities, higher salaries, better services, and better lifestyles. The perceived better conditions attract poor people from rural areas. People move into urban areas mainly to seek economic opportunities. In rural areas, often on small family farms, it is difficult to improve one's standard of living beyond basic sustenance. Farm living is dependent on unpredictable environmental conditions, and during of drought, flood or pestilence, survival becomes extremely problematic. Cities, in contrast, are known to be places where money, services and wealth are centralized. Cities are places where fortunes are made and where social mobility is possible. Businesses that generate jobs and capitals are usually located in urban areas. Whether the source is trade or tourism, it is also through the cities that foreign money flows into a country. People living on a farm may wish to move to the city and try to make enough money to send back home to their struggling family.

In the cities, there are better basic services as well as other specialist services that are not found in rural areas. There are more job opportunities and a greater variety of jobs in the cities. Health is another major factor. People, especially the elderly are often forced to move to cities where there are doctors and hospitals that can cater for their health needs. Other factors include a greater variety of entertainment (restaurants, movie theatres, theme parks, etc.) and a better quality of education. Due to high populations, urban areas can also have much more diverse social communities allowing others to find people like them.

These conditions are heightened during times of change from a pre-industrial society to an industrial one. At this transition time many new commercial enterprises are made possible, thus creating new jobs in cities. It is also a result of industrialization that farms become more mechanized, putting many farm laborers out of work. Developing nations are currently passing through the process of industrialization. As a result, growth rate of urban population is very high in these countries comparing industrialized countries. In industrialized countries the future growth of urban populations will be comparatively modest since their population growth rates are low and over 80% of their population already live in urban areas. In contrast, developing countries are in the middle of the transition process, when urban population growth rates are very high.

According to the United Nations report (UNFPA 2007), the number and proportion of urban dwellers will continue to rise quickly. Urban global population will grow to 4.9 billion by 2030. In comparison, the world's rural population is expected to decrease by some 28 million between 2005 and 2030. At the global level, all future population growth will thus be in towns and cities; most of which will be in developing countries. The urban population of Africa and Asia is expected to be doubled between 2000 and 2030. This huge growth in urban population may force to cause uncontrolled urban growth resulting in sprawl. The rapid growth of cities strains their capacity to provide services such as energy, education, health care, transportation, sanitation, and physical security. Since governments have less revenue to spend on the basic upkeep of cities and the provision of services, cities become areas of massive sprawl and serious environmental problems.

1.4 Population Growth in Greater Cairo

Egypt's rapid population growth is placing severe pressures on the country's resources. According to the population censuses, Egypt's population has doubled from 9.7 million to more than 18 million in fifty years since 1897 to 1947. The second doubling took almost thirty years from 1947 to 1976 reaching around 36 million according to 1976 census. In 1986, population reached 48.3 million, and by 1996 it was 59.3 million. During the twentieth century the population of Egypt has increased by more than 5 times. Population is projected to reach 94 million by 2020.

The Greater Cairo Region now represents about 22 per cent of the total population of Egypt, and 43 per cent of the urban population, totaling approximately 22.8 million inhabitants (2017). The Greater Cairo agglomeration, a continuous urbanized area, which can be roughly identified as the cities of Cairo, Giza, and Shubra al-Khima, with a population of about 8 6 million (1982) of which 62 per cent are in the Cairo Governorate 25 per cent in the Giza Governorate and 13 per cent in the Qalyubia Governorate). If the present trend of growth continues, a large encroachment on agricultural land can be expected in Giza and Qalyubia. Migration was the main reason for the population growth in the Greater Cairo Region between 1935 and 1965, accounting for 35 per cent of it. According to the 1976 census, migration into the Cairo and Giza governorates were 1 236 million and 0.234 million inhabitants respectively, whereas emigration was only about 20 per cent of these totals. Migration into Qalyubia was 71,000 inhabitants and emigration about 60 per cent of the total, oriented chiefly toward the industrial areas on the Ismailia road. Migration within the governorates of the Greater Cairo Region has always been an important factor and has been increasing. In 1980 the net migration into the Cairo Governorate represented 23 per cent of the population, 33 per cent into the Giza Governorate and 16 per cent into the Qalyubia Governorate.

1.5 Literature Review

(Pham and Yamaguchi, 2011) Urban growth and change analysis using remote sensing and spatial metrics from 1975 to 2003 for Hanoi, Vietnam. The objective of this study was to combine remotely sensed data and spatial metrics to characterize the urbanization of Hanoi for the period from 1975 to 2003. Firstly, surface land cover maps of Hanoi were generated from satellite images using a mixel filtering method. This enhances the accuracy of image classification by removing the effect of mix pixels (mixel). Secondly, the 'percentage like of adjacency', was used to quantify urban fragmentation and to produce urban change-pattern maps of Hanoi. The maps provide information on urban structure and help to visualize the nature, timing and location of urbanization. Three urban growth patterns were identified: infill growth, expansion growth and outlying growth.

To detect urban change in Hanoi, mid-resolution ASTER and Landsat satellite images, which had a spatial resolution of 15 and 30 m, respectively, were used in this study. All of the images were geo-rectified to the resolution of ASTER images (15 m) before a supervised maximum likelihood classification was applied to generate surface cover maps of the urban areas, which could then be extracted from satellite data. The results of the classification made it possible to visualize the expansion of Hanoi City for the period from 1975 to 2003.

This study demonstrated that a combination of both remote sensing and spatial metrics is both useful and effective for analyzing urbanization. Spatial metrics provide quantitative thematic information which complements the visual information provided by a remotely sensed classification.

(Ayad et al., 2013) Investigating urban growth scenarios in Wadi El Natrun area, Egypt, using the UPlan land use allocation model. This study aims at establishing an approach for the analysis of urban growth dynamics to support urban planning decisions in Egypt. And in order to understand the current growth trends in Wadi El Natrun, existing urban features are

digitized from topographic maps produced by the Egyptian Surveying Agency (years 1954 and 1990) and satellite imageries acquired from the Landsat Thematic Mapper (TM) (year 1984) and Enhanced Thematic Mapper Plus (ETM+) sensors (years 1999 and 2005).

(Maktav and Erbek, 2005) Analysis of urban growth using multi-temporal satellite data in Istanbul, Turkey. The objective of this study to investigate the impact of urban growth on land-use changes, especially the agricultural land in the district of Buyukcekmece in suburban Istanbul. In this study, multi-temporal satellite data of Landsat Thematic Mapper (TM) (12 June, 1984 and 16 April, 1998), and IKONOS XS+Pan (13 February, 2002) data were utilized. In addition, SPOT P (11 July, 1998) data were used for visual analysis and interpretation of the classification results.

In this study, land-use changes in the Buyukcekmece district of Istanbul were analysed, benefiting mainly from the spectral properties of multi-temporal satellite data.

Urban growth was mainly driven by population migration into this area. This intensive migration and natural population growth in Istanbul has caused continuous urban growth to be detected. In this study, parallel to the continuous population growth (.40% in some regions), rapid urbanization has been detected. Also, a decrease or total loss of agricultural fields in various sections of the area due to the rapid increase of settlement areas has been determined.

(YAGOUB, M. M. 2004) Monitoring of urban growth of a desert city through remote sensing: Al-Ain, UAE, between 1976 and 2000. The objective of this study is to investigate the development of Al Ain city, in the United Arab Emirates (UAE), between 1976 and 2000, with particular reference to the space–time relationship. Al Ain is the fastest changing city in the Arabian Peninsula. It has gone from a desert oasis to a thriving modern city in just over 30 years. Maps, color aerial photographs, satellite imagery, Global Positioning System (GPS), and Geographical Information System (GIS) were used as an aid for understanding the

development of the city. Change and development in the city is evident from comparison of old maps, aerial photographs, and satellite imagery taken during 1976, 1978, 1984, 1994, 1998 and 2000. The city was found to have a tendency for major expansion in the direction of the west and south-west. Expansion in any direction was found to be governed by the availability of utilities (water, electricity), economic activities along roads (agriculture, industry), geographical constraints (valleys, sand dunes, mountains), and legal factors (boundary with Sultanate of Oman, planning and institutional rules).

1.6 Statement of the problem

In terms of Greater Cairo history, a lot of problems were appeared. They are mainly related to the random extensions and informal housing. High population density, over crowded streets, high rise buildings and informal areas are other problems. All these reasons are sufficient to encourage environmental damage and failure of Cairo infrastructure The absence of good following for urban laws (which guide urban growth) represent major factor of Cairo problems. Therefore researchers direct their studies to solve all interacting problems of Cairo urban region. In this framework the idea of this study was done. It was aim of this study is analyze the urban land cover and existing land use changes, and produce land use and cover map for the Greater Cairo area at varied periods to monitor possible changes that may occurred, particularly in the urban areas and agriculture and subsequently predict likely changes in Greater Cairo Region.

1.7 Research Aims

The aim of this study is analyze the urban land cover and existing land use changes, and produce land use and cover map for the Greater Cairo area at varied periods to monitor possible changes that may occurred, particularly in the urban areas and agriculture and subsequently predict likely changes.

1.8 Research Objectives

The main objective of the present study was to highlight and analyze the exchange between the land cover components at Greater Cairo with focusing on urban area and agricultural land between 1984, 1992, 2000, 2008 and 2016 using Landsat satellite data.

1.9 Study Area

The selected area of study is the Greater Cairo, which is known as the capital of Egypt and one of the fastest growing megacities worldwide. The study area is located at 30°02'N and 31°21'E, in the middle of the Delta Region, and covers an area of 1991 km2. Consisting of all cities in the Cairo Governorate as well as Giza, 6th of October, Sheikh Zayed City in the Giza Governorate and Shubra El Kheima and Obour in the Qalyubia Governorate. The Nile forms the administrative division between these governorates (Cairo and Giza), with locate Cairo and Helwan on the east bank of the river and, Giza and Six October and Sheikh Zayed City on the west bank. And Shubra El Kheima and Obour city north of Cairo Governorate. The area includes a variety of land uses associated with a complex mix of land cover, such as a central business district (CBD), urban/ suburban residential areas and some rural areas (e.g. cultivated areas and soil). This area has encountered rapid urban development and population growth in the last 20 years.

The region has the highest population and population density among Egyptian governorates, and is considered one of the most populous regions worldwide. The internal migration from Upper Egypt and the Delta began just after the Second World War, especially in the middle of 1950s due to the massive industrialization policy.

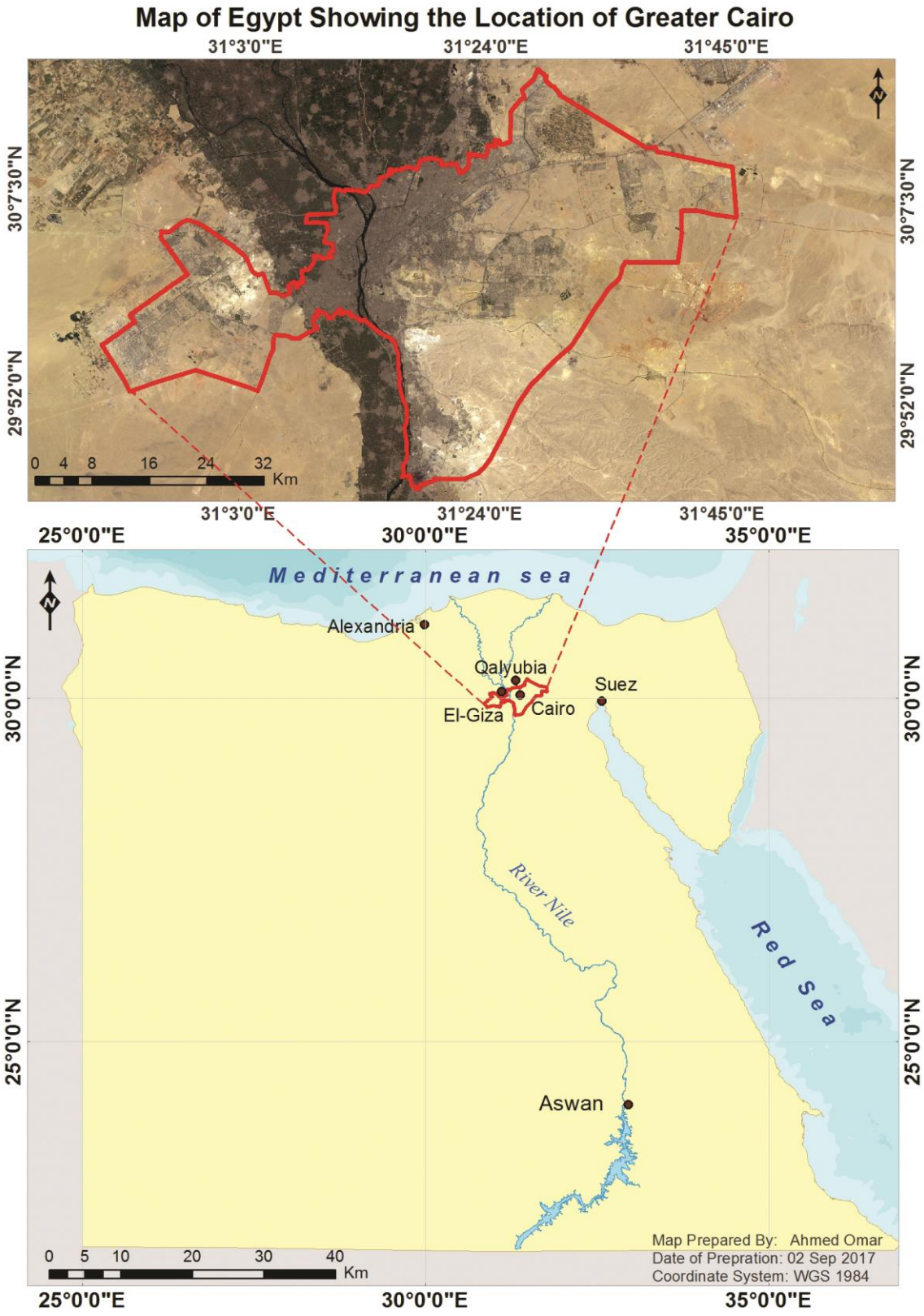

Map1: Egypt Map Showing the Location of study area.

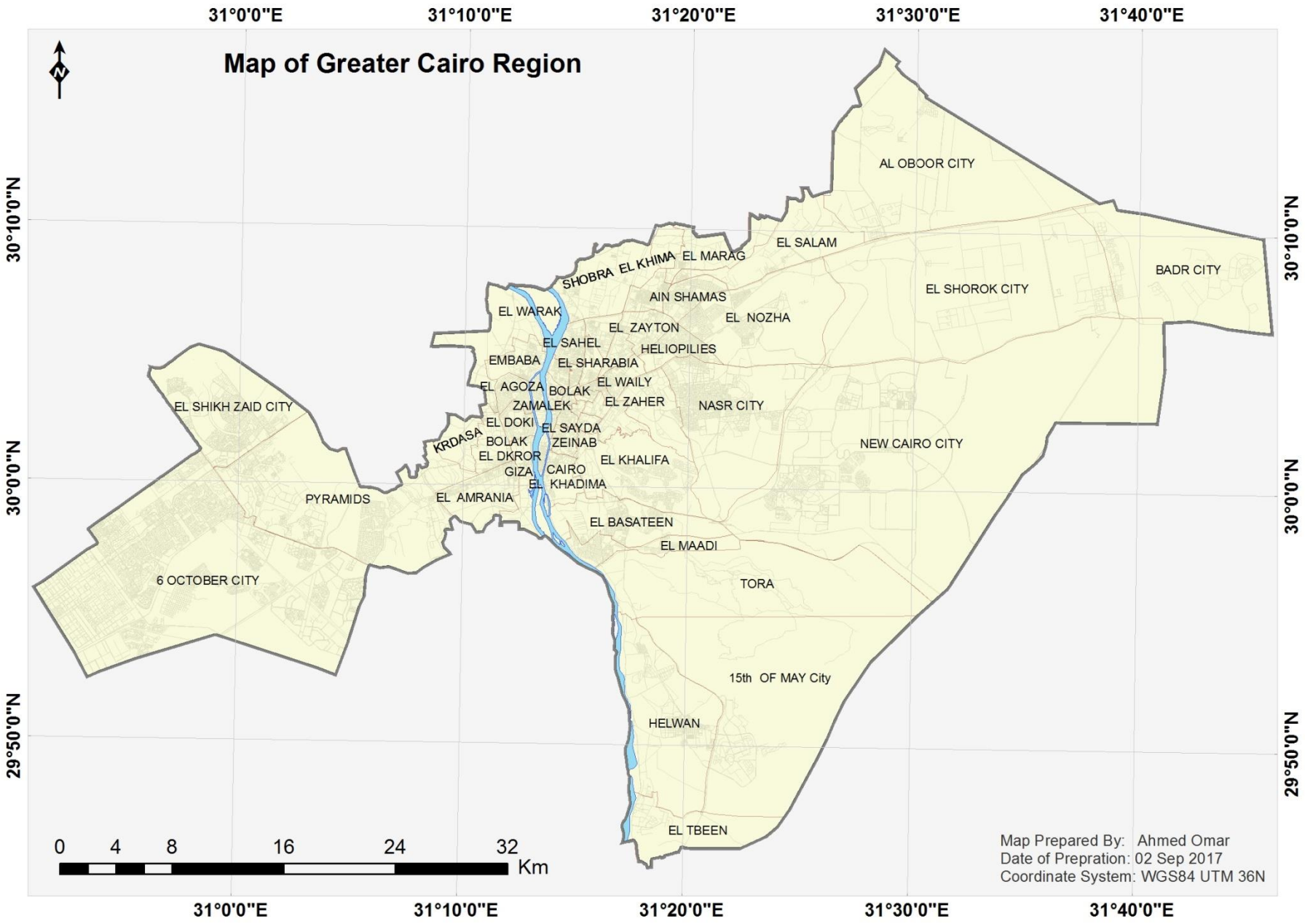

Map2: Map Showing the Cities and urban Communities in Greater Cairo Region.

Chapter-2

2. Methodology

2.1 Introduction

Research methodology is a systematic way to solve a problem. It is a science of studying how research is to be carried out. Essentially, the procedures by which researchers go about their work of describing, explaining and predicting phenomena are called research methodology. It is also defined as the study of methods by which knowledge is gained. Its aim is to give the work plan of research. It is also defined as the systematic, theoretical analysis of the methods applied to a field of study. It comprises the theoretical analysis of the body of methods and principles associated with a branch of knowledge. Typically, it encompasses concepts such as paradigm, theoretical model, phases and quantitative or qualitative techniques. (Irny, 2005)

It has been defined also as the base of any research. It involves all methods and approaches that have been used in any given study. This chapter deals with the methodology issue of this research. It commences with the first stage of the research, the Data collection phase, which contains collection, and chooses the appropriate satellite images for this research. Pre-processing images and processing images come in the following sections. And consists of some elements Geometric correction, Radiometric Correction, Atmospheric correction, Image Enhancement, Supervised Classification, Accuracy Assessment, land use/cover classification, change detection analysis, physical expansion analysis, and modeling urban growth.

2.2 Software used

Basically, four software were used for this project;

- ENVI 5.3: this was used for Images pre-processing, Classification and change detection analysis of the study area.

- ArcGIS 10.2: this was used partly in GIS analysis and producing Land use/cover Maps.
- Microsoft word: was used basically for the presentation of the research.
- Microsoft Excel was used for statistical analysis and producing the bar graph.

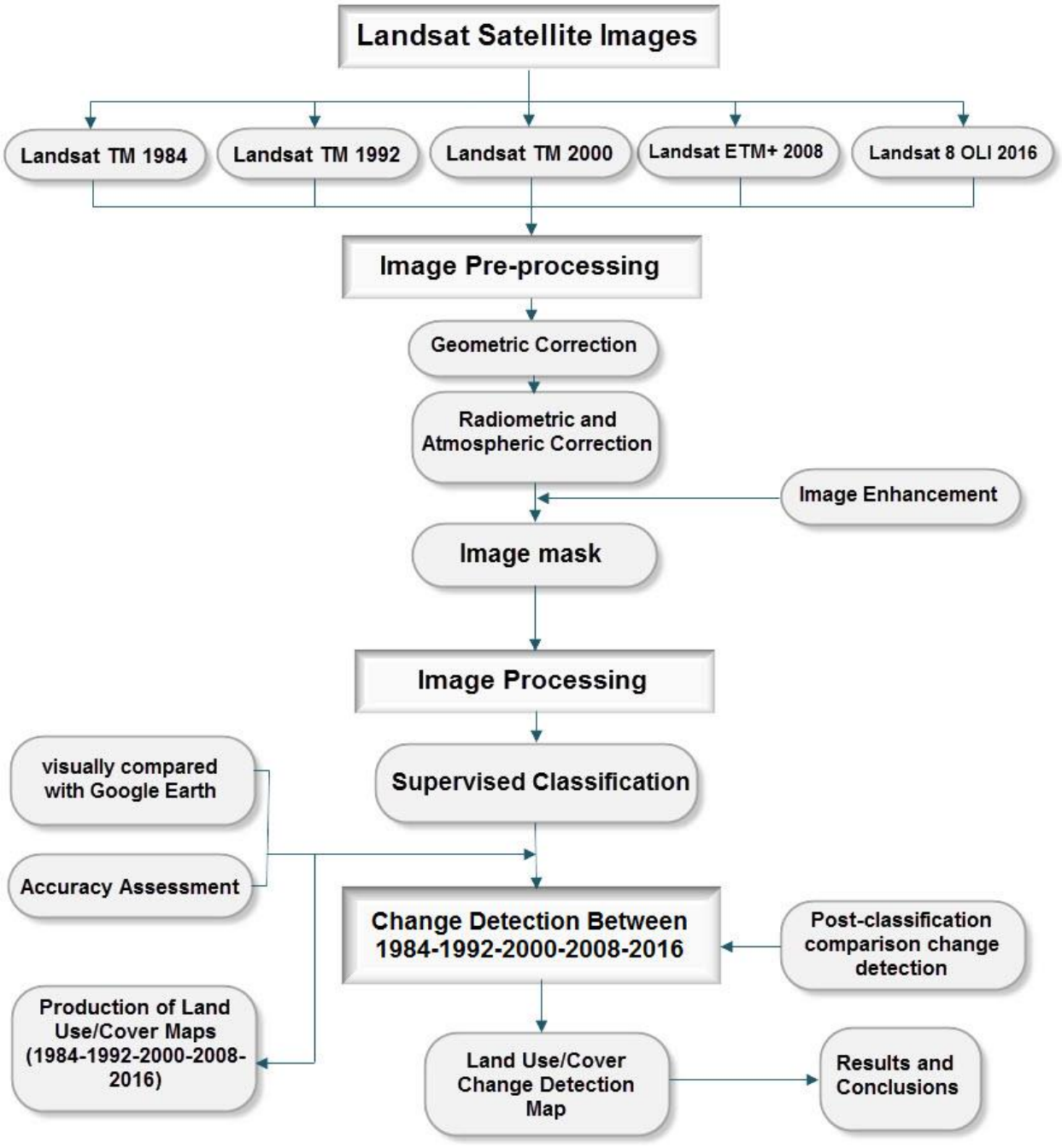

Figure1: Flow Chart Depicting the Change Detection Methodology.

2.3 Data Collection

Data collection is the first, most important and critical stage of any research or study as this step may control the direction of the research. And it is a complicated task especially for a developing country. Many tough security checks have to be done, even for "unimportant" data. Data cost is very expensive compared to similar applications in developed countries and it has to be undertaken through complicated procedures that consume long time periods. In addition, it may be difficult to get up-to-date data. In this study, five available satellite images were obtained from the United States Geological Survey (USGS) databases online resources, were downloaded at no cost from Earth Explorer (Landsat TM, Landsat ETM+ and Landsat 8 (OLI) images acquired in August 1984, August 1992, August 2000, August 2008 and August 2016 respectively).

Although there were a plenty of satellite images covering the study period, it was important to utilized images covering the summer season to ensure that agricultural land encompassing Greater Cairo are fully cultivated, and to have images with the sun elevation angle most closer to nadir. All the images were originally dereferenced to the Universal Transverse Mercator (UTM, zone 36°N).

2.4 Landsat Satellite Images

Landsat satellite images are available since 1972 up to date in eight successive generations, therefore, a long time series of data is potentially available for analysis. Landsat data are received and downlinked to ground stations worldwide, and are archived at the USGS EROS Center in Sioux Falls, South Dakota. Landsat data products are processed and made available for download to all users at no charge via EarthExplorer, GloVis, and the LandsatLook Viewer.

It was launched the first civilian Earth observation satellite. Their goal was achieved on July

23, 1972, with the launch of the Earth Resources Technology Satellite (ERTS-1), which was later renamed Landsat 1. The launches of Landsat 2, Landsat 3, and Landsat 4 followed in 1975, 1978, and 1982, respectively. When Landsat 5 launched in 1984, no one could have predicted that the satellite would continue to deliver high quality, global data of Earth's land surfaces for 28 years and 10 months, officially setting a new Guinness World Record for "longest-operating Earth observation satellite." Landsat 6 failed to achieve orbit in 1993; however, Landsat 7 successfully launched in 1999 and continues to provide global data. Landsat 8, launched in 2013, continues the mission, and Landsat 9 is tentatively planned to launch in 2020.

Date	Satellite	Path and Row	Ground Coverage
03 August 1984	LS5 TM	P - 176 , R - 39	South and Southeast of Nile Delta
25 August 1992	LS5 TM	P - 176 , R - 39	South and Southeast of Nile Delta
15 August 2000	LS5 TM	P - 176 , R - 39	South and Southeast of Nile Delta
29 August 2008	LS7 ETM+	P - 176 , R - 39	South and Southeast of Nile Delta
27 August 2016	LS 8 OLI	P - 176 , R - 39	South and Southeast of Nile Delta

Table1: Details of the Landsat Images Used in the Study.

2.4.1 Characteristics of Landsat 5 TM

Landsat TM data has a 30-m ground spatial resolution cell for all bands except band 6, which has a 120m spatial resolution. Although, the Landsat TM bands are finely tuned for vegetation discrimination, other applications benefit from the enhanced characteristics of Landsat TM. Band one is the best for bathymetry investigations. Bands five and seven have proven to be extremely valuable in discrimination of rock types. Meanwhile, band five is used to differentiate between snow and cloud covered areas. In addition, band six is useful in thermal mapping (Lillesand and Kieffer 1994).

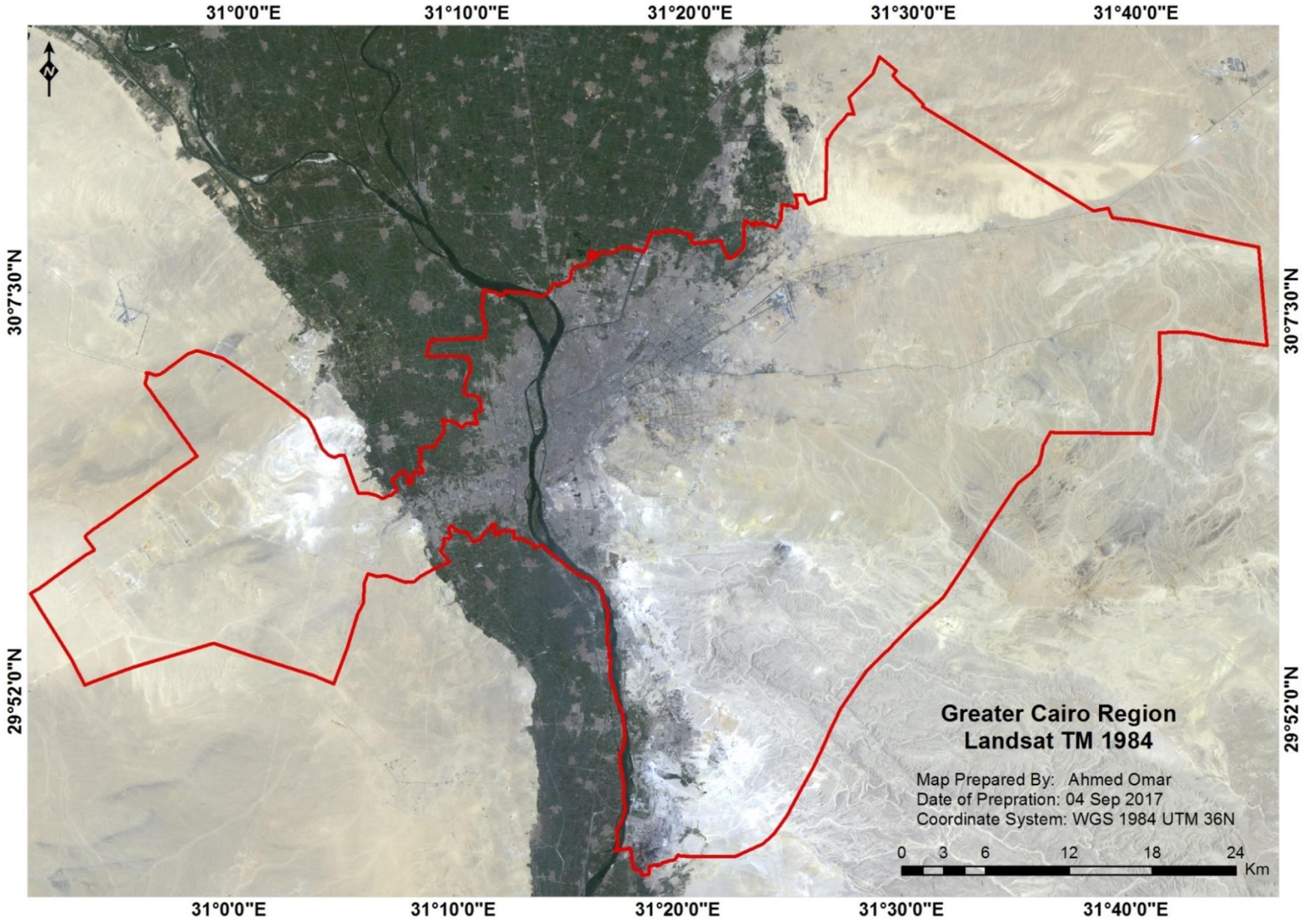

Map3: Landsat Thematic Mapper (TM) 1984 for Greater Cairo Region.

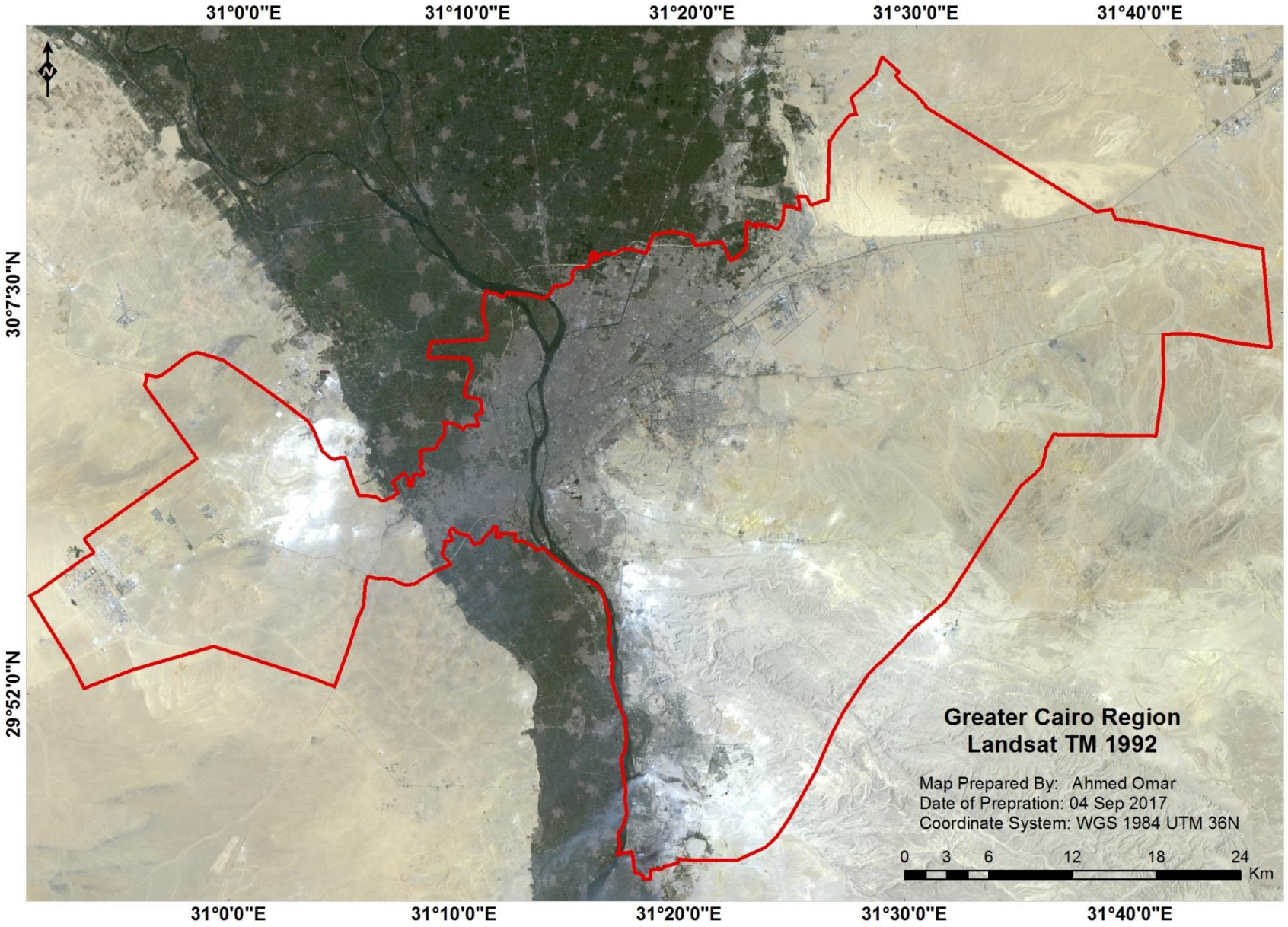

Map4: Landsat Thematic Mapper (TM) 1992 for Greater Cairo Region.

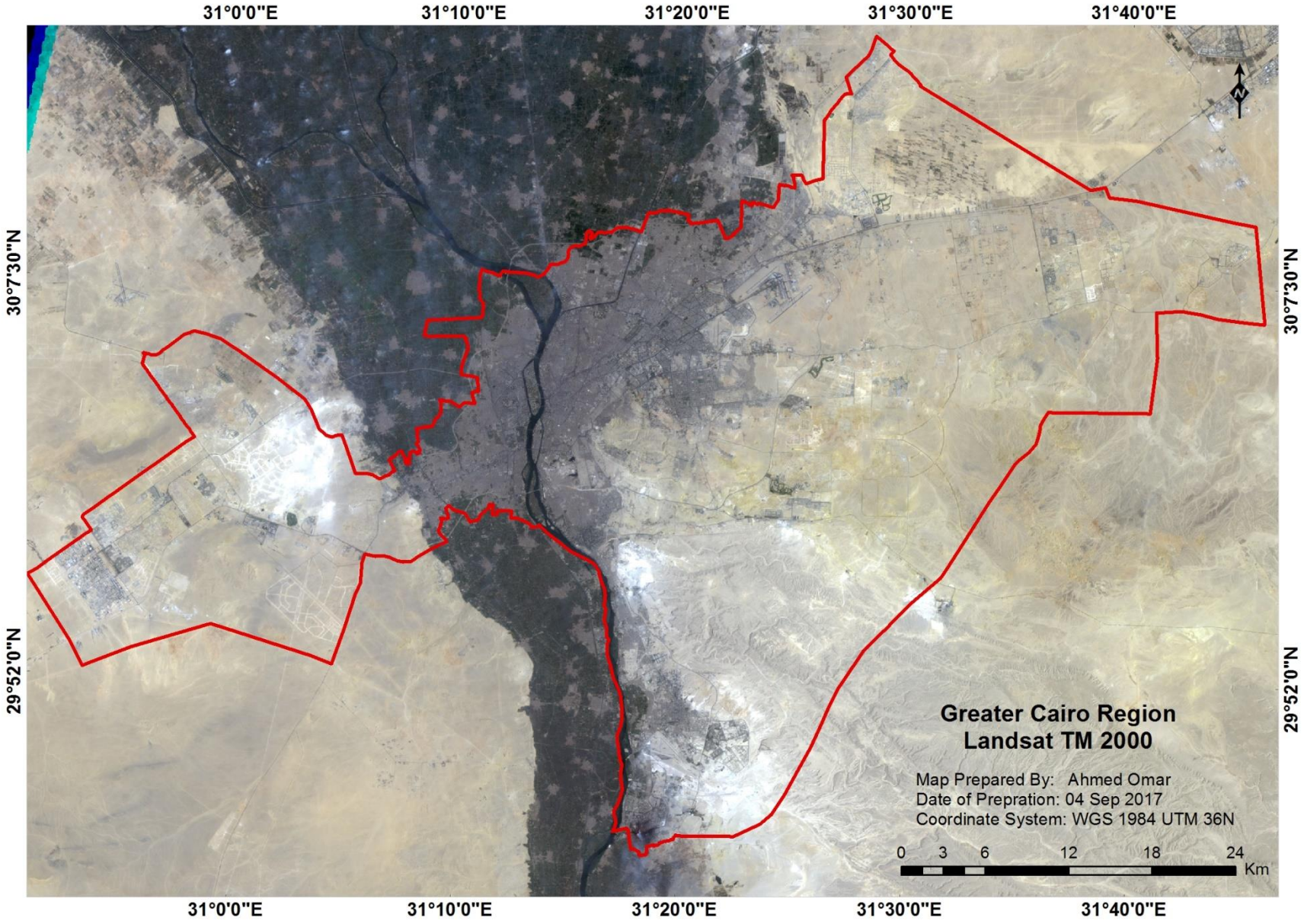

Map5: Landsat Thematic Mapper (TM) 2000 for Greater Cairo Region.

2.4.2 Characteristics of Landsat 7 ETM+

Landsat 7 ETM+ images consist of eight spectral bands with a spatial resolution of 30 meters for bands 1 to 7. The panchromatic band 8 has a resolution of 15 meters. All bands can collect one of two gain settings (high or low) for increased radiometric sensitivity and dynamic range, while Band 6 collects both high and low gain for all scenes. Approximate scene size is 170 km north-south by 183 km east-west (106 mi by 114 mi). All Landsat 7 scenes collected since May 30, 2003 have data gaps due to the Scan Line Corrector (SLC) failure. Since that time all Landsat ETM images have had wedge-shaped gaps on both sides of each scene, resulting in approximately 22% data loss.

Scaramuzza, et al (2004) developed a technique which can be used to fill gaps in one scene with data from another Landsat scene (Scaramuzza, et al 2004). I solved fill gaps problem by more accurate technique to fill gaps in one scene with data from another Landsat scene taken in the same month by using known category values from one Landsat 7 image to fill in areas of "no data" in another Landsat 7 image (Such as shown in the figure 2). After finishing this process I used historical imagery tool in Google earth to make sure the image is accurate.

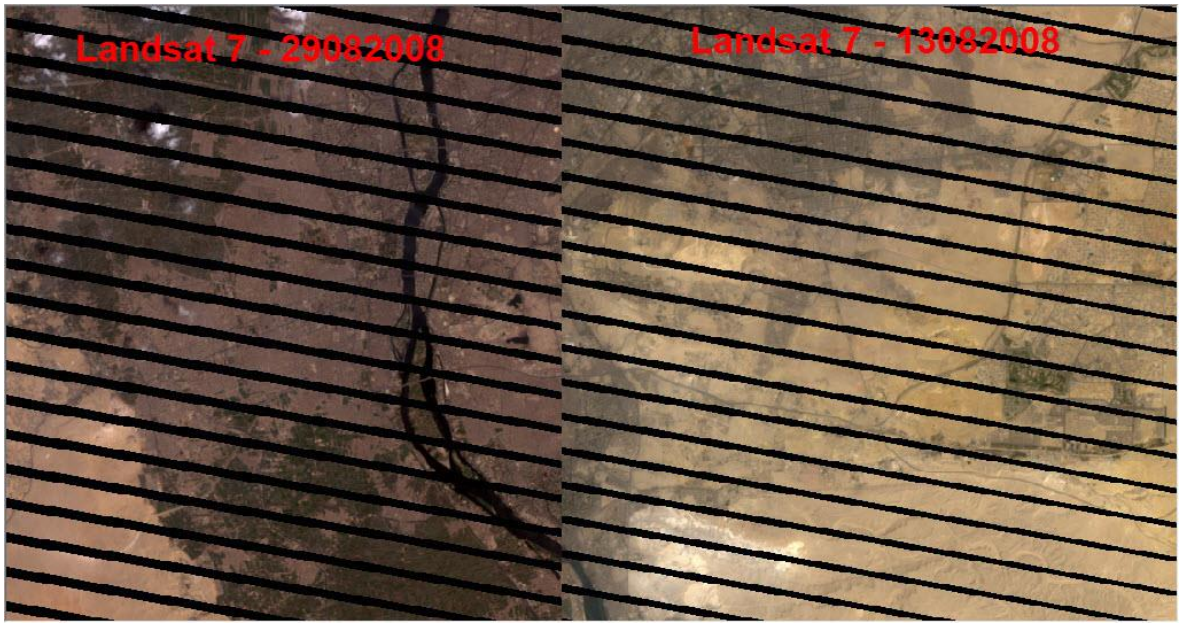

Figure2: Showing two Landsat 7 ETM+ 2008 images taken in the same month.

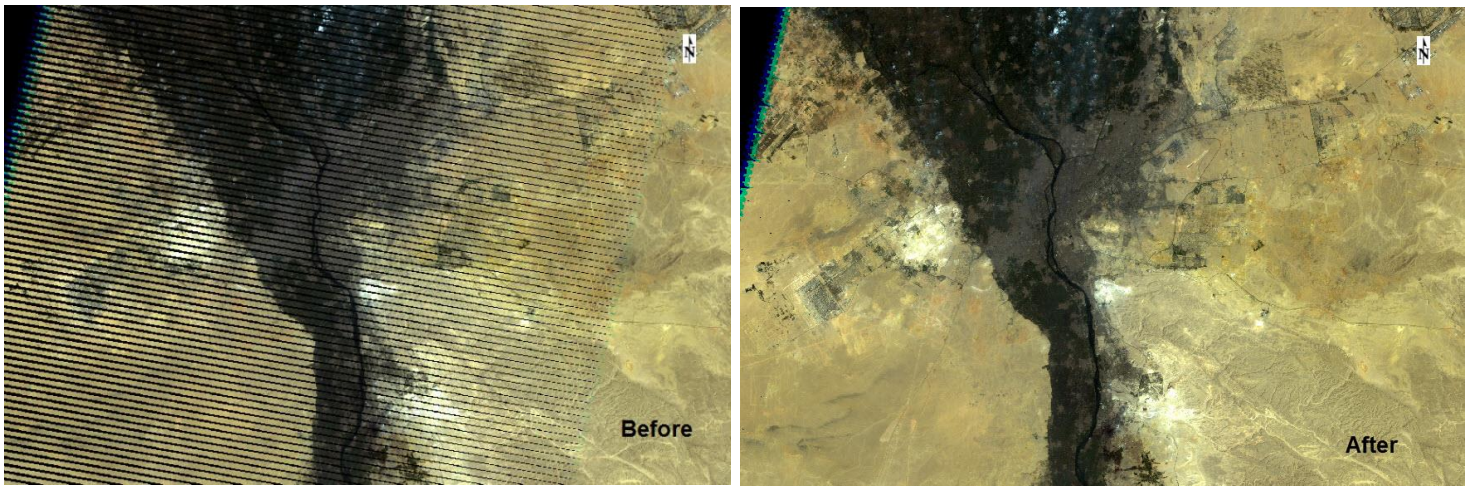

Figure2-1: Showing Landsat 7 ETM+ 2008 image before and after apply filling gaps.

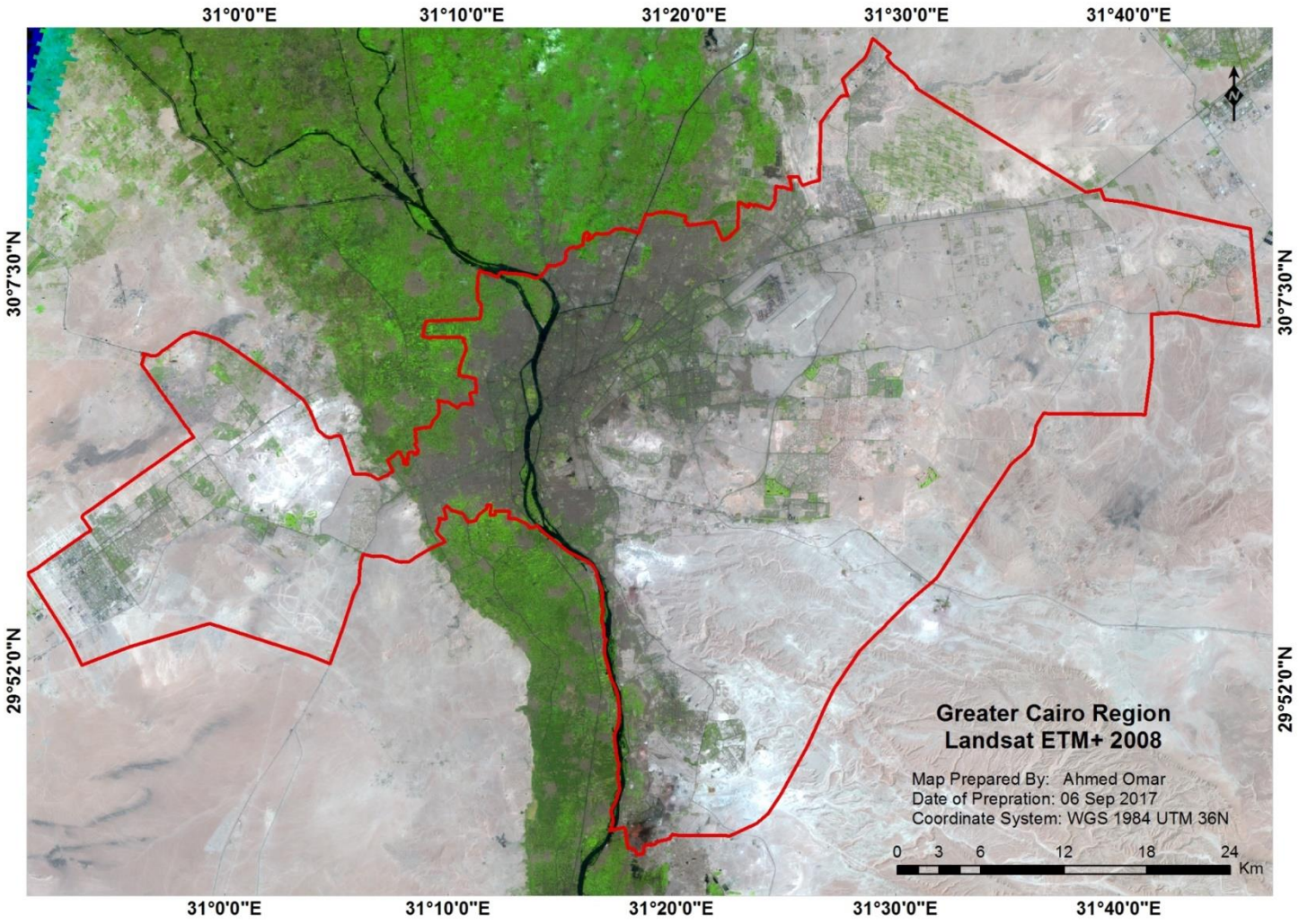

Map6: Landsat 7 ETM+ 2008 for Greater Cairo Region.

2.4.3 Characteristics of Landsat 8 (OLI)

The Operational Land Imager (OLI) 30-meter multi spectral spatial resolutions along a 185 km wide swath. The entire Earth falls within view once every 16 days due to LDCM's near-polar orbit. Landsat 8 (launched 11 February 2013) measures different ranges of frequencies along the electromagnetic spectrum – a color, although not necessarily a color visible to the human eye. Each range is called a band, and Landsat 8 has 11 bands. Landsat numbers its red, green, and blue sensors as 4, 3, and 2, so when we combine them we get a true-color image.

Satellite Sensor	Acquired Date	Coordinate System/ Datum	Zone	Bands	Wavelength (micrometers)	Resolution (meters)
Landsat 5 TM	03-08-1984	UTM/WGS 84	36 N	1-Blue	0.45 - 0.52	30
				2-Green	0.52 - 0.60	30
	25-08-1992			3-Red	0.63 - 0.69	30
				4-NIR	0.76 - 0.90	30
	15-08-2000			5-SWIR1	1.55 - 1.75	30
				7-SWIR2	2.08 - 2.35	30
Landsat 7 ETM+	29-08-2008	UTM/WGS 84	36 N	1-Blue	0.45 - 0.52	30
				2-Green	0.52 - 0.60	30
				3-Red	0.63 - 0.69	30
				4-NIR	0.77 - 0.90	30
				5-SWIR1	1.55 - 1.75	30
				7-SWIR2	2.09 - 2.35	30
Landsat 8 OLI	27-08-2016	UTM/WGS 84	36 N	2-Blue	0.45 - 0.51	30
				3-Green	0.53 - 0.59	30
				4-Red	0.64 - 0.67	30
				5-NIR	0.85 - 0.88	30
				6-SWIR1	1.57 - 1.65	30
				7-SWIR2	2.11 - 2.29	30

Table2: Landsat (5 TM, 7 ETM+, 8 OLI) sensors and their characteristics.

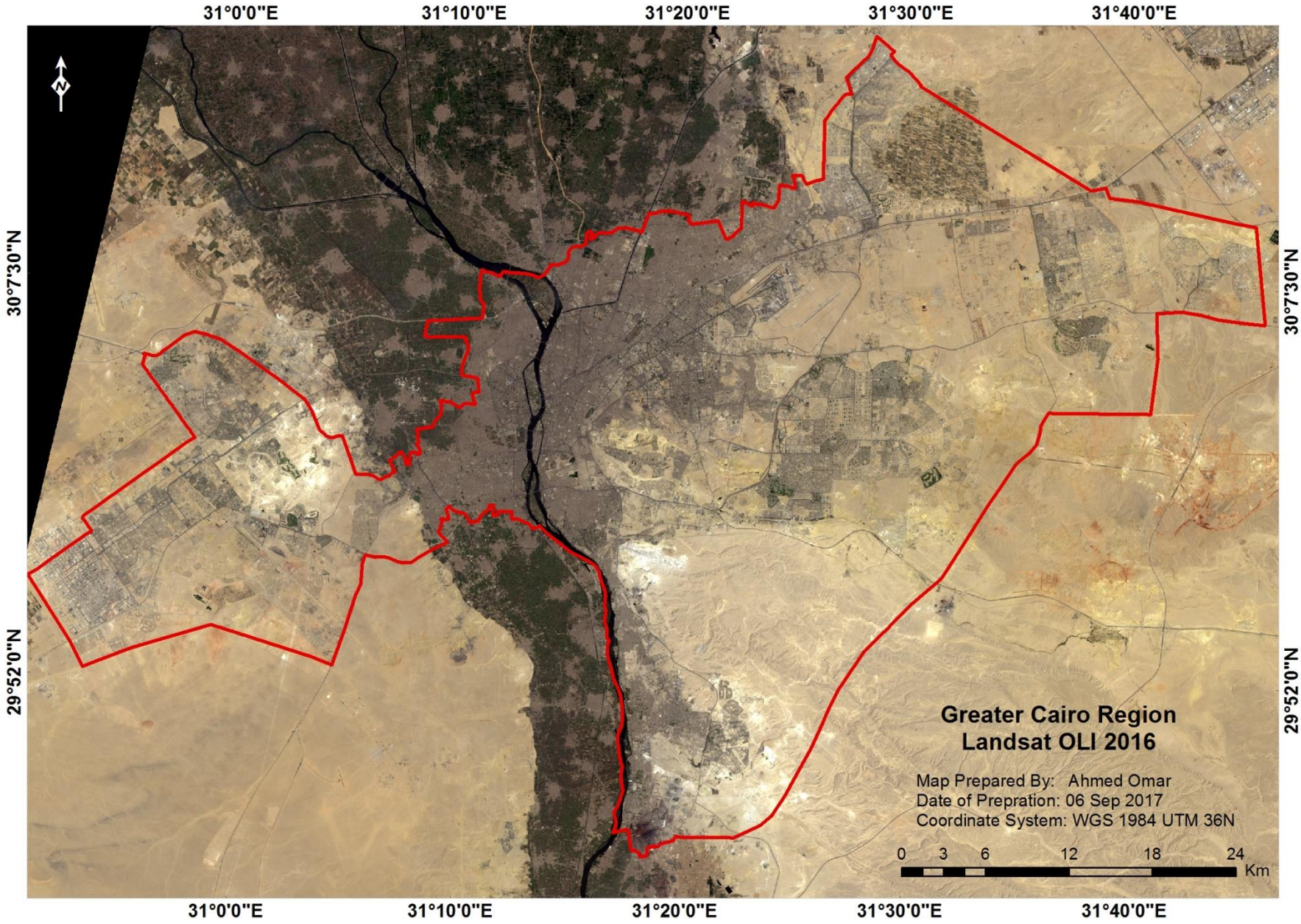

Map7: Landsat 8 OLI 2016 for Greater Cairo Region.

2.5 Image Pre-processing

Satellite image pre-processing is crucial step in any analytical remote sensing workflow and it is prior to data analysis process. Satellite image processing composed of techniques and procedures which follow in pre-processing the image data (Furtado et al. 2010). Satellite image pre-processing includes procedures of radiometric calibration of, atmospheric correction of the variations of the viewing geometry and instrument response of spectral characteristics (Schowengerdt 2007). The other important procedure in image pre-processing is the geometric correction of the image data, where the objective of geometric correction of image is to overcome the distortion which introduced by atmospheric refraction, relief of the earth surface. Also image enhancement increase the visual interpretation of image objects and elements by increasing the visual distinction between surface features (Acharya et al. 2005).

Landsat images were used in this study were of the same season and date of acquisition almost the same. All image scenes subjected to image processing procedures were carried out using Envi 5.3.

2.5.1 Geometric Correction

The geometric correction of image data is an important prerequisite which must be performed prior to using images in geographic information systems (GIS) and other image processing programs. To process the data with other data or maps in a GIS, all of the data must have the same reference system. The acquired Landsat images used in this study are ortho-rectified. They are in world geodetic system (WGS 84) datum and with Universal Transverse Mercator (UTM) projection system.

A geometrical correction, also called geo-referencing, is a procedure where the content of a map will be assigned a spatial coordinate system. Change detection analysis is basically

performed on pixel-by-pixel basis; so the accurate per-pixel registered multi-temporal satellite images data because the registration errors could effect on the LULC change detection result, and lead to an overestimation of actual changes (Stow, 1999).

In geo-referencing, image points and pass points need to be searched, which then can be recognized in the coordinates. Pass points are usually determined with a GPS receiver on the terrain or with maps. Visual street crossings, bridges over water, etc. can be identified, and their coordinates will be noted. These points will then be coordinated with identical image points of the not yet geo-referenced satellite image. These correlations can ensure projections with the help of various additional procedures.

When execute visual investigation between Landsat images no significant discrepancies between images scenes were observed. The investigation process revealing a high geometric matching between images, with shift between images about 2 and 3 pixels. Therefore, image to image registration technique using Envi (5.3) image to image registration with Ground Control Point (GCP) were used to enhance both images with maximum accurate matching between images. Landsat 8 OLI image placed as a base image, and Landsat TM, ETM images as wrap images. The Landsat TM, ETM images is registered to Landsat 8 OLI image with RMS error less than 1 pixel.

Base image	Wrap image	Matching method	Resampling method	Model	Number of GCP	RMS Error
Landsat 8 2016	Landsat TM 1984	Cross Correlation	Bilinear	Polynomial	64	0.42

Table3: Image to image registration information of Landsat TM 1984 to Landsat 8 OLI.

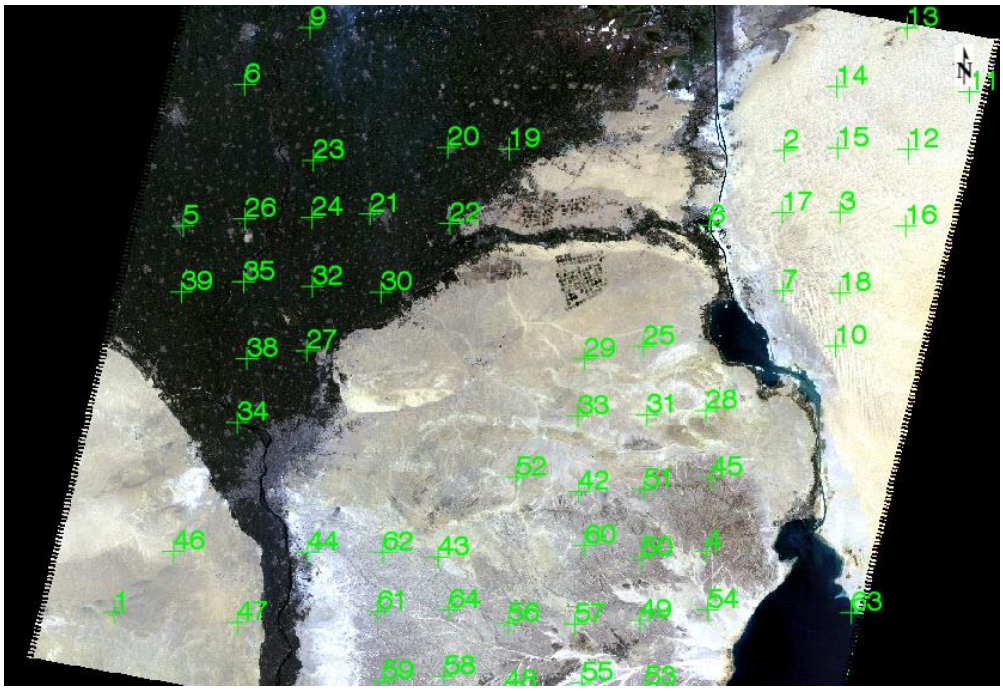

Figure 3: Image to image registration (Landsat 1984 – Landsat 2016) in Envi.

After finishing image registration, the registered image were visually assessed by comparing between base image (Landsat 8 OLI 2016) and wrapped image (Landsat TM 1984) using linear features such as streets. As shown in Figure 4.

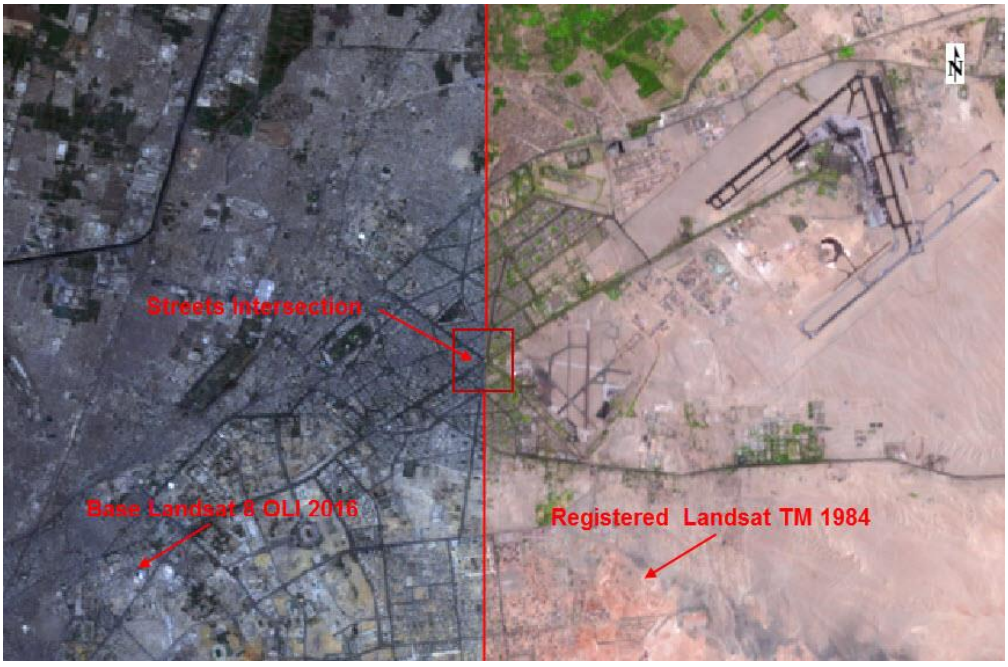

Figure 4: Comparison between the registered image LS 1984 and the base image LS 2016.

Base image	Wrap image	Matching method	Resampling method	Model	Number of GCP	RMS Error
Landsat 8 2016	Landsat TM 1992	Cross Correlation	Bilinear	Polynomial	64	0.23

Table4: Image to image registration information of Landsat TM 1992 to Landsat 8 OLI.

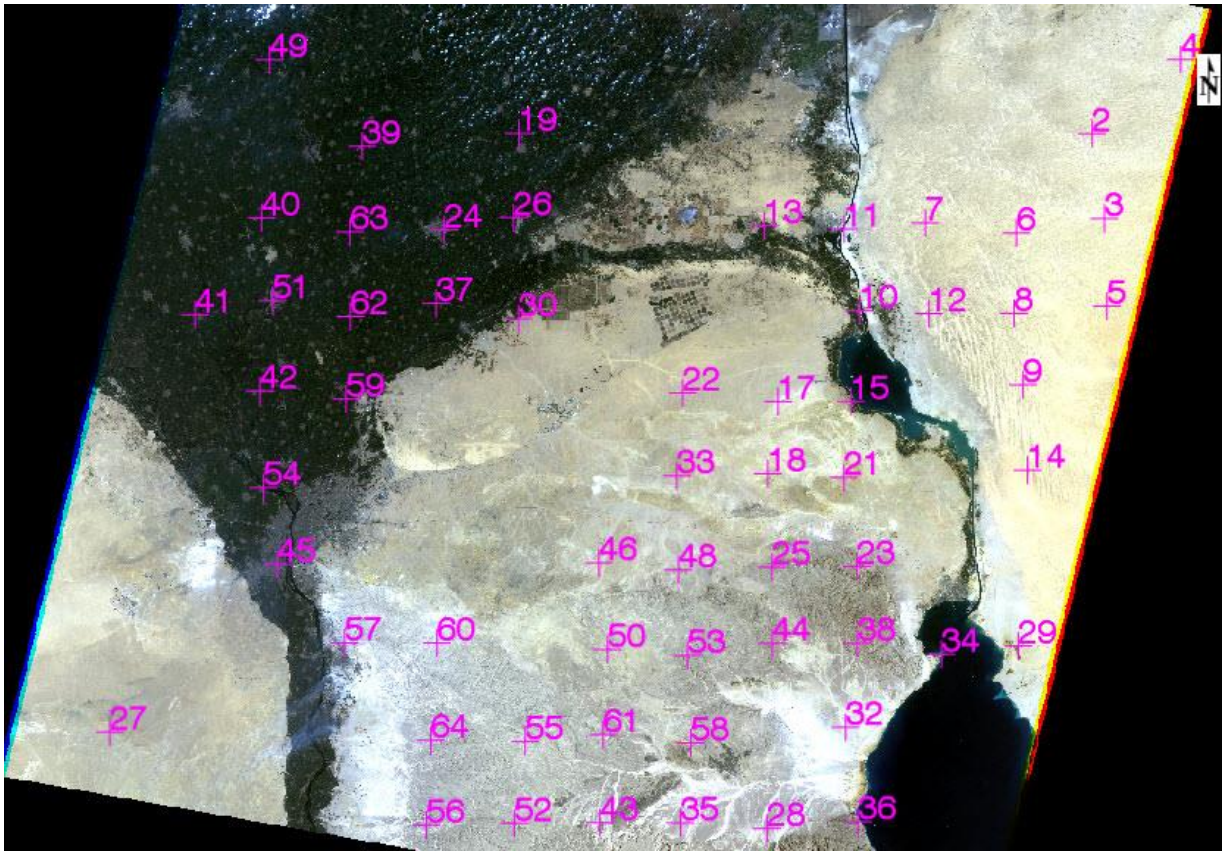

Figure 5: Image to image registration (Landsat 1992 – Landsat 2016) in Envi.

After finishing image registration, the registered image were visually assessed by comparing between base image (Landsat 8 OLI 2016) and wrapped image (Landsat TM 1992) using linear features such as streets. As shown in Figure 6.

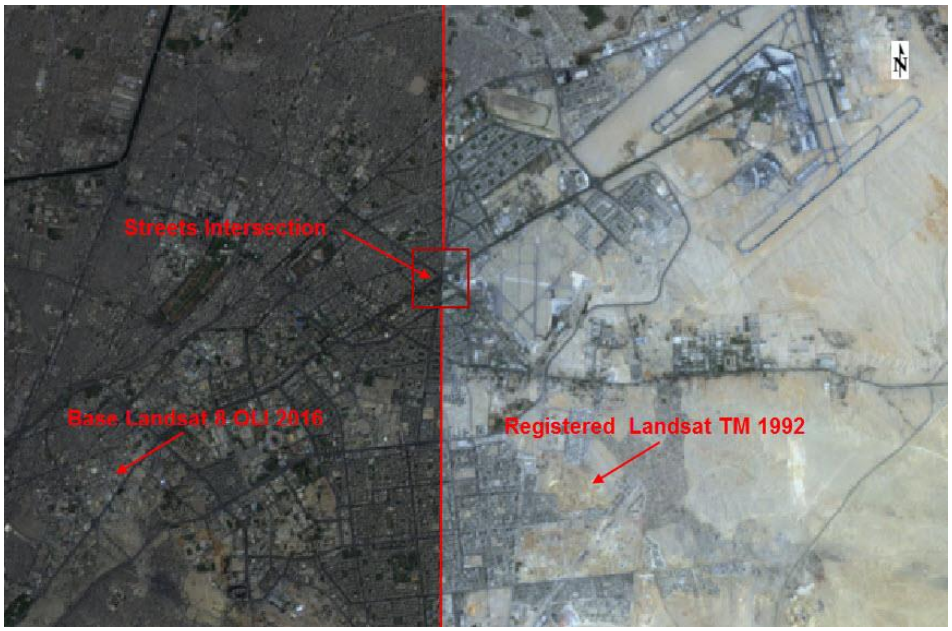

Figure 6: Comparison between the registered image LS 1992 and the base image LS 2016.

Base image	Wrap image	Matching method	Resampling method	Model	Number of GCP	RMS Error
Landsat 8 2016	Landsat TM 2000	Cross Correlation	Bilinear	Polynomial	82	0.24

Table5: Image to image registration information of Landsat TM 2000 to Landsat 8 OLI.

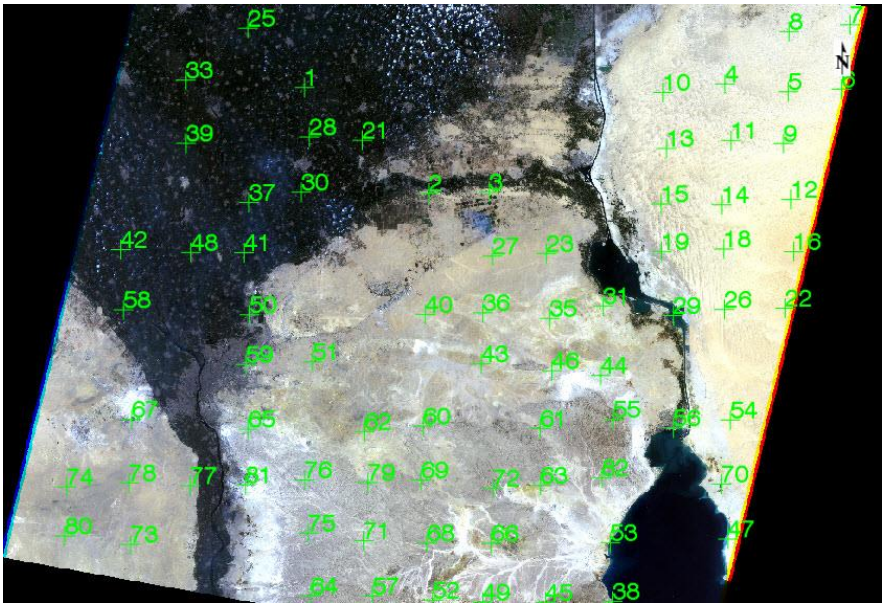

Figure 7: Image to image registration (Landsat 2000 – Landsat 2016) in Envi.

After finishing image registration, the registered image were visually assessed by comparing between base image (Landsat 8 OLI 2016) and wrapped image (Landsat TM 2000) using linear features such as streets. As shown in Figure 8.

Figure 8: Comparison between the registered image LS 2000 and the base image LS 2016.

Base image	Wrap image	Matching method	Resampling method	Model	Number of GCP	RMS Error
Landsat 8 2016	Landsat ETM+ 2008	Cross Correlation	Bilinear	Polynomial	87	0.19

Table6: Image to image registration information of Landsat 7 ETM+ 2008 to Landsat 8 OLI.

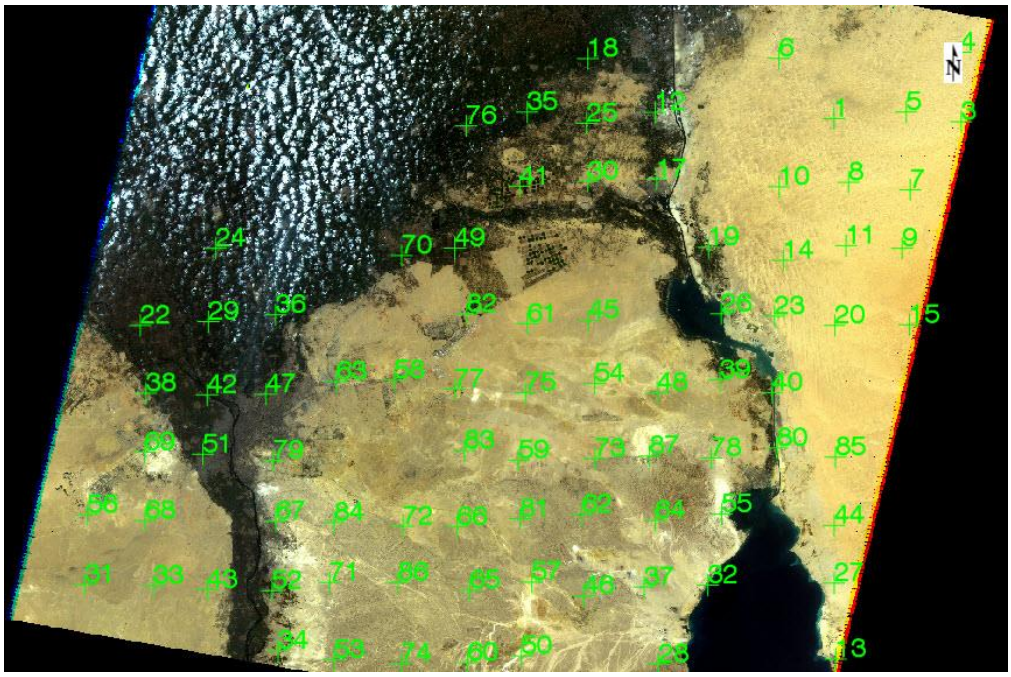

Figure 9: Image to image registration (Landsat 2008 – Landsat 2016) in Envi.

After finishing image registration, the registered image were visually assessed by comparing between base image (Landsat 8 OLI 2016) and wrapped image (Landsat 7 ETM+ 2008) using linear features such as streets. As shown in Figure 10.

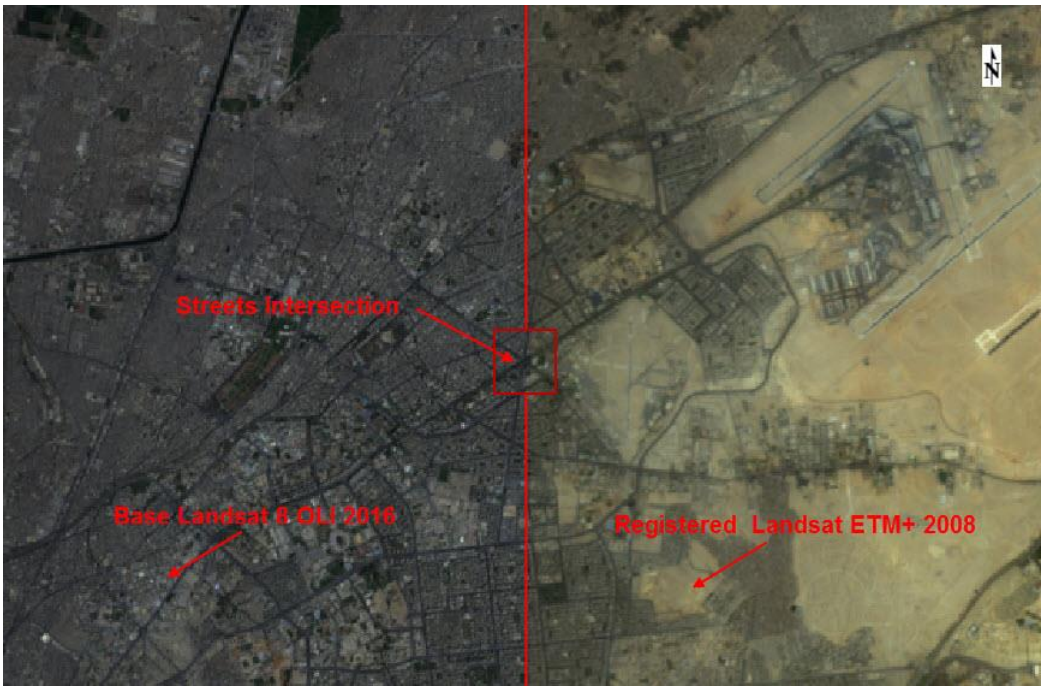

Figure 10: Comparison between the registered image LS 2008 and the base image LS 2016.

2.5.2 Radiometric Correction

System corrections are important, when technical defects and deficiencies of the sensor and data transfer systems lead to mistakes in the image data construction. The radiometric correction or normalization is required to perform more accurate change detection process using supervised classification. Radiometric correction is done to reduce or correct errors in the digital numbers of images. The process improves the interpretability and quality of remote sensed data. Radiometric calibration and correction are particularly important when comparing data sets over a multiple time periods. The energy that sensors onboard aircrafts or satellites record can differ from the actual energy emitted or reflected from a surface on the ground. This is due to the sun's azimuth and elevation and atmospheric conditions that can influence the observed energy. Therefore, in order to obtain the real ground irradiance or reflectance, radiometric errors must be corrected.

In order to make a meaningful measure of radiance at the Earth's surface, the atmospheric interferences must be removed from the data. This process is called "atmospheric correction". The entire process of radiometric correction involves several steps as the following.

Manually Converting Landsat TM and ETM data to TOA Reflectance. This is a two-step process. First, converting DNs to radiance values, and then converting these radiance values to reflectance values. A considerable amount of additional information is needed to carry out the radiometric correction of an image. Much of this is contained in header files which come with the imagery (MTL.txt).

- Step 1. Calibrated DN to Spectral Radiance Conversion.

$$L\lambda = ((LMAX\lambda - LMIN\lambda)/(QCALMAX - QCALMIN)) * (QCAL - QCALMIN) + LMIN\lambda$$

Where:

$L\lambda$ = spectral radiance at the sensor's aperture

$QCAL$ = the quantized calibrated pixel value in DN

$LMIN\lambda$ = the spectral radiance scaled to QCALMIN in watts/(meter squared * ster * μm)

$LMAX\lambda$ = the spectral radiance scaled to QCALMAX in watts/(meter squared * ster * μm)

$QCALMIN$ = the minimum quantized calibrated pixel value (corresponding to LMINλ) in DN 1 for LPGS products, 0 for NLAPS products

$QCALMAX$ = the maximum quantized calibrated pixel value (corresponding to LMAXλ) in DN = 255

- Step 2. Conversion of spectral radiance to TOA reflectance

$$P\rho = \pi * L\lambda * d / ESUN\lambda * \cos(\vartheta)S$$

Where:

$P\rho$ = unitless TOA or planetary reflectance

$L\lambda$ = spectral radiance at the sensor's aperture

d = Earth-Sun distance in astronomical units from nautical handbook or interpolated values

$ESUN\lambda$ = mean solar exoatmospheric spectral irradiance

$\cos(\vartheta)S$ = solar zenith angle in degrees

Manually Converting Landsat 8 OLI data to ToA Reflectance. The products are delivered in 16-bit unsigned integer format and can be rescaled to the Top Of Atmosphere (TOA) reflectance and/or radiance using radiometric rescaling coefficients provided in the product metadata file (MTL file), as briefly described below. The MTL file also contains the thermal constants needed to convert TIRS data to the at-satellite brightness temperature as the following steps.

- Step 1: Conversion to TOA Radiance.

$$L\lambda = M_L Q_{cal} + A_L$$

where:

$L\lambda$ = TOA spectral radiance (Watts/(m2 * srad * μm))

M_L = Band-specific multiplicative rescaling factor from the metadata (RADIANCE_MULT_BAND_x, where x is the band number)

A_L = Band-specific additive rescaling factor from the metadata (RADIANCE_ADD_BAND_x, where x is the band number)

Q_{cal} = Quantized and calibrated standard product pixel values (DN)

- Step 2: Conversion to TOA Reflectance.

$$\rho\lambda = \frac{M_\rho Q_{cal} + A_\rho}{\cos(\theta_{SZ})}$$

where:

$\rho\lambda$ = TOA planetary reflectance.

M_ρ = Band-specific multiplicative rescaling factor from the metadata (REFLECTANCE_MULT_BAND_x, where x is the band number)

A_ρ = Band-specific additive rescaling factor from the metadata (REFLECTANCE_ADD_BAND_x, where x is the band number)

Q_{cal} = Quantized and calibrated standard product pixel values (DN)

θ_{SE} = Local sun elevation angle. The scene center sun elevation angle in degrees is provided in the metadata (SUN_ELEVATION).

θ_{SZ} = Local solar zenith angle; $\theta_{SZ} = 90° - \theta_{SE}$

- Step 3: Conversion to At-Satellite Brightness Temperature.

$$T = \frac{K_2}{\ln\left(\frac{K_1}{L\lambda} + 1\right)}$$

where:

T = At-satellite brightness temperature (K)

$L\lambda$ = TOA spectral radiance (Watts/(m2 * srad * μm))

K_1 = Band-specific thermal conversion constant from the metadata (K1_CONSTANT_BAND_x, where x is the thermal band number)

K_2 = Band-specific thermal conversion constant from the metadata (K2_CONSTANT_BAND_x, where x is the thermal band number)

To achieve an accurate radiometric correction, the atmospheric correction first is performed on the image scenes of Landsat TM 1984, 1992, 2000 and Landsat 7 ETM+ 2008 and Landsat 8 2016, to get rid of atmospheric effects (e.g. haze, dust or smoke). Then, the radiometric correction was implemented in one step using radiometric correction tool using Envi software (FLAASH Atmospheric Correction) which require a combination of parameters such as sun and view angle effects and the sensor calibration. These parameters have been obtained from Landsat metadata information for each image.

After run FLAASH atmospheric correction in ENVI, checked the Minimum and Maximum of reflectance images (by use statistics calculation). And the results were not normal and there are negative values, so I used bellow formula in Band math in ENVI software:

```
(b1 le 0)*0+(b1 ge 10000)*1+(b1 gt 0 and b1 lt 10000)*float(b1)/10000
```

Figure 11 showing the difference between the Minimum and Maximum of reflectance image before and after using Band Math formula.

Figure 11: Landsat TM 1984 before and after execution Post FLAASH Band Math Equation.

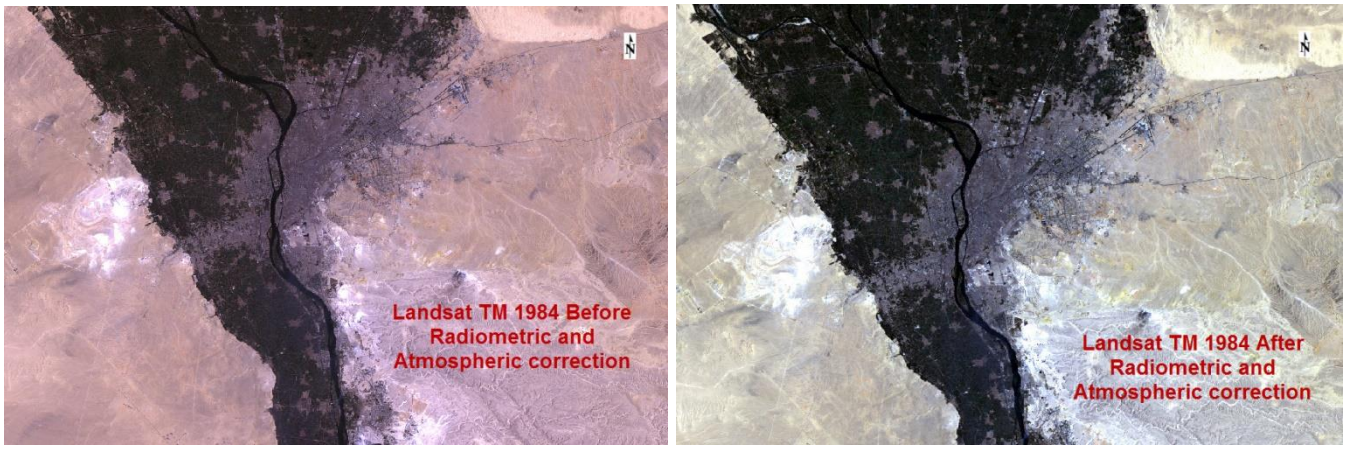

Figure 12: Landsat TM 1984 image before and after radiometric and atmospheric correction.

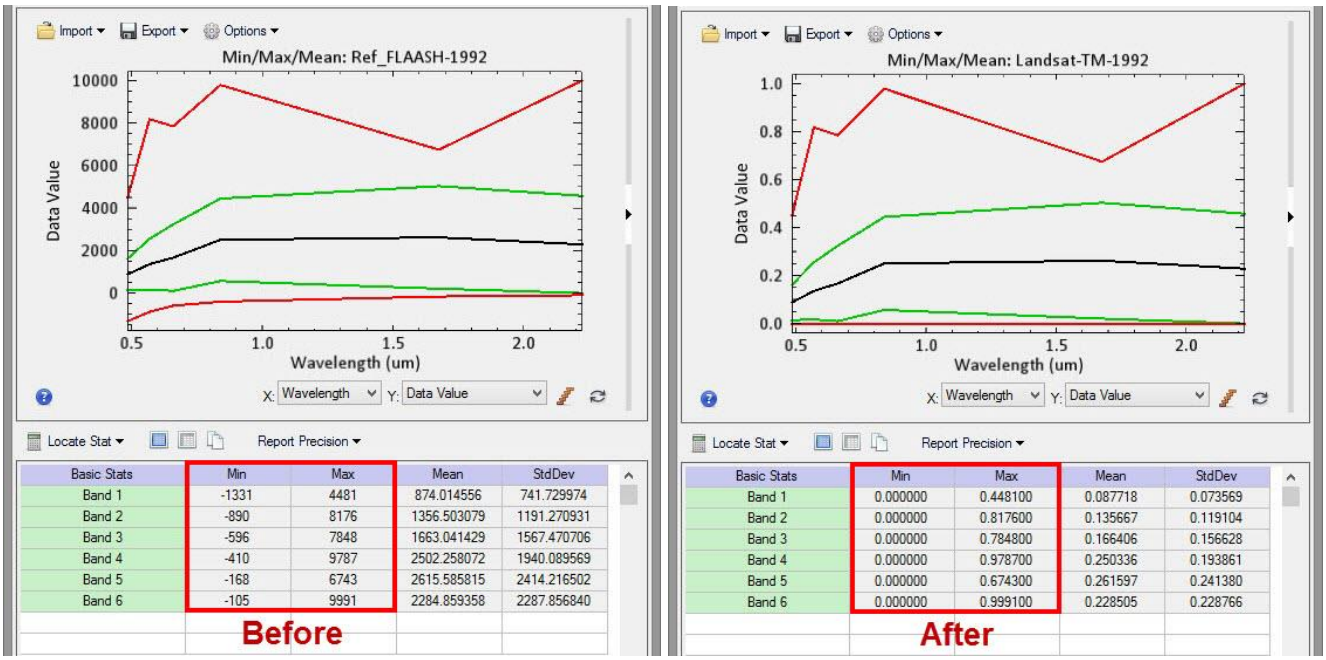

Figure 13: Landsat TM 1992 before and after execution Post FLAASH Band Math Equation.

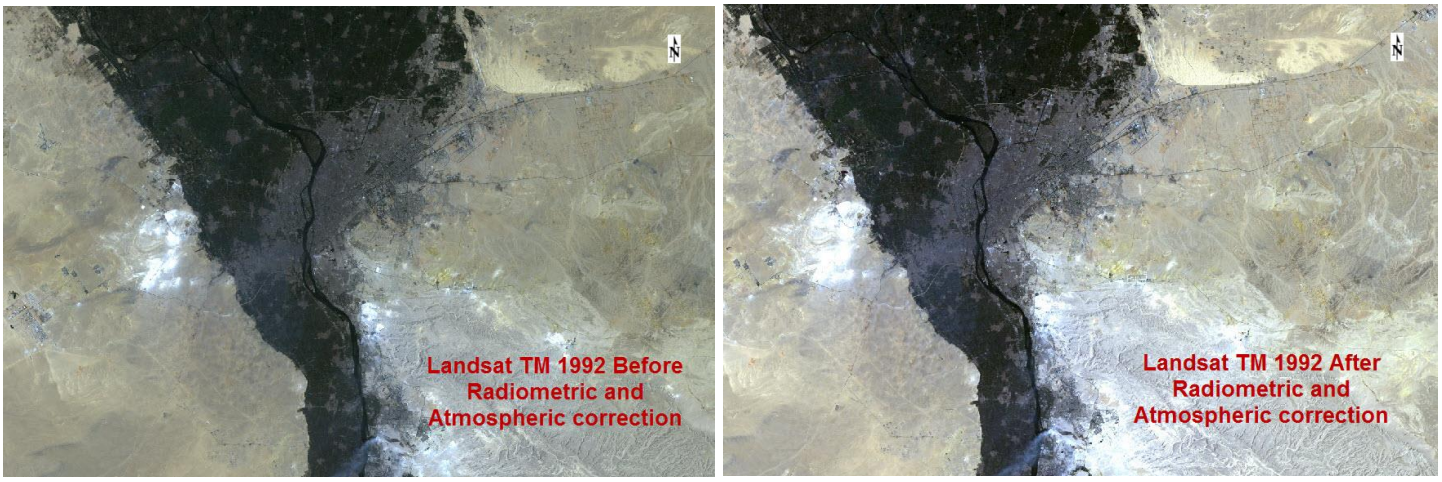

Figure 14: Landsat TM 1992 image before and after radiometric and atmospheric correction.

Figure 15: Landsat TM 2000 before and after execution Post FLAASH Band Math Equation.

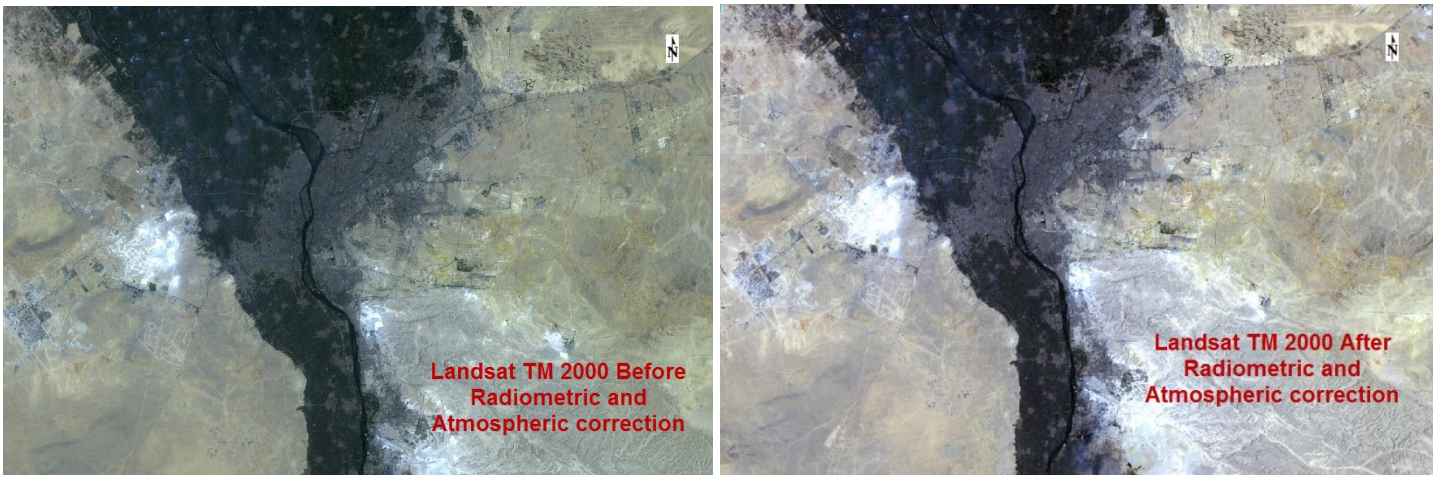

Figure 16: Landsat TM 2000 image before and after radiometric and atmospheric correction.

Figure 17: Landsat ETM+ 2008 before and after execution Post FLAASH Band Math Equation.

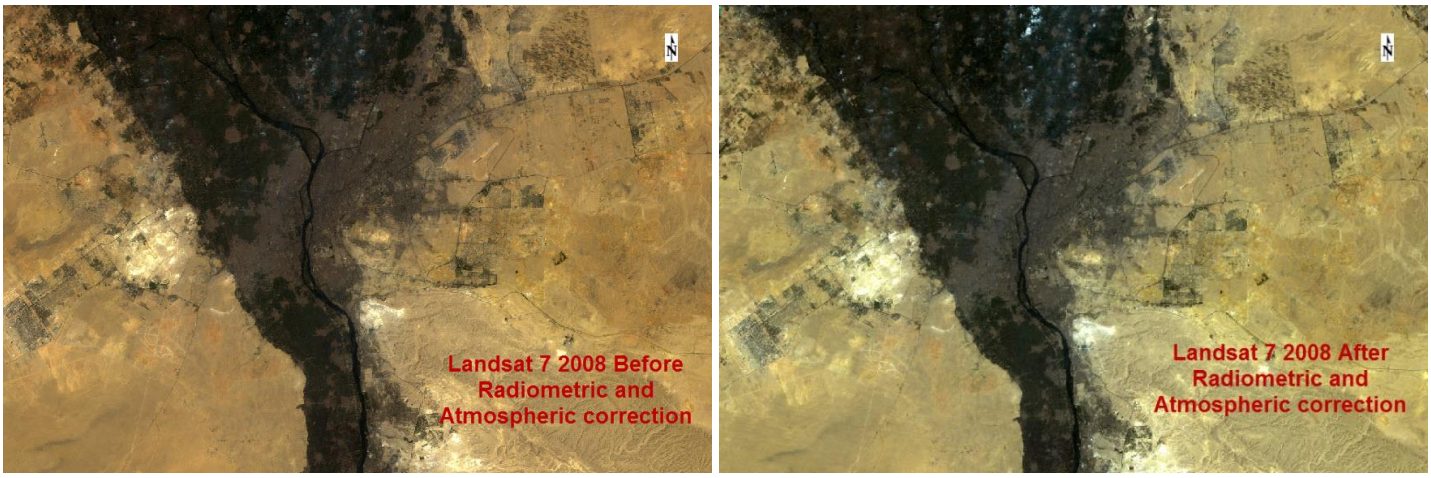

Figure 18: Landsat ETM+ 2008 image before and after radiometric and atmospheric correction.

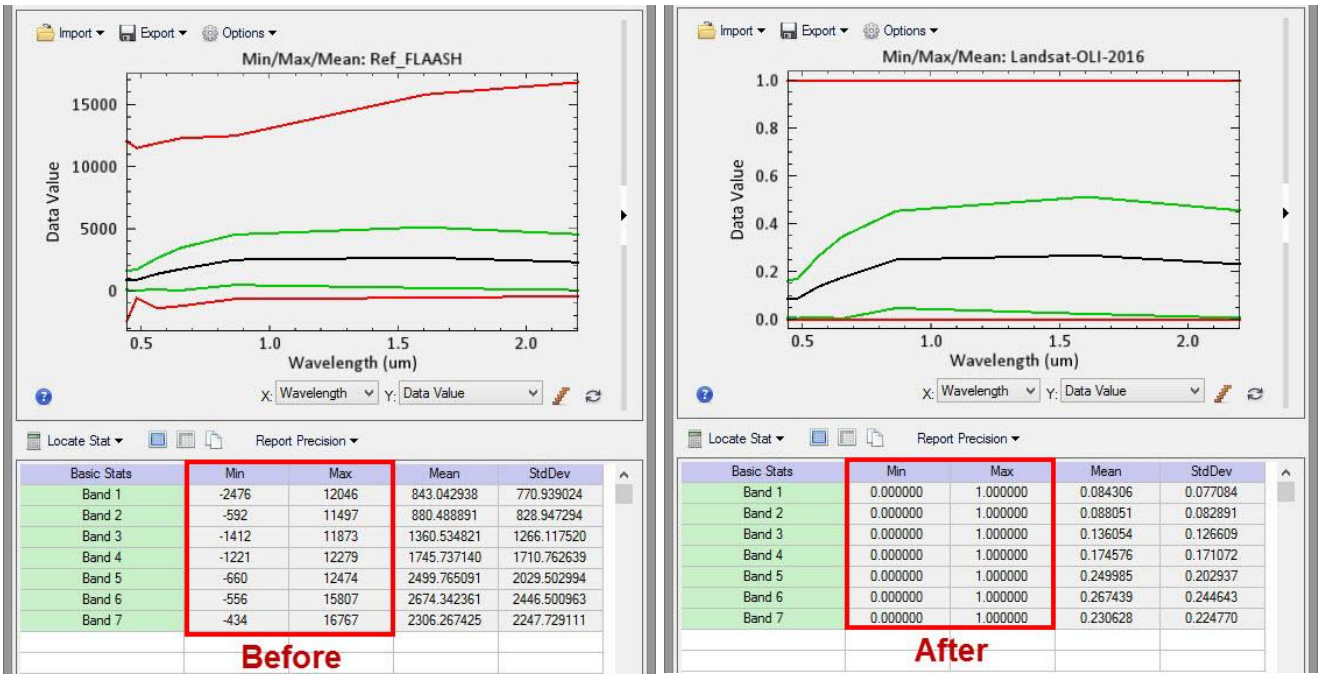

Figure 19: Landsat 8 2016 before and after execution Post FLAASH Band Math Equation.

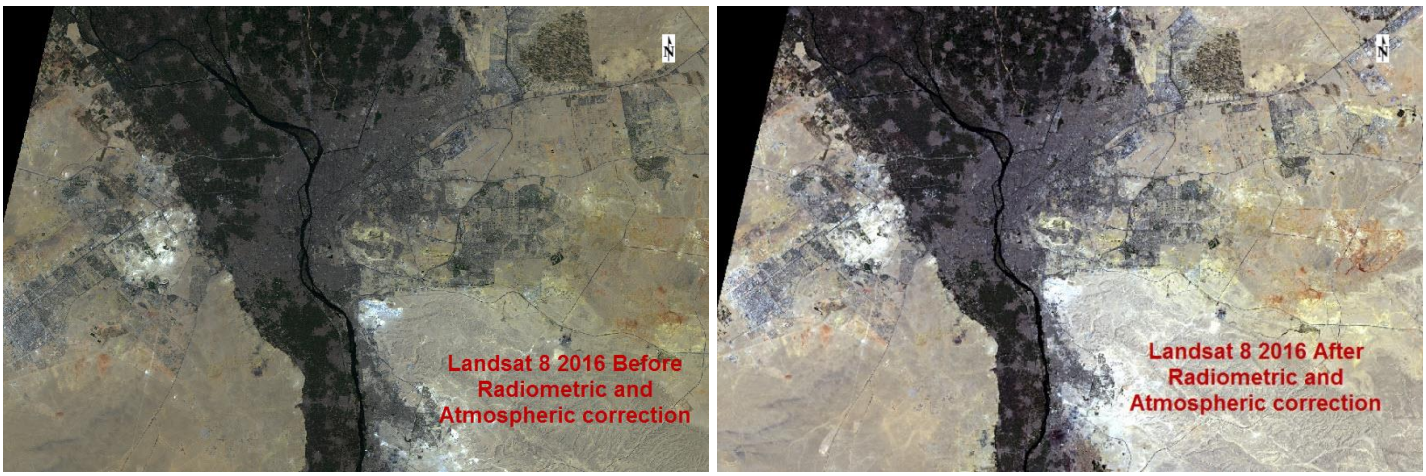

Figure 20: Landsat 8 2016 image before and after radiometric and atmospheric correction.

2.5.3 Image Enhancement

Enhancements are used to make it easier for visual interpretation and understanding of imagery. The advantage of digital imagery is that it allows us to manipulate the digital pixel values in an image. Although radiometric corrections for illumination, atmospheric influences, and sensor characteristics may be done prior to distribution of data to the user, the image may still not be optimized for visual interpretation. Remote sensing devices, particularly those operated from satellite platforms, must be designed to cope with levels of target/background energy which are typical of all conditions likely to be encountered in routine use. With large variations in spectral response from a diverse range of targets (e.g. Built-up areas, Deserts, Green Lands, Water Bodies, etc.) no generic radiometric correction could optimally account for and display the optimum brightness range and contrast for all targets. Thus, for each application and each image, a custom adjustment of the range and distribution of brightness values is usually necessary.

2.5.4 Image masking

The masking process is useful to clip images to a certain study area, and exclude the area out of study from the classification and change detection. I have boundary of Greater Cairo Region I got it from CAPMAS, and applied masking process for five satellite images Landsat 5 TM 1984, 1992, 2000 and Landsat 7 ETM+ 2008 and Landsat 8 OLI 2016 by using Envi software.

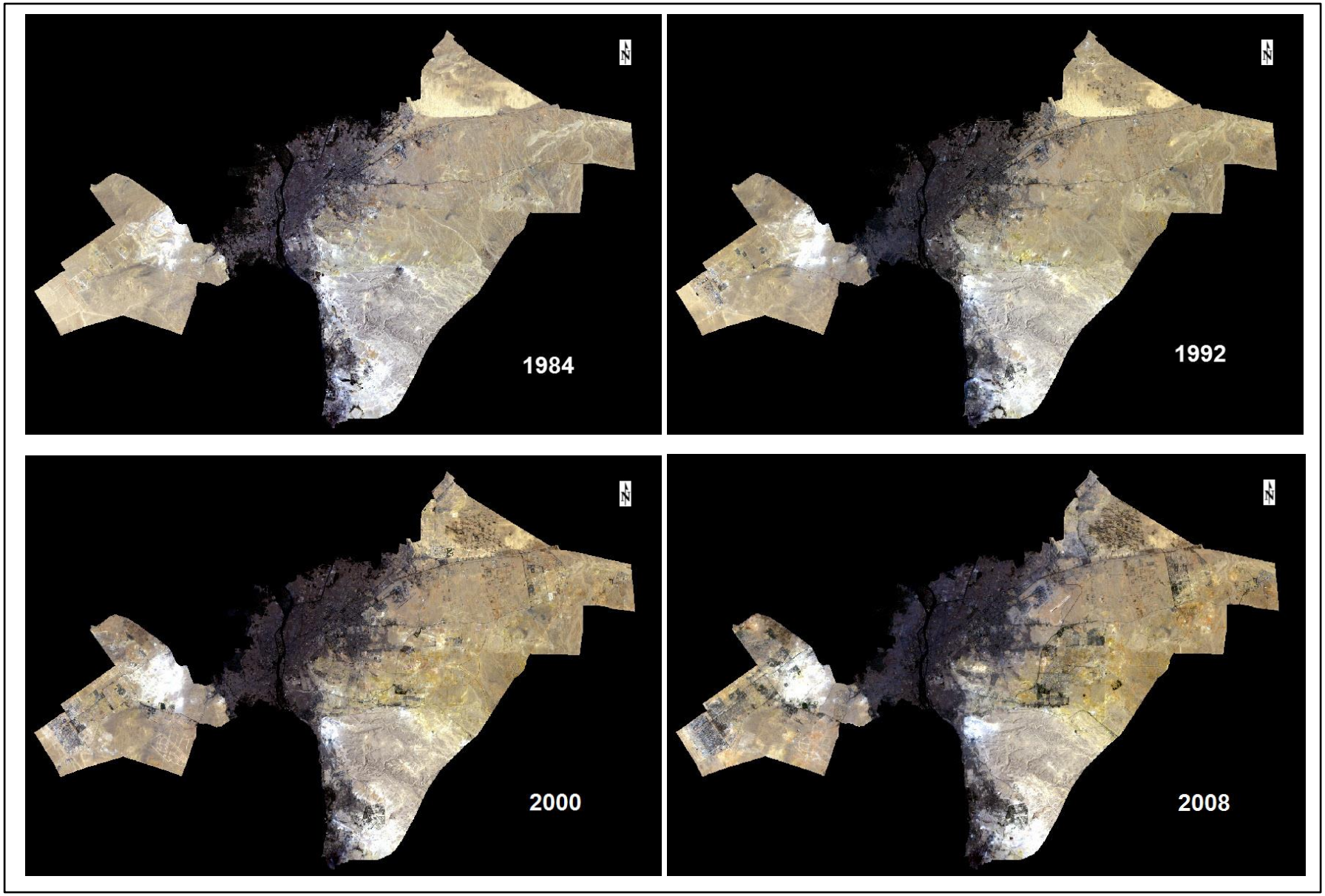

Figure 21: Landsat 5 TM and Landsat 7 ETM+ for Greater Cairo Region after masking.

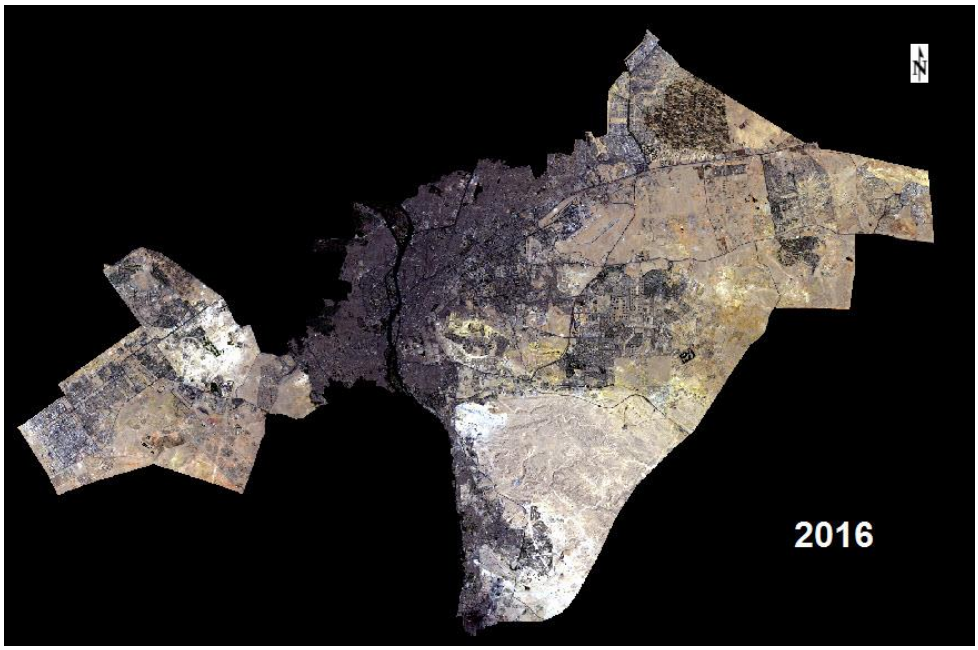

Figure 22: Landsat 8 (OLI) 2016 for Greater Cairo Region after masking.

2.6 Image Processing

There are many processing and analysis techniques have been developed to interpret remote sensing images to extract land us/land cover information as possible and detecting and monitoring urban growth. The choice of specific technique or algorithm depends on the aim of the study or the project. Image classification process is one of image processing and analysis. Image classification use the quantitative spectral information that contained in satellite image. Image analysis and classification can be performed using multispectral or hyperspectral imagery. There are two basic approaches commonly used for image classification; supervised and unsupervised classification. In this study supervised classification approach were used in image classification of Landsat datasets.

2.6.1 Image Classification

The intent of the classification process is to categorize all pixels in a digital image into one of several land cover classes, or "themes". This categorized data may then be used to produce thematic maps of the land cover present in an image. Normally, multispectral data are used to perform the classification and, indeed, the spectral pattern present within the data for each pixel is used as the numerical basis for categorization (Lillesand and Kiefer, 1994). The objective of image classification is to identify and portray, as a unique gray level (or color), the features occurring in an image in terms of the object or type of land cover these features actually represent on the ground.

A human analyst attempting to classify features in an image uses the elements of visual interpretation to identify homogeneous groups of pixels which represent various features or land cover classes of interest. Digital image classification uses the spectral information represented by the digital numbers in one or more spectral bands, and attempts to classify each individual pixel based on this spectral information. This type of classification is termed spectral pattern recognition. In either case, the objective is to assign all pixels in the image to particular classes or themes (e.g. water, coniferous forest, deciduous forest, corn, wheat, etc.). The resulting classified image is comprised of a mosaic of pixels, each of which belong to a particular theme, and is essentially a thematic "map" of the original image.

2.6.2 Supervised Classification

Supervised classification is a technique which usually used for quantitative analysis of remote sensing image data. Supervised classification technique has developed for satellite image processing where it is applied to the classification of spectral response of features on earth surface which recorded in the satellite image spectral layers. Supervised classification primarily depends on the prior knowledge of land cover types of the area under study through satellite image. Supervised technique process is a process of using

samples or signature of identified feature or objects (which represented as a group of pixels that assigned with numeric values represent the spectral reflectance of this object) to classify and group the objects or features with same pixel signature or reflectance values. Samples of known identity are pixels located within training areas (Campbell, 2002). So, the selection of the samples of object(s) of the study area considered the key of supervised classification technique. The application software of image processing is using the identified samples area to calculate the statistical characteristics for each information class, then image classified into classes by examining the reflectance information of each pixel and group them according to the information of each class that resemble the most. There are many possible elements of error correlated with supervised classification (Campbell, 2002). One of these elements is that defined classes may not match real classes that exist in the image data, and as consequence may not well distinct. Also, the selected classes' samples may not be delegated of conditions over the image of study area, so the user may face a problem in coupling or matching some classes as he defined on image.

Supervised classification coupled with four different classification algorithms, Maximum likelihood, Minimum distance, Mahalanobis Distance and Spectral Angle Mapper. Maximum likelihood is the most common and accurate algorithm that used for image classification, and was used in this for performing supervised classification of the two images of the study area. In order to perform the algorithm five classes have been defined from image namely, water bodies, cultivated land, Soil, Bushes and grass, Coastal sands and dunes.

The analyst identifies in the imagery homogeneous representative samples of the different surface cover types (information classes) of interest. These samples are referred to as training areas. The selection of appropriate training areas is based on the analyst's familiarity with the geographical area and their knowledge of the actual surface cover types

present in the image. Thus, the analyst is "supervising" the categorization of a set of specific classes. The numerical information in all spectral bands for the pixels comprising these areas are used to "train" the computer to recognize spectrally similar areas for each class. The computer uses a special program or algorithm (of which there are several variations), to determine the numerical "signatures" for each training class. Once the computer has determined the signatures for each class, each pixel in the image is compared to these signatures and labeled as the class it most closely "resembles" digitally. Thus, in a supervised classification we are first identifying the information classes which are then used to determine the spectral classes which represent them.

Class ID	Class Name	Class Description	Number of trained samples – Landsat Images				
			1984	1992	2000	2008	2016
1	Built-up areas	Residential, industrial and other uses.	46	49	44	52	90
2	Desert	Desert, Rocky outcrop and bare soils.	45	40	42	45	30
3	Green Lands	Agriculture, crop land and gardens.	39	34	24	23	20
4	Water Bodies	River and Artificial lakes.	12	11	9	9	7

Table7: Image Classification Schema and training samples.

Identifying land cover features and training sample was difficult and time consuming process, but band combination of Landsat imagery make it better to identify samples features. The band combination were used to identify the six classes are shown in Table 5.

Land Cover Type	Band Combination
Built Up Area	Band 1, 4, 7 - Band 1 , 4, 5 - Band 1 , 2, 3
Desert	Band 1, 4, 7 - Band 2, 4, 5
Green Lands	Band 1, 4, 7 - Band 1 , 4, 5
Water Bodies	Band 1, 4 & 7 - Band 1, 2 ,3 - Band 1 , 4, 5

Table8: Band combination to identify land cover type.

The supervised classification was applied using ENVI for the classification process. At least 100 training sites (signatures) were chosen to represent land cover classes, such as Green Lands, Built-up areas, Water Bodies (the Nile) and Desert. The maximum likelihood classifier (MLC) was the algorithm applied for the clustering process. The six spectral bands in the TM and ETM image and the nine bands in the Landsat 8 image (the thermal band was excluded) were incorporated in the classification process.

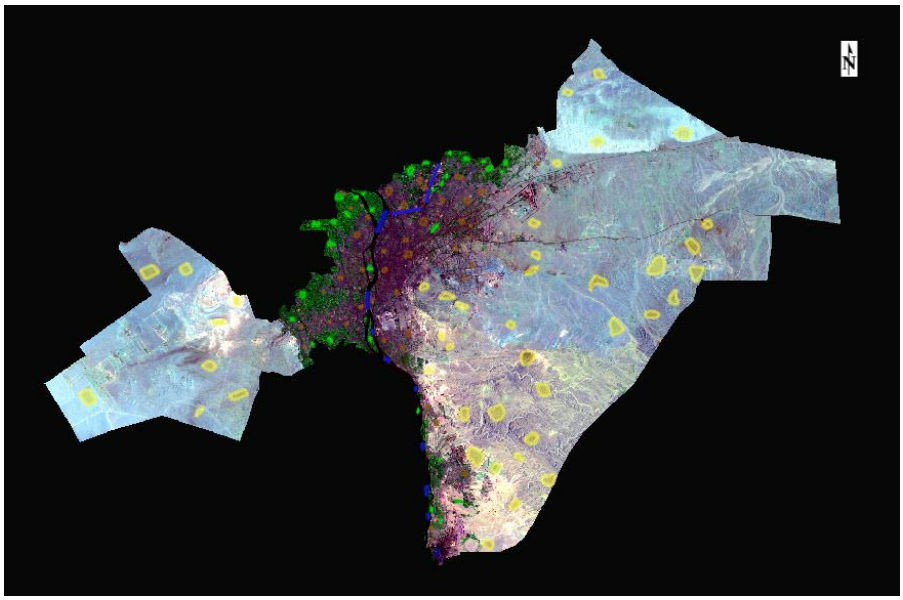

Figure 23: Showing the location of the training areas on Landsat TM 1984.

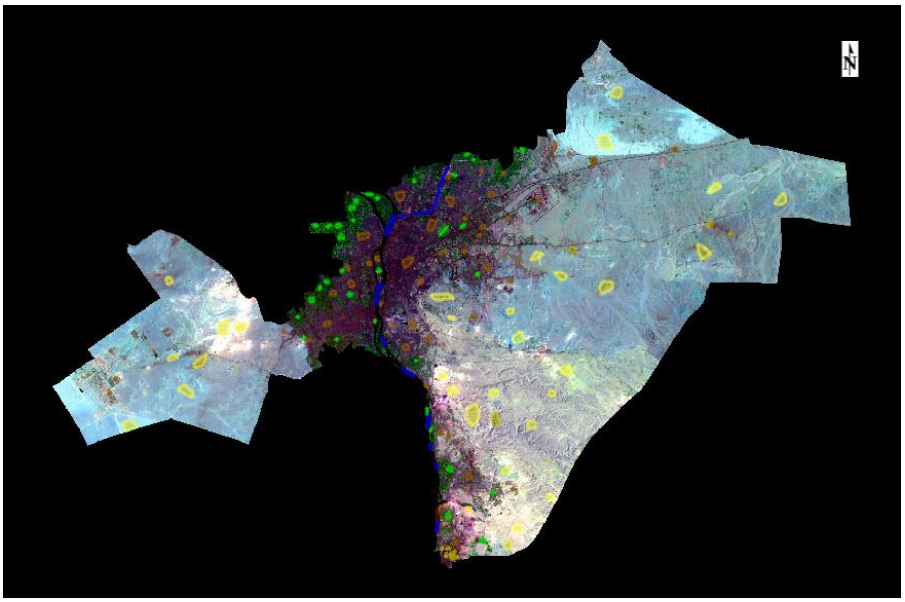

Figure 24: Showing the location of the training areas on Landsat TM 1992.

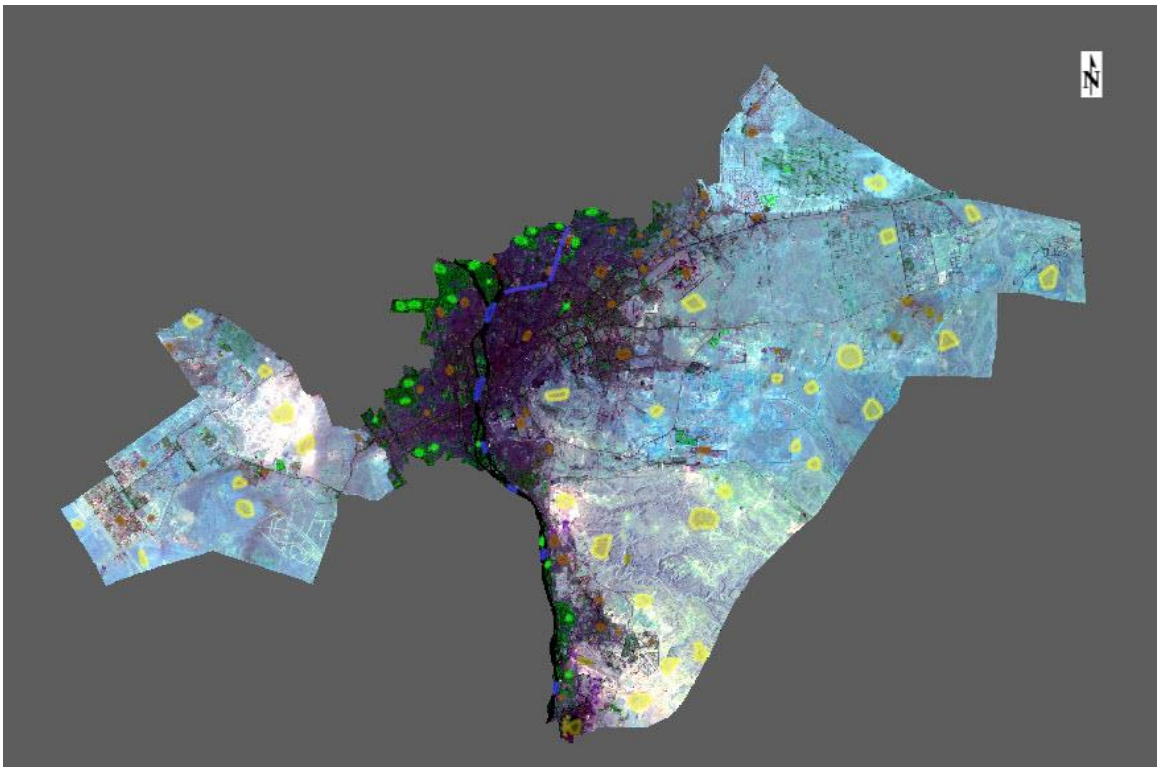

Figure 25: Showing the location of the training areas on Landsat TM 2000.

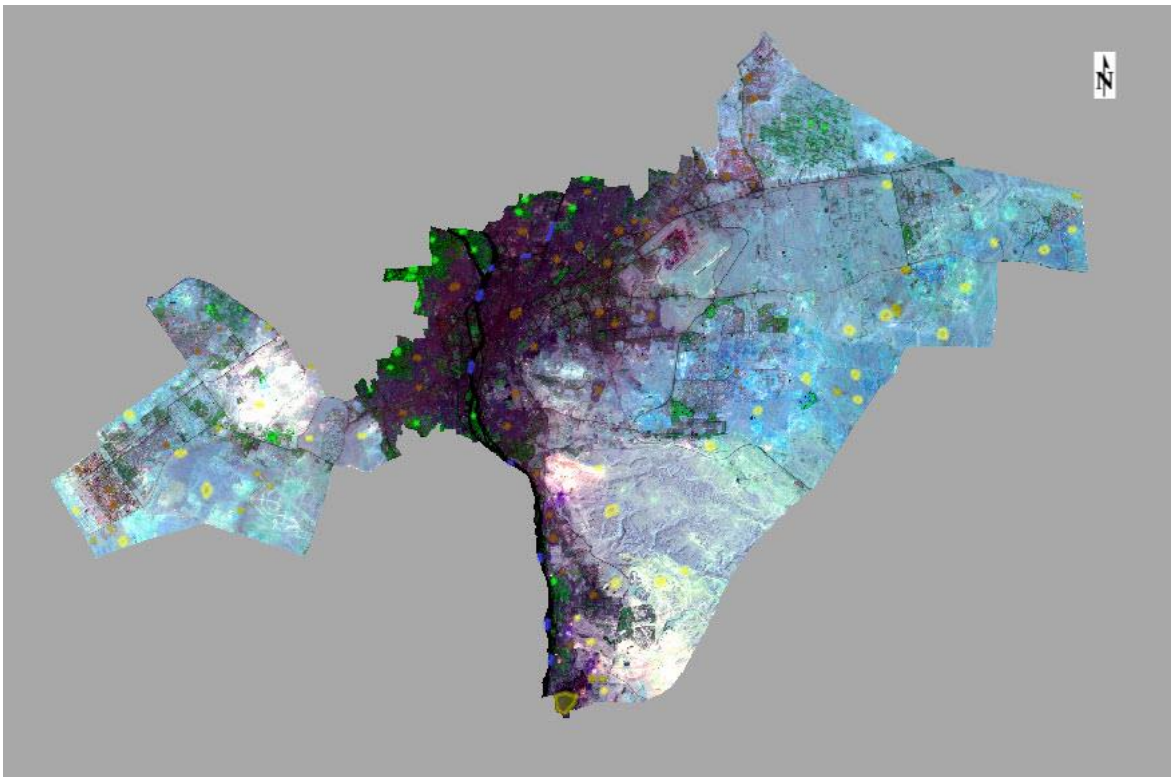

Figure 26: Showing the location of the training areas on Landsat ETM 2008.

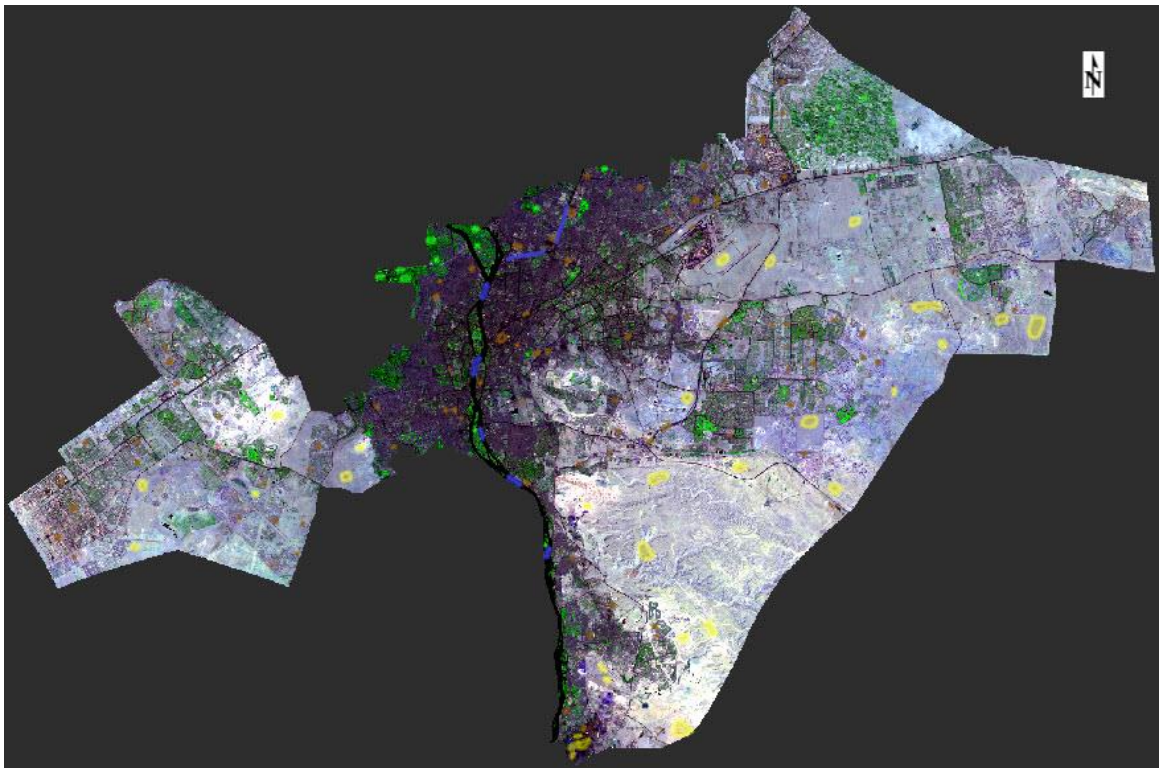

Figure 27: Showing the location of the training areas on Landsat OLI 2016.

After classification, a major 3 × 3 filter was applied to remove anomalous pixels from the matrix. All pixels pertaining to each class were recoded together and the gross area of this class was counted. With the help of the final version of the Google Earth, the Landsat 5, 7 and 8 classified images of 1984, 1992, 2000, 2008 and 2016 was visually compared with the true color and finer spatial resolution image of Greater Cairo Region as appeared in the Google Earth. In addition, 100 random points were selected at each classified TM, ETM and Landsat 8 image on a stratified random approach and compared digitally with the corresponding pixels of the original TM, ETM and Landsat 8 images as a reference data. If reference pixels are selected randomly, the possibility of bias is lowered and classification accuracy rises. The producer and user accuracies were obtained for each land cover map.

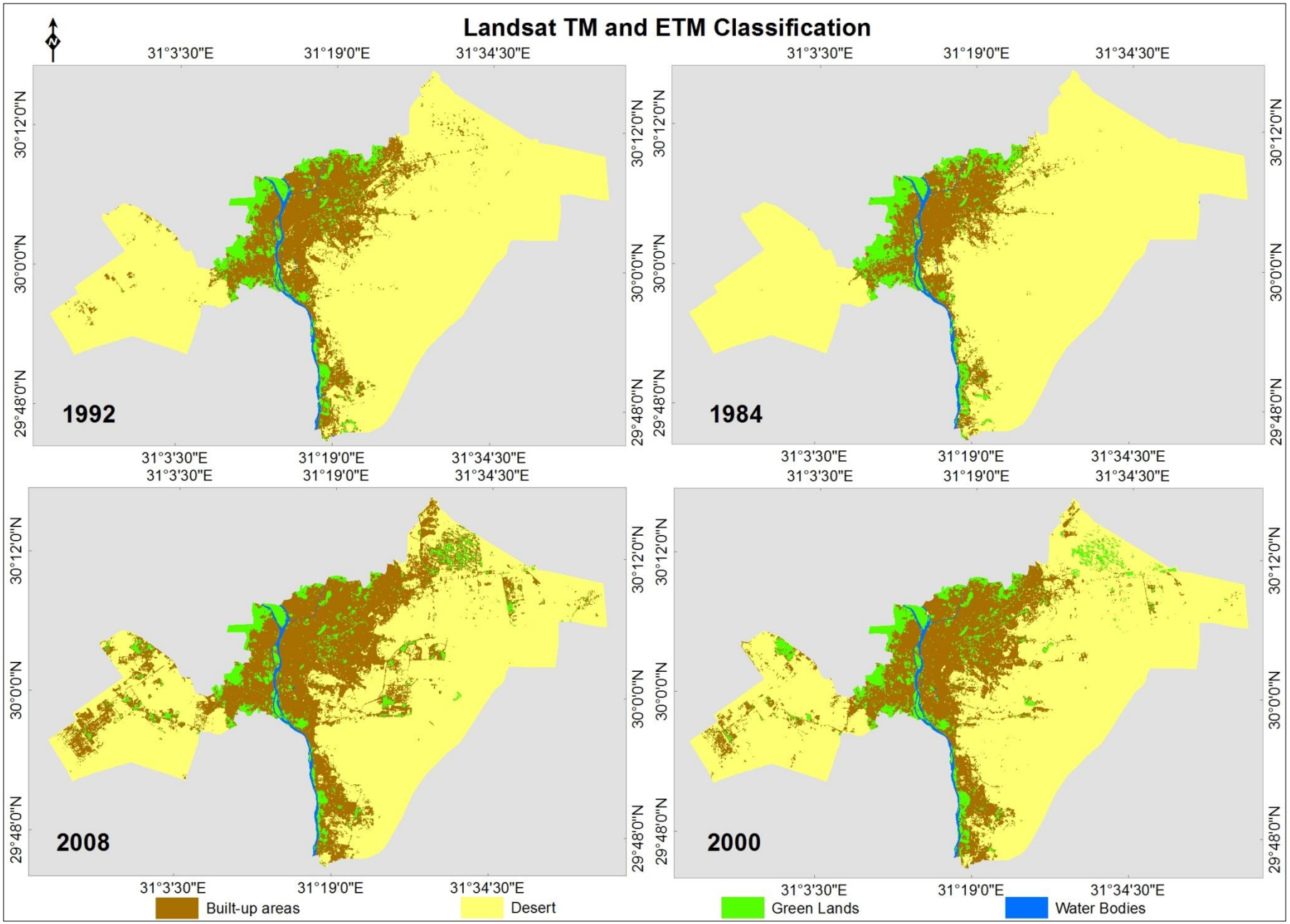

Map 8: Landsat TM and ETM+ Classification.

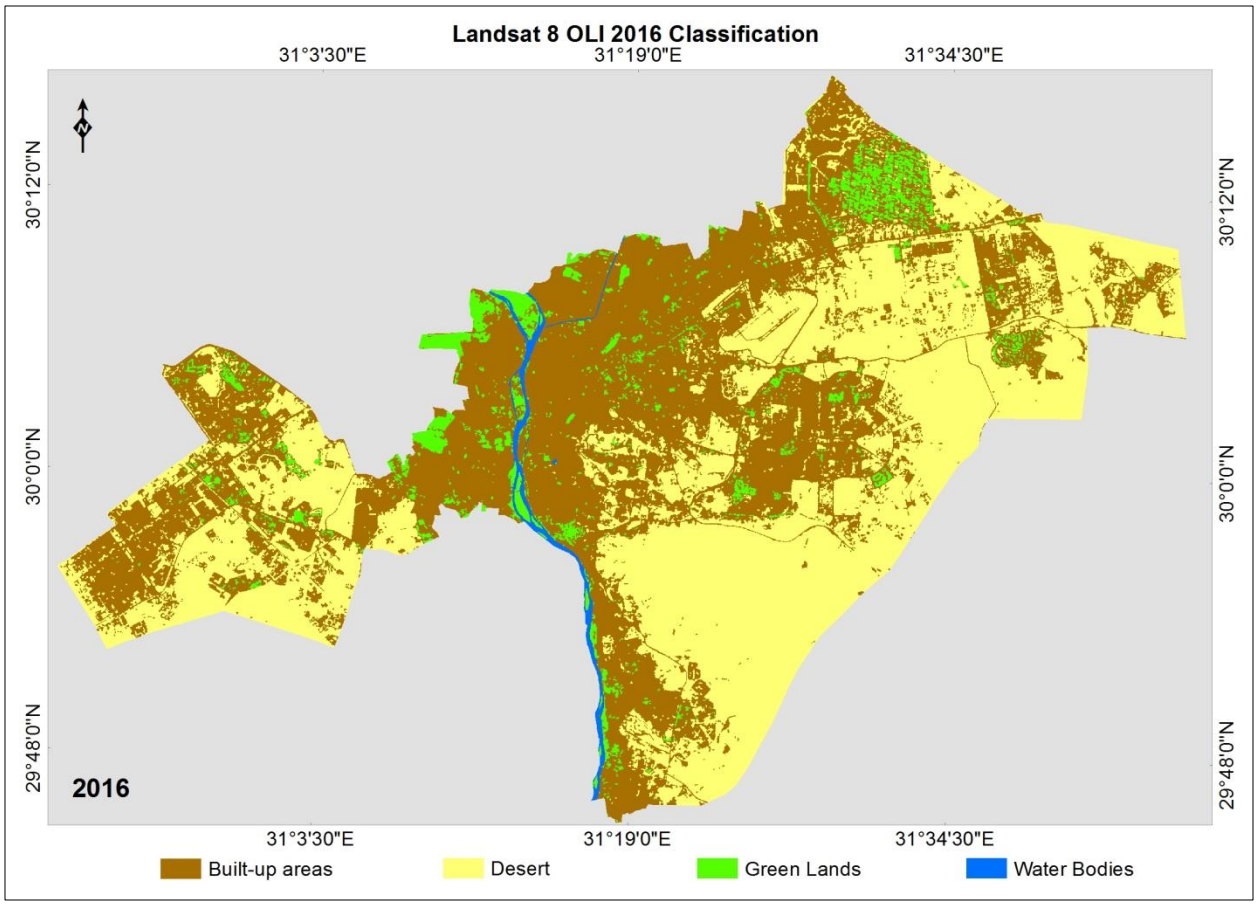

Map 9: Landsat 8 (OLI) 2016 Classification.

2.6.3 Accuracy Assessment

In the context of information extraction by image analysis, accuracy "measures the agreement between a standard assumed to be correct and a classified image of unknown quality." Precision defines the level of detail found within the classification. It is possible to increase the accuracy of a classification by decreasing the amount of detail or by generalizing to broad classes rather than very specific ones. For example, a scheme which generally categorizes trees vs. crops presents less opportunity for classification error than one that distinguishes many types of trees and many types of crops. In this case, lower precision provides the potential for higher accuracy. However, the user of the map that offers only general classes cannot make precise statements about any given point on the map.

Classification error occurs when a pixel (or feature) belonging to one category is assigned to another category. Errors of omission occur when a feature is left out of the category being evaluated; errors of commission occur when a feature is incorrectly included in the category being evaluated. An error of omission in one category will be counted as an error in commission in another category.

Accuracy assessment is performed by comparing the map created by remote sensing analysis to a reference map based on a different information source. One might ask why the remote sensing analysis is needed if the reference map to compare it to already exists. One of the primary purposes of accuracy assessment and error analysis in this case is to permit quantitative comparisons of different interpretations. Classifications done from images acquired at different times, classified by different procedures, or produced by different individuals can be evaluated using a pixel-by-pixel, point-by-point comparison. The results must be considered in the context of the application to determine which is the “most correct” or “most useful” for a particular purpose.

In order to be compared, both the map to be evaluated and the reference map must be accurately registered geometrically to each other. They must also use the same classification scheme, and they should have been classified at the same level of detail. One simple method of comparison is to calculate the total area assigned to each category in both maps and to compare the overall figures. This type of assessment is called non-site-specific-accuracy. On the other hand, site-specific accuracy is based on a comparison of the two maps at specific locations (i.e., individual pixels in two digital images). In this type of comparison, it is obvious that the degree to which the pixels in one image spatially align with the pixels in the second image contributes to the accuracy assessment result. Errors in classification should be distinguished from errors in registration or positioning of boundaries. Another useful form of site-specific accuracy assessment is to compare field

data or training data at a number of locations within the image, similar to the way spatial accuracy assessment using ground checkpoints is performed for digital orthophotos and terrain models.

Accuracy of image classification is most often reported as a percentage correct. The consumer's accuracy (CA) is computed using the number of correctly classified pixels to the total number of pixels assigned to a particular category. It takes errors of commission into account by telling the consumer that, for all areas identified as category X, a certain percentage are actually correct. The producer's accuracy (PA) informs the image analyst of the number of pixels correctly classified in a particular category as a percentage of the total number of pixels actually belonging to that category in the image. Producer's accuracy measures errors of omission.

The accuracy of Post-classification comparison method depends on the accuracy of the classified satellite images being used. The overall accuracy of the 1984 classified image is 90%, and the overall accuracy of the 1992 classified image is 92%, and the overall accuracy of the 2000 classified image is 94%, and the overall accuracy of the 2008 classified image is 94%, and the overall accuracy of the 2016 classified image is 96%. According to this, it is expected that the accuracy of the change detection product in this study is high as classification results.

Error Matrix					
Classified Data	Built-up areas	Desert	Water Bodies	Green Lands	Row Total
Built-up areas	20	3	0	2	25
Desert	3	22	0	0	25
Water Bodies	0	0	25	0	25
Green Lands	2	0	0	23	25
Column Total	25	25	25	25	100

Table9: Error Matrix for the classified satellite image 1984.

ACCURACY TOTALS					
Class Name	Reference Totals	Classified Totals	Number Correct	Producers Accuracy	Users Accuracy
Built-up	25	25	20	100.00%	80.00%
Desert	25	25	22	100.00%	88.00%
Water Bodies	25	25	25	100.00%	100.00%
Green Lands	25	25	23	100.00%	92.00%
Totals	100	100	90		
	Overall Classification Accuracy = 90.00%				

Table10: Accuracy Totals for the classified satellite image 1984.

Error Matrix					
Classified Data	Built-up areas	Desert	Water Bodies	Green Lands	Row Total
Built-up areas	21	2	0	2	25
Desert	2	23	0	0	25
Water Bodies	0	0	25	0	25
Green Lands	2	0	0	23	25
Column Total	25	25	25	25	100

Table11: Error Matrix for the classified satellite image 1992.

ACCURACY TOTALS					
Class Name	Reference Totals	Classified Totals	Number Correct	Producers Accuracy	Users Accuracy
Built-up	25	25	21	100.00%	84.00%
Desert	25	25	23	100.00%	92.00%
Water Bodies	25	25	25	100.00%	100.00%
Green Lands	25	25	23	100.00%	92.00%
Totals	100	100	92		
	Overall Classification Accuracy = 92.00%				

Table12: Accuracy Totals for the classified satellite image 1992.

Error Matrix					
Classified Data	Built-up areas	Desert	Water Bodies	Green Lands	Row Total
Built-up areas	22	2	0	1	25
Desert	2	23	0	0	25
Water Bodies	0	0	25	0	25
Green Lands	1	0	0	24	25
Column Total	25	25	25	25	100

Table13: Error Matrix for the classified satellite image 2000.

ACCURACY TOTALS					
Class Name	Reference Totals	Classified Totals	Number Correct	Producers Accuracy	Users Accuracy
Built-up	25	25	22	100.00%	88.00%
Desert	25	25	23	100.00%	92.00%
Water Bodies	25	25	25	100.00%	100.00%
Green Lands	25	25	24	100.00%	96.00%
Totals	100	100	94		
	Overall Classification Accuracy = 94.00%				

Table14: Accuracy Totals for the classified satellite image 2000.

Error Matrix					
Classified Data	Built-up areas	Desert	Water Bodies	Green Lands	Row Total
Built-up areas	22	2	0	1	25
Desert	2	23	0	0	25
Water Bodies	0	0	25	0	25
Green Lands	1	0	0	24	25
Column Total	25	25	25	25	100

Table15: Error Matrix for the classified satellite image 2008.

ACCURACY TOTALS					
Class Name	Reference Totals	Classified Totals	Number Correct	Producers Accuracy	Users Accuracy
Built-up	25	25	22	100.00%	88.00%
Desert	25	25	23	100.00%	92.00%
Water Bodies	25	25	25	100.00%	100.00%
Green Lands	25	25	24	100.00%	96.00%
Totals	100	100	94		
	Overall Classification Accuracy = 94.00%				

Table16: Accuracy Totals for the classified satellite image 2008.

Error Matrix					
Classified Data	Built-up areas	Desert	Water Bodies	Green Lands	Row Total
Built-up areas	23	1	0	1	25
Desert	1	24	0	0	25
Water Bodies	0	0	25	0	25
Green Lands	1	0	0	24	25
Column Total	25	25	25	25	100

Table17: Error Matrix for the classified satellite image 2016.

ACCURACY TOTALS					
Class Name	Reference Totals	Classified Totals	Number Correct	Producers Accuracy	Users Accuracy
Built-up	25	25	23	100.00%	92.00%
Desert	25	25	24	100.00%	96.00%
Water Bodies	25	25	25	100.00%	100.00%
Green Lands	25	25	24	100.00%	96.00%
Totals	100	100	96		
	Overall Classification Accuracy = 96.00%				

Table18: Accuracy Totals for the classified satellite image 2016.

2.7 Change Detection

2.7.1 Introduction

Timely and accurate change detection of Earth's surface features is extremely important for understanding relationships and interactions between human and natural phenomena in order to promote better decision making. And there are various methods of addressing change detection using satellite images (Lu et al., 2004). Satellite images offer a repetitive coverage of the Earth. This is a significant advantage for environmental monitoring (Gibson and Power 2000). Some satellites systems have been operational for several decades, thus they provide a record of change. Change detection is the process of identifying difference in the state of an object or phenomenon by observing it at different times (Deer 1995). Change detection techniques provide systematic methods to record and analysis the change. The principal basis in using remotely sensed data for change detection projects is that changes in land cover result in changes in radiance values (Mas 1999). These changes are often caused by human activities. Change detection has a number of applications within the environmental sphere. Urban growth is one of the most dynamic phenomena in the modern world. The accelerated growth and changes in the urban landscape has a great impact on the environment. The growth and direction of urban development should be monitored.

2.7.2 Change Detection Method Selection

The selection of an appropriate change detection algorithm is very important. And will define the type of classification to be applied. Jensen (1996) stated that at least seven change detection algorithms are commonly used from the following,

(1) Change detection using write function memory insertion.

(2) Multi-date composite image change detection.

(3) Image Algebra change detection (Band differencing or band ratioing).

(4) Multi-date change detection using a binary mask applied to date 2.

(5) Multi-date change detection using ancillary data source as date 1.

(6) Manual, on screen digitising of change.

(7) Post-classification comparison change detection.

These will be discussed in brief using (Jensen 1996) to help the selection of the appropriate method for this study.

2.7.2.1 Change detection using write function memory insertion

In this method, the individual bands of the images can be inserted into specific write function memory banks (red, green, and or blue) to identify visually the changes. The main advantage of this method is the possibility of investigating two or even three images of different dates at one time. The method unfortunately does not give any information about the size of change from one land cover class to another.

2.7.2.2 Image Algebra change detection (Band differencing or band ratioing)

The quantity of change between two images can be identified by image (or band) differencing or band ratioing. Image differencing involves subtracting the rectified imagery of one date from another. The results of subtracting will be positive and negative values in areas of radiance change and zero values in areas of no change. Band ratioing applies the

same concept except the results will be a ratio rather than an absolute value where the area of "no change" will have a ratio value of 1. The analysts have the choice to decide where to place the threshold between change and no change values so it is important to have previous experience with the study area. It is also recommended to perform illumination and atmospheric correction before applying this method (Lillesand and Kieffer 1994). Although this method provides quantitative information about the change, it does not give any information on the nature of change.

2.7.2.3 Multi-date change detection using a binary mask applied to date 2

In this method, one of the images should be rectified and classified, then, a certain band from both images will be placed in a new dataset. This new dataset will be analyzed using some image algebra functions producing a new change image file. The change image is then recoded into a binary mask file to contain only the area (s) of change between the two dates. The change mask is then overlaid onto date 2. Finally, change pixels only will be classified in date 2 imagery. To obtain information about the nature of change, the post-classification comparison method can be applied.

2.7.2.4 Multi-date change detection using ancillary data source as date 1

Some analysts suggested another source of data rather than remotely sensed data as a base map for change detection projects. Jensen (1996) recommended using digital maps as date 1 in the absence of satellite images and this data should be recoded to be compatible with the classification scheme being used with the image of date 2. Then the date 2 image should be classified and compared on a pixel-by-pixel basis with date 1 information using post classification comparison method. This method has many advantages:

(1) The detailed information about the nature of change can be obtained.

(2) Only a single classification of date 2 image is required.

(3) Old maps can be updated through this method.

On the other hand, this method needs the ancillary data to be digitized, recoded, and converted to raster format to be compatible with remotely sensed data. This means every error from manual digitising and subsequent processes can lead to unacceptable results of change detection analysis.

2.7.2.5 Image regression

In this method, pixel values from one time are assumed to be a (normally) linear function of pixel values at some other time. The function that relates the pixel values can be determined using a least squares regression. The changed pixels will have values that differ significantly from that predicted by the determined function, threshold is applied to detect areas of change (Deer 1995). This method has been used in many studies such as (Singh 1986).

2.7.2.6 Manual, on screen digitising of change

Aerial photographs of high resolution from different dates can be scanned into digital image files, then, they can be displayed on a CRT screen at the same time. The displayed images can be analyzed using photo interpretation techniques to identify change. This method can be applied also with satellite images of high resolution.

2.7.2.7 Post-classification comparison change detection

This method is based on comparing two rectified and classified images pixel by pixel. That means every error in the classification of the images will reflect on the accuracy of the final change map. Hence, it is essential to produce high accuracy classified images for using with this method. This method provides detailed information about the nature and size of change that is valuable for accepted change detection results. In many studies, the post-

classification comparison method has provided the highest accuracy of change detection compared to the other methods (Mas 1999). Post classification comparison method has been used to detect changes in many studies such as detecting changes from nonurban to urban categories (Riordan 1980), and detecting changes in general land use (Gordon 1980).

2.8 Change detection using Post-classification Comparison.

There are various methods of addressing change detection using satellite images (Lu et al., 2004). The post-classification change detection approach is one of the most common, accurate and quantitative techniques (Jensen 1995). The purpose of conducting this method of change detection was not only to estimate the difference of urban land area between 1984 and 2016, but also to highlight areas added to urban landscape from agricultural land and from the adjacent desert separately. In other words, it was important to distinguish pixels which were recorded as agricultural land in 1984 and were added to urban land in 2016 from those which were recorded as desert area in 1984 and were added to urban land in 2016. This process was carried out using the Modeler in ERDAS Imagine. First, each Landsat TM and Landsat 8 (OLI) classified image was recoded to have unique ordinal classes. Then the two images were multiplied together to yield a composite image containing the number of pixels converted to urban area either from agricultural land or from desert areas. A “from -to” change matrix was then prepared to extract the separated pixels.

Two rectified, classified images with high accuracy (94% as an average for both images) were compared pixel by pixel in ENVI to perform change detection using post-classification comparison method. The method involves subtracting one image from another image of the same area acquired at different dates. If the result for some classes is zero, this means there is no change. If there is any value more/less than zero, this implies change.

Chapter-3

3. Data Analysis and Results

Urbanization is a major cause of land use changes and land conversions. It makes unpredictable and long lasting changes on the landscape. An important aspect of change detection is to determine what is actually changing to what i.e. which land use class is changing to the other. Analyzing the spatial and temporal changes in land use and land cover is one of the effective ways to understand the current environmental status of an area and ongoing changes (Arvind et al., 2006, Yuan et al., 2005; Zubair, 2006).

The objective of this study forms the basis of all the analysis carried out in this chapter. The results are presented inform of maps, charts and statistical tables. They include the static, change and projected land use land cover of each class.

3.1 Detecting urban growth in Greater Cairo Region

The dominant causative factors of the different types of land degradation were identified. The main type of human induced land degradation in the investigated areas is urbanization. These degradation variables were assessed showing the changes that occurred during the period of 1984, 1992, 2000, 2008 and 2016 for human induced land degradation using multi-dates satellite images.

The total investigated area was determined by (1991 Km^2). In the year 1984, urbanized area covered 244.4 Km^2. In the year 1992, extra urbanized area covered 344.3 Km^2. In the year 2000, extra urbanized area covered 452.4 Km^2. In the year 2008, extra urbanized area covered 593 Km^2. In the year 2016, extra urbanized area covered 921.2 Km^2.

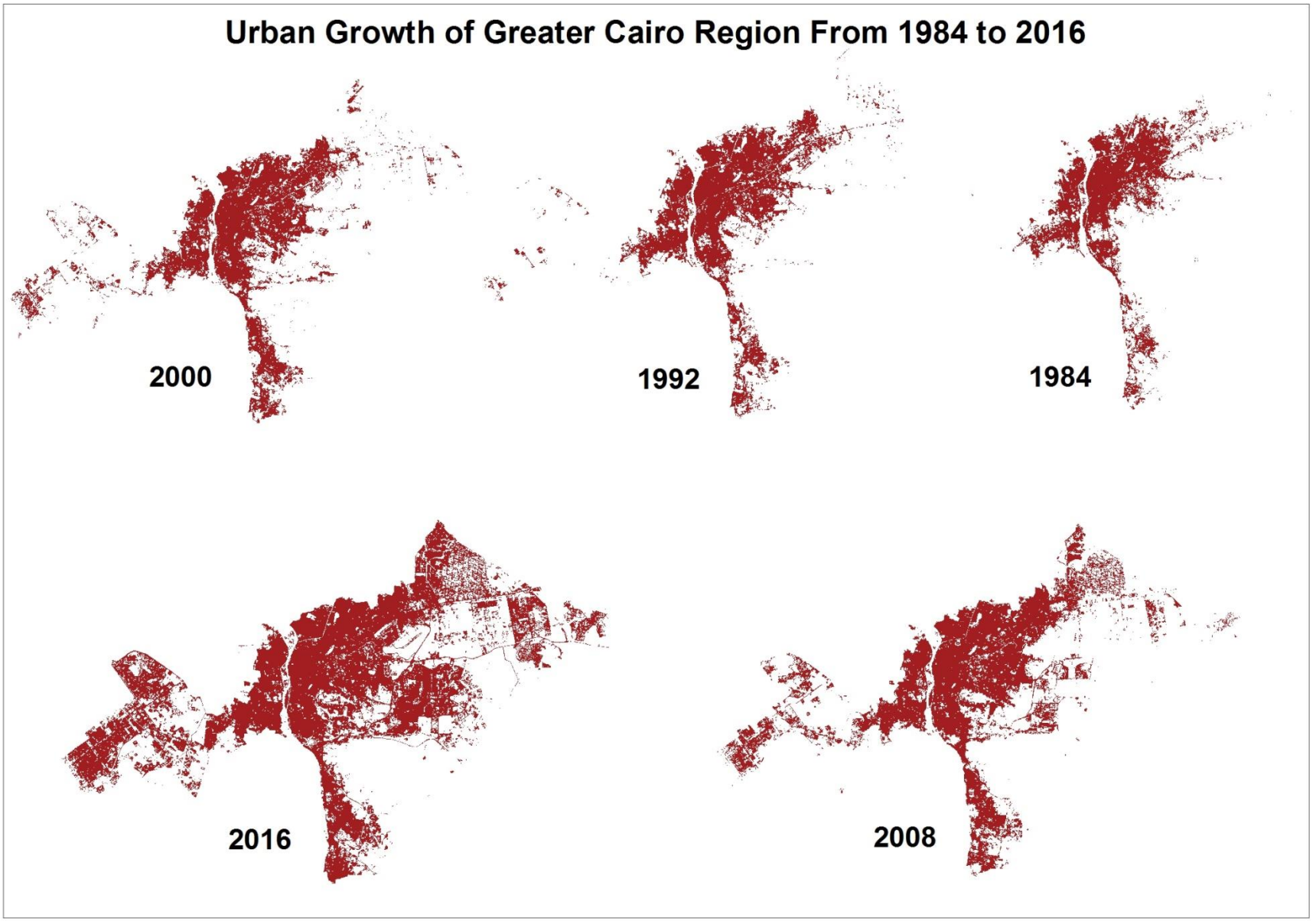

Figure 28: Showing Urban Growth in 1984, 1992, 2000, 2008 and 2016.

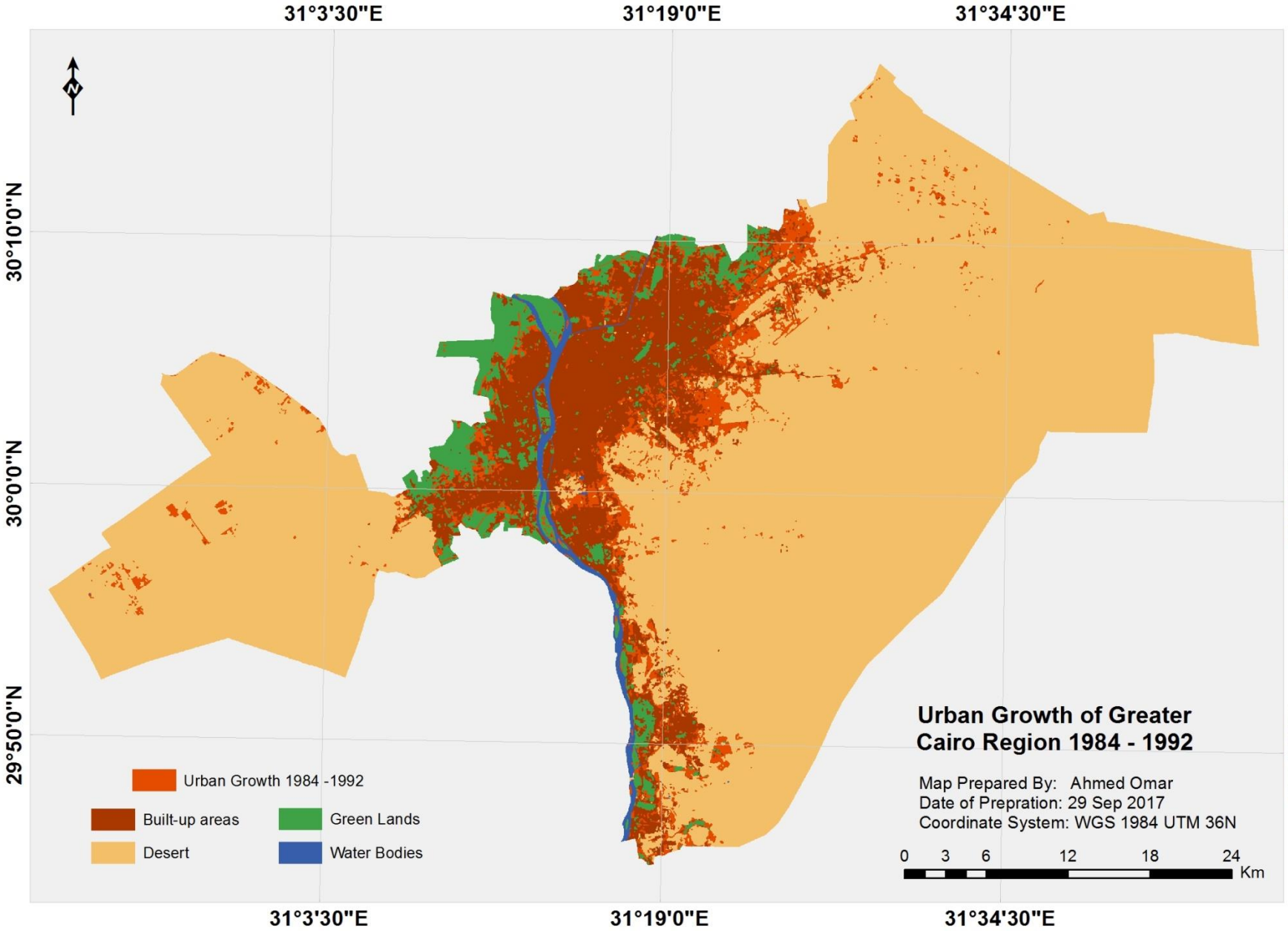

Map 10: Showing Urban Growth of Greater Cairo Region 1984 - 1992.

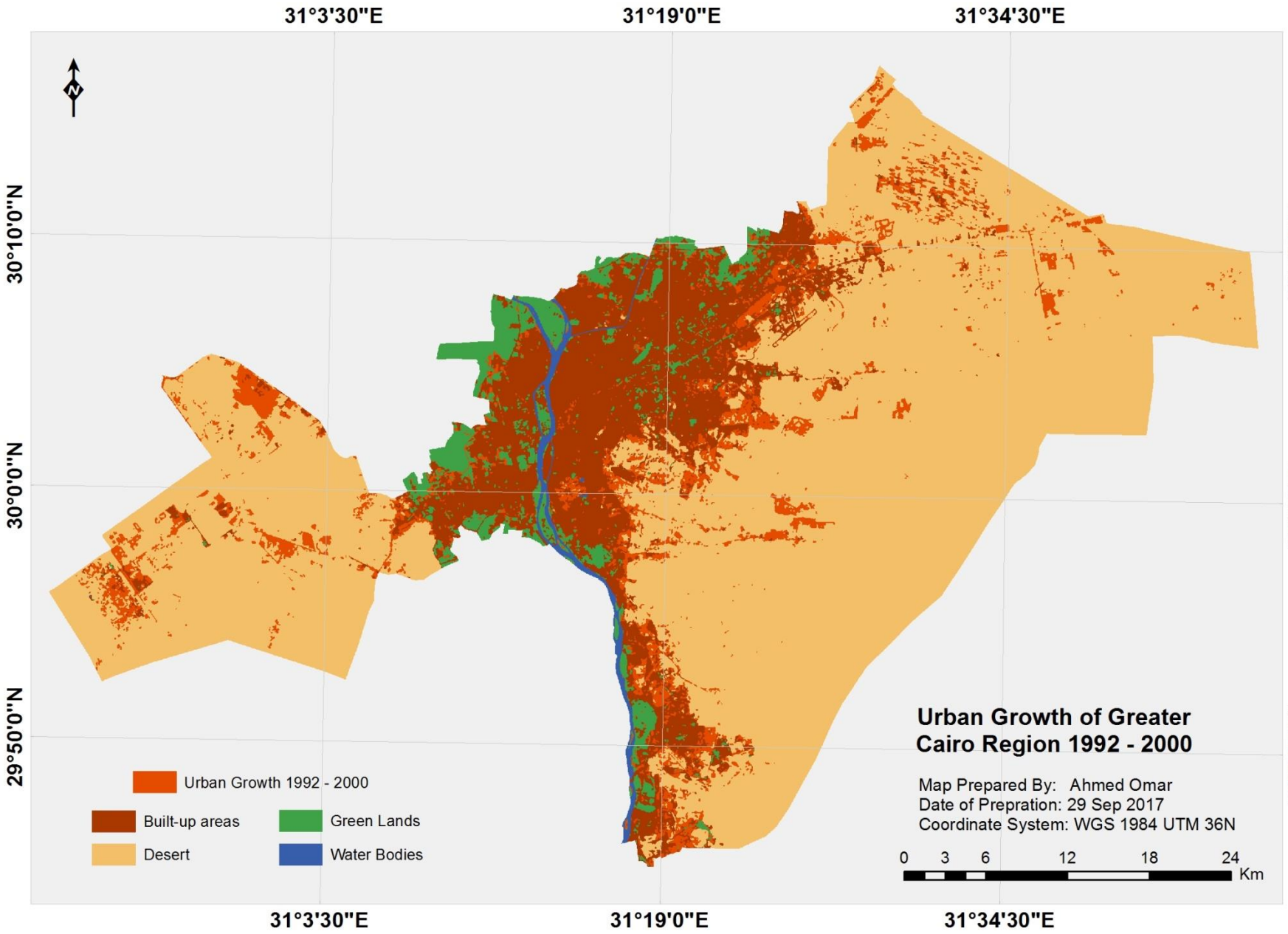

Map 11: Showing Urban Growth of Greater Cairo Region 1992 - 2000.

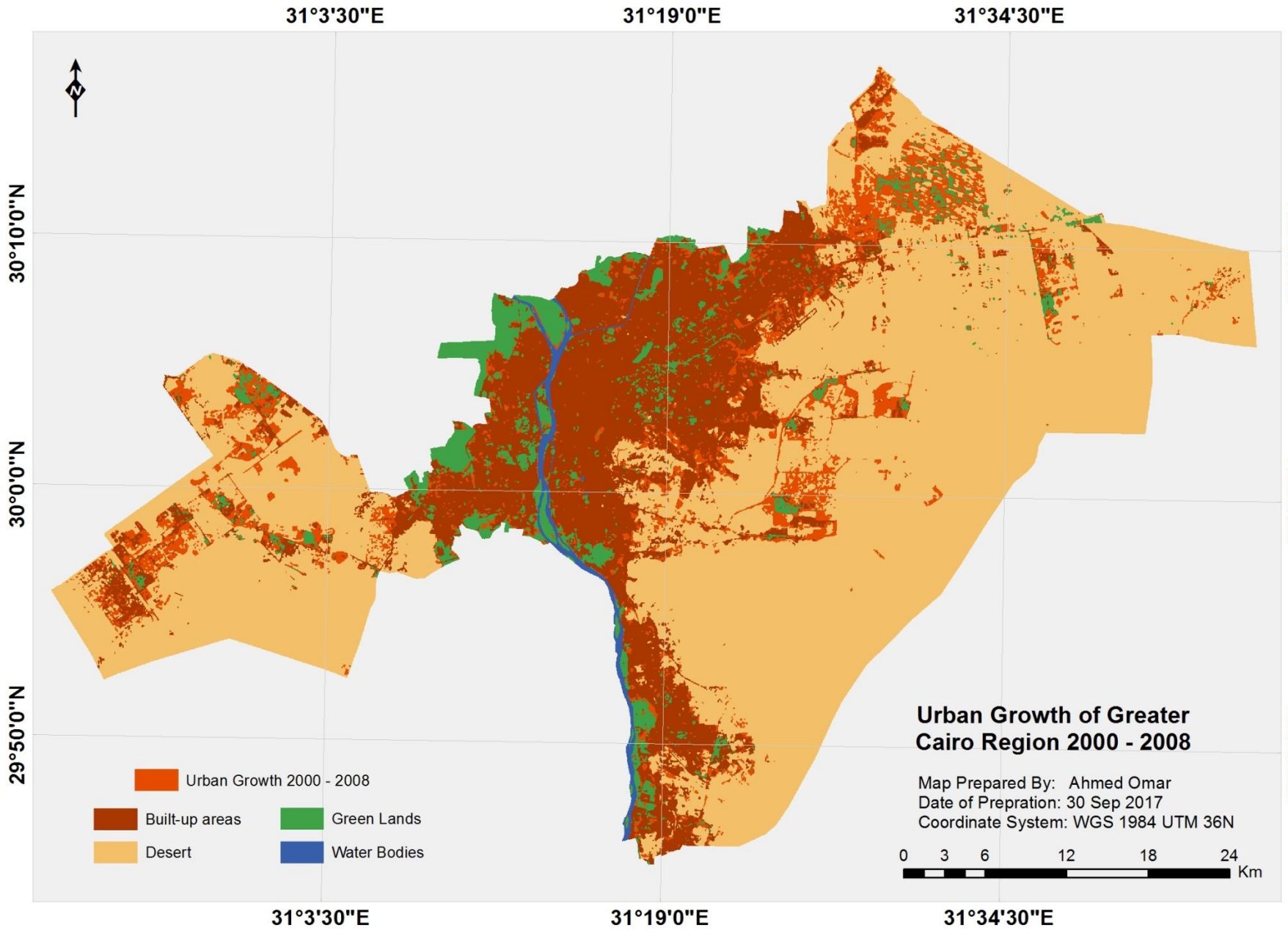

Map 12: Showing Urban Growth of Greater Cairo Region 2000 - 2008.

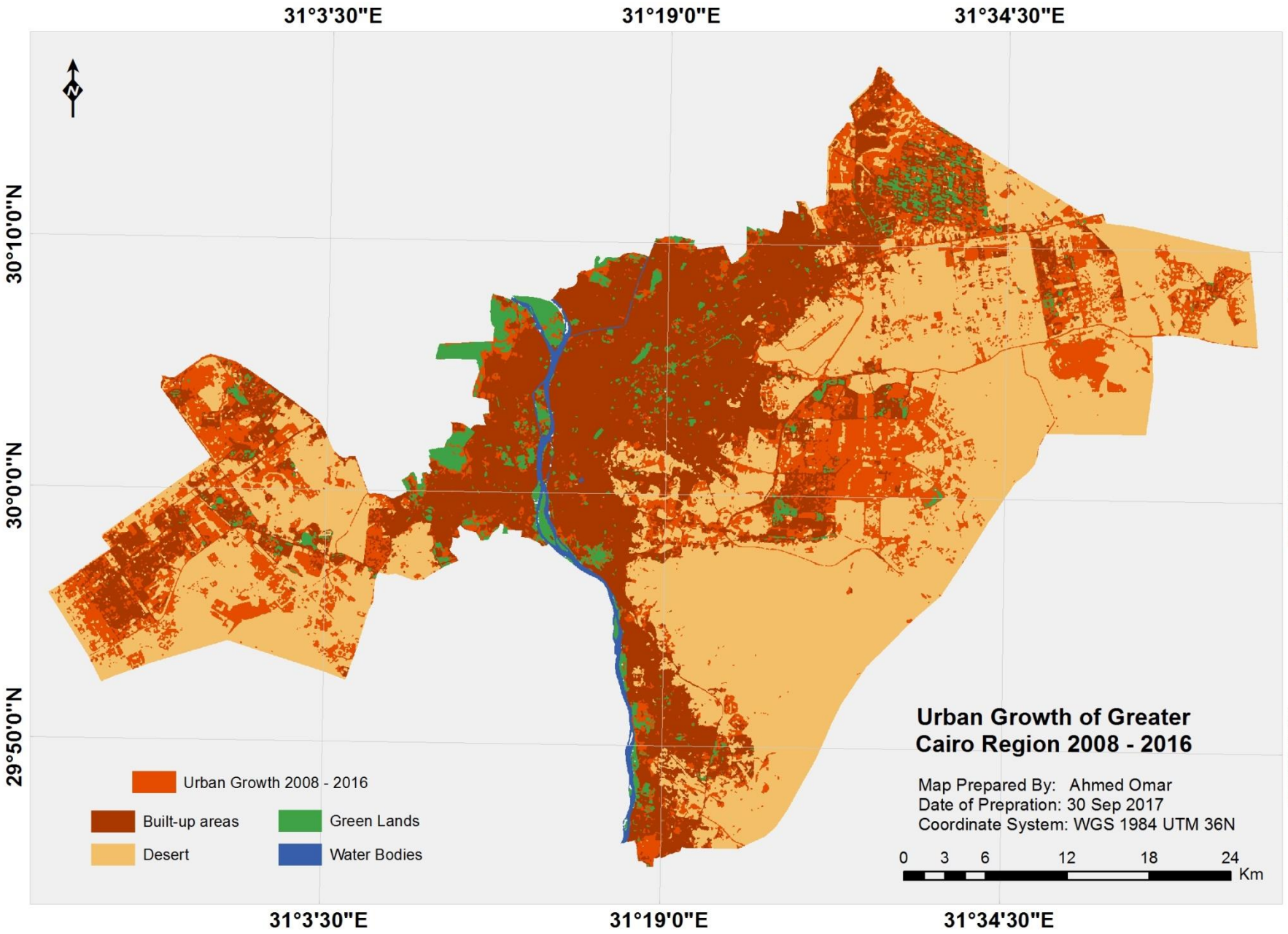

Map 13: Showing Urban Growth of Greater Cairo Region 2008 - 2016.

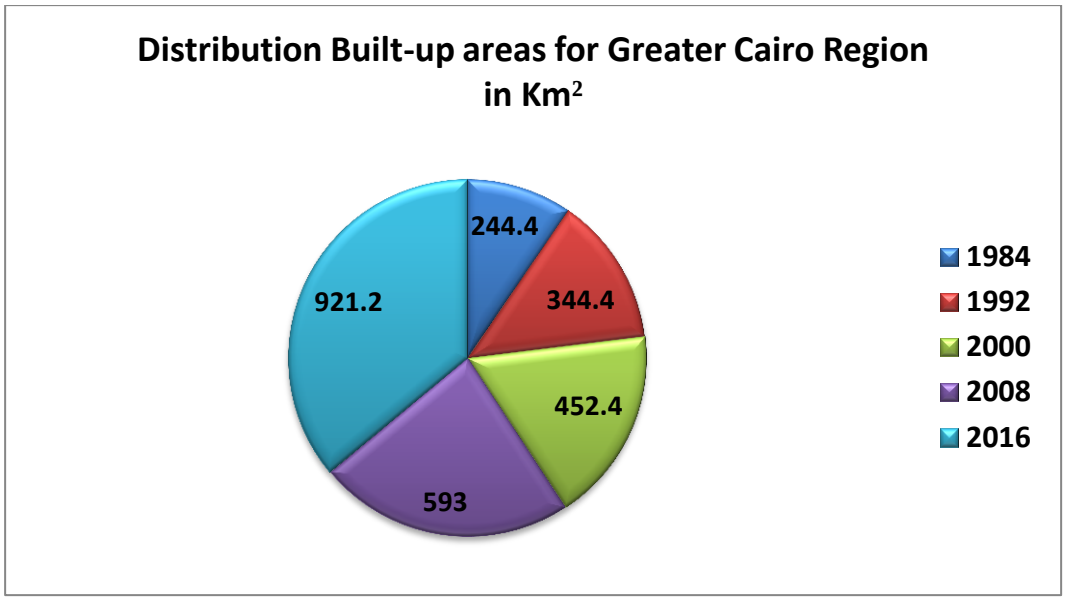

Figure 29: Distribution of Built-up areas Growth from 1984 to 2016.

3.2 Land Use/Cover Classification Maps

Land use/cover map 1984 is generated by classification of Landsat Thematic Mapper (TM) 1984. This map is processed by supervised classification, Built-up areas with an area 244.6 Km^2 and Green Lands with an area 111.5 Km^2, and Desert is on the east with an area 1613.7 Km^2 (Table 19) (Map 14).

Class	1984 (Area / Km^2)	Percentage
Built-up areas	244.6	12.3 %
Green Lands	111.5	5.6 %
Deserts	1613.7	81 %
Water Bodies	21.9	1.1 %
Total	1991.7	100 %

Table19: Land Use/Cover Categories in Greater Cairo (1984)

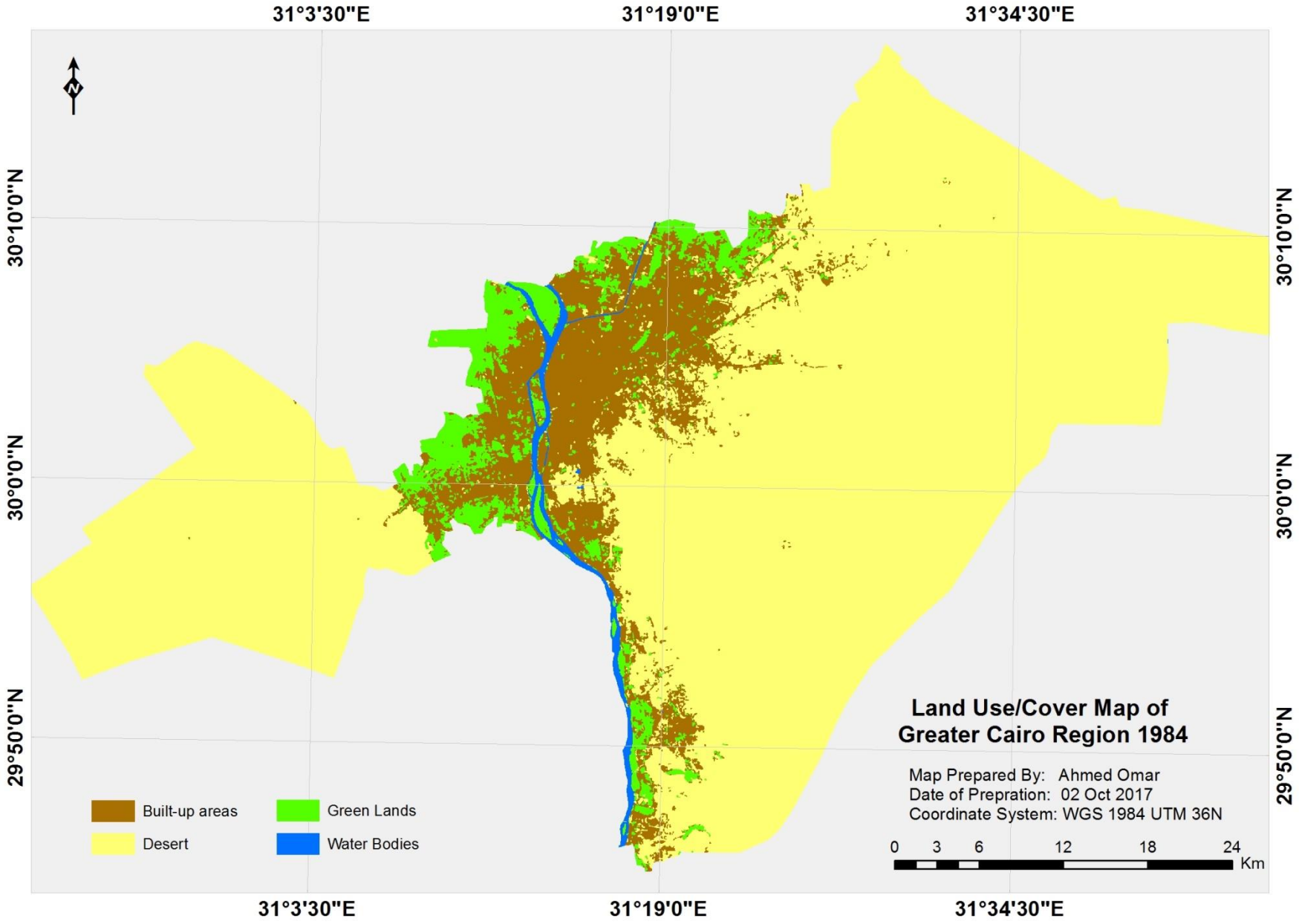

Map14: Greater Cairo Region Land Use Land Cover 1984.

Land use/cover map 1992 is generated by classification of Landsat Thematic Mapper (TM) 1992. This map is processed by supervised classification, Built-up areas with an area 344.6 Km^2 and Green Lands with an area 104.2 Km^2, and Desert is on the east with an area 1522.6 Km^2 (Table 20) (Map 15).

Class	1992 (Area / Km2)	Percentage
Built-up areas	344.6	17.3 %
Green Lands	104.2	5.2 %
Deserts	1522.6	76.4 %
Water Bodies	20.3	1.1 %
Total	1991.7	100 %

Table20: Land Use/Cover Categories in Greater Cairo (1992)

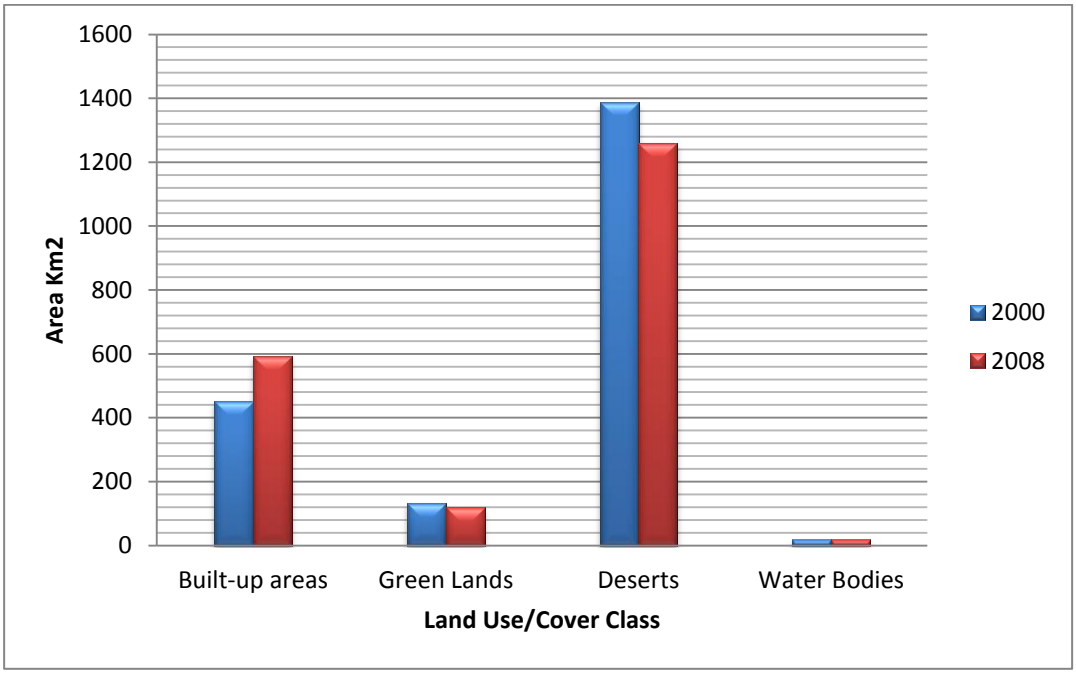

Figure30: Chart of Land Use/Cover change in Greater Cairo (1984-1992).

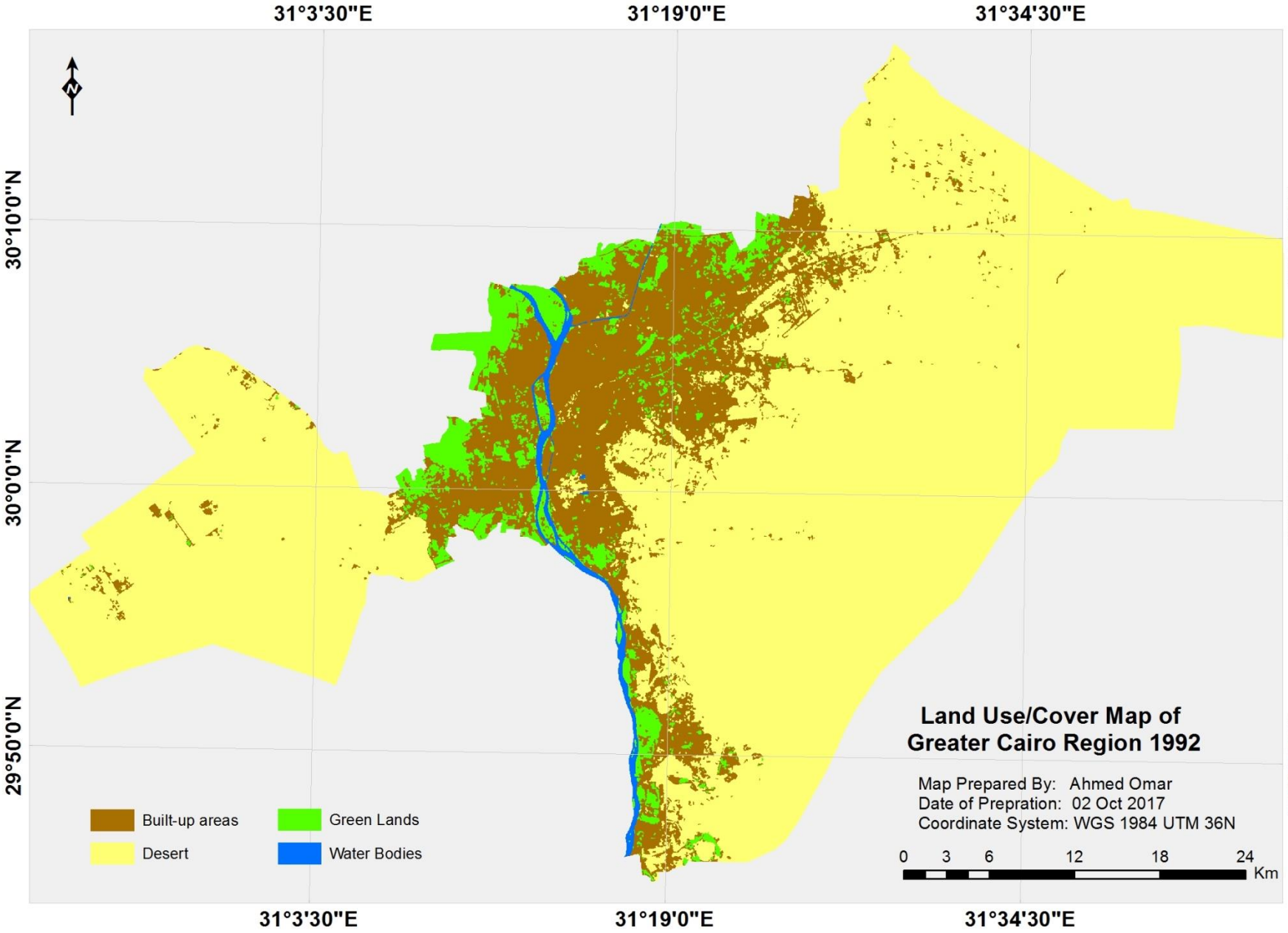

Map15: Greater Cairo Region Land Use Land Cover 1992.

Land use/cover map 2000 is generated by classification of Landsat Thematic Mapper (TM) 2000. This map is processed by supervised classification, Built-up areas with an area 452.7 Km^2 and Green Lands with an area 132.9 Km^2, and Desert is on the east with an area 1386.8 Km^2 (Table 21) (Map 16).

Class	2000 (Area / Km2)	Percentage
Built-up areas	452.7	22.7 %
Green Lands	132.9	6.7 %
Deserts	1386.8	69.6 %
Water Bodies	19.3	1 %
Total	1991.7	100 %

Table21: Land Use/Cover Categories in Greater Cairo (2000)

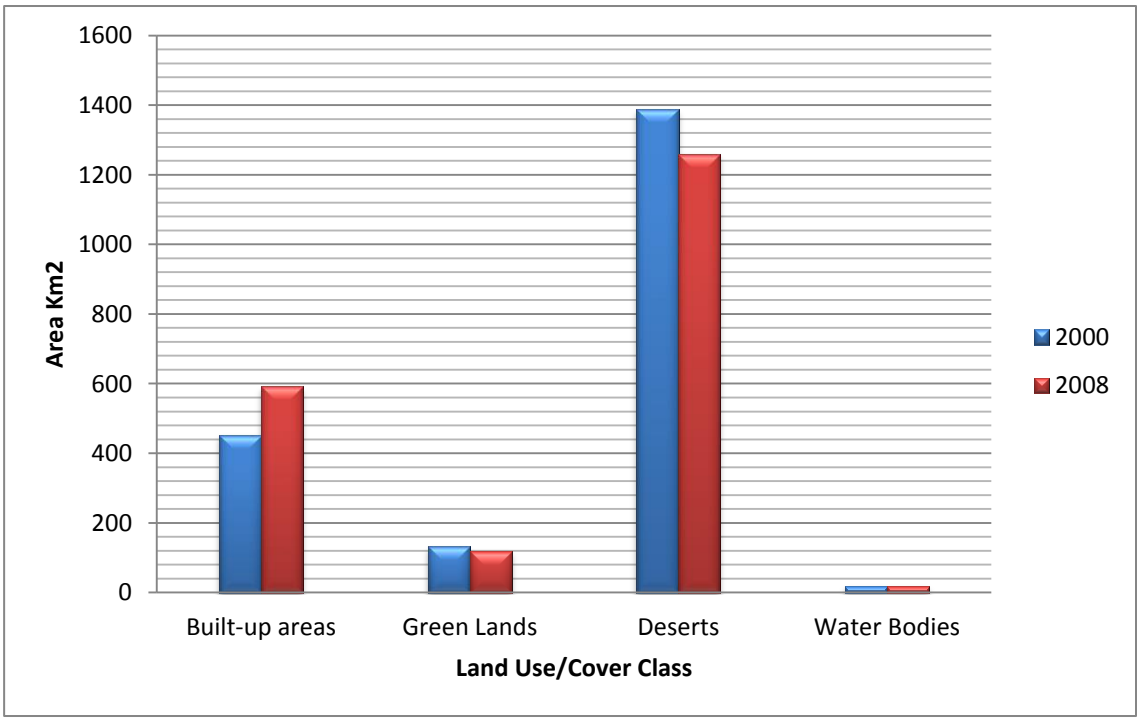

Figure31: Chart of Land Use/Cover change in Greater Cairo (1992-2000).

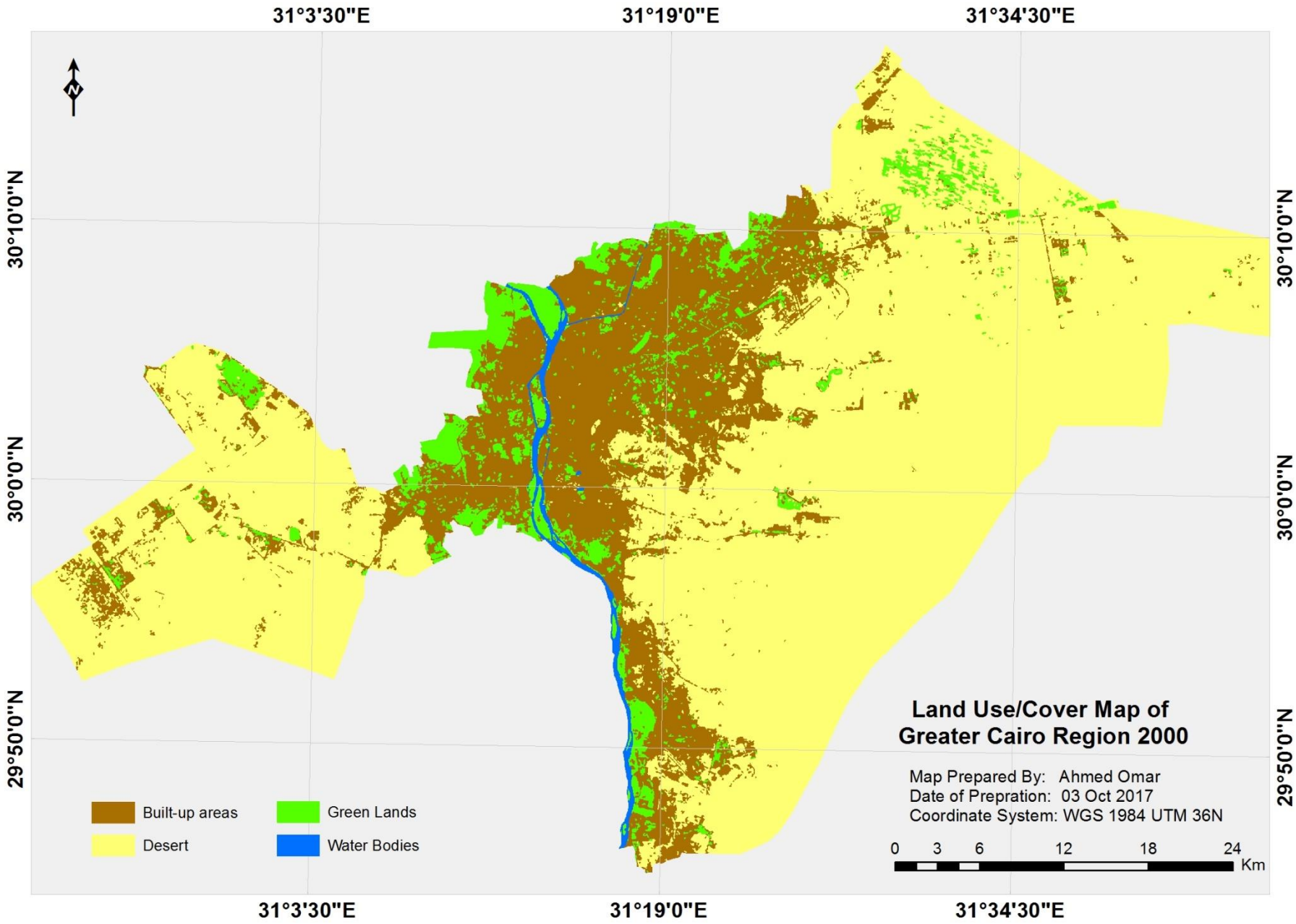

Map16: Greater Cairo Region Land Use Land Cover 2000.

Land use/cover map 2008 is generated by classification of Landsat Enhanced Thematic Mapper (ETM) 2008. This map is processed by supervised classification, Built-up areas with an area 592.9 Km^2 and Green Lands with an area 120 Km^2, and Desert is on the east with an area 1259.8 Km^2 (Table 22) (Map 17).

Class	2008 (Area / Km2)	Percentage
Built-up areas	592.9	29.8 %
Green Lands	120	6 %
Deserts	1259.8	63.3 %
Water Bodies	19	0.9 %
Total	1991.7	100 %

Table22: Land Use/Cover Categories in Greater Cairo (2008)

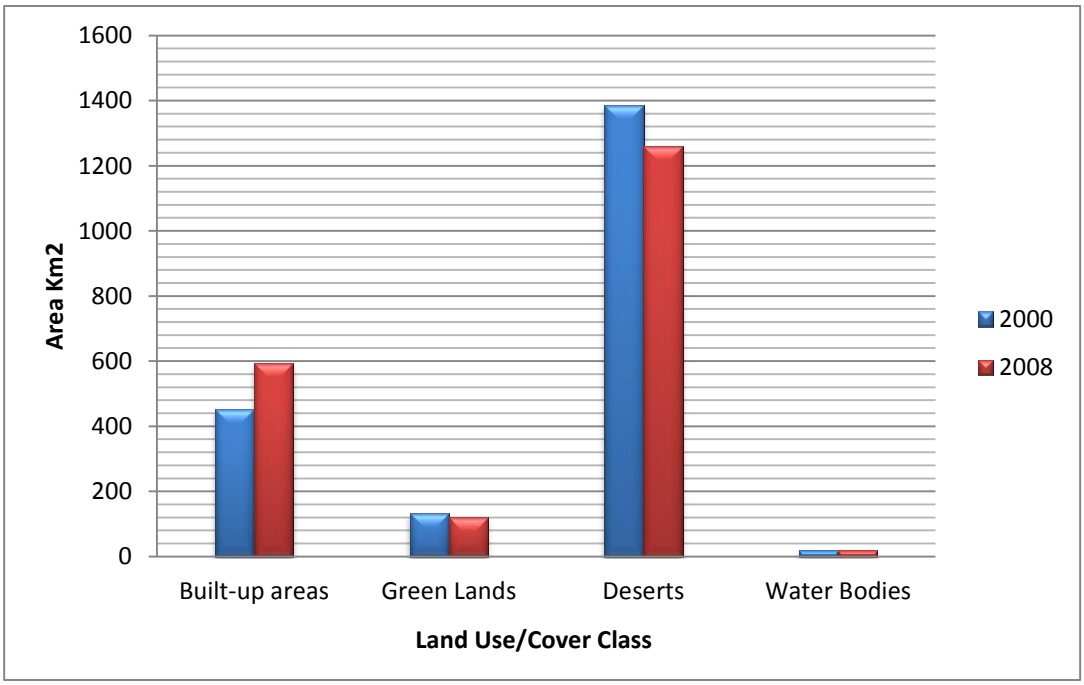

Figure32: Chart of Land Use/Cover change in Greater Cairo (2000-2008).

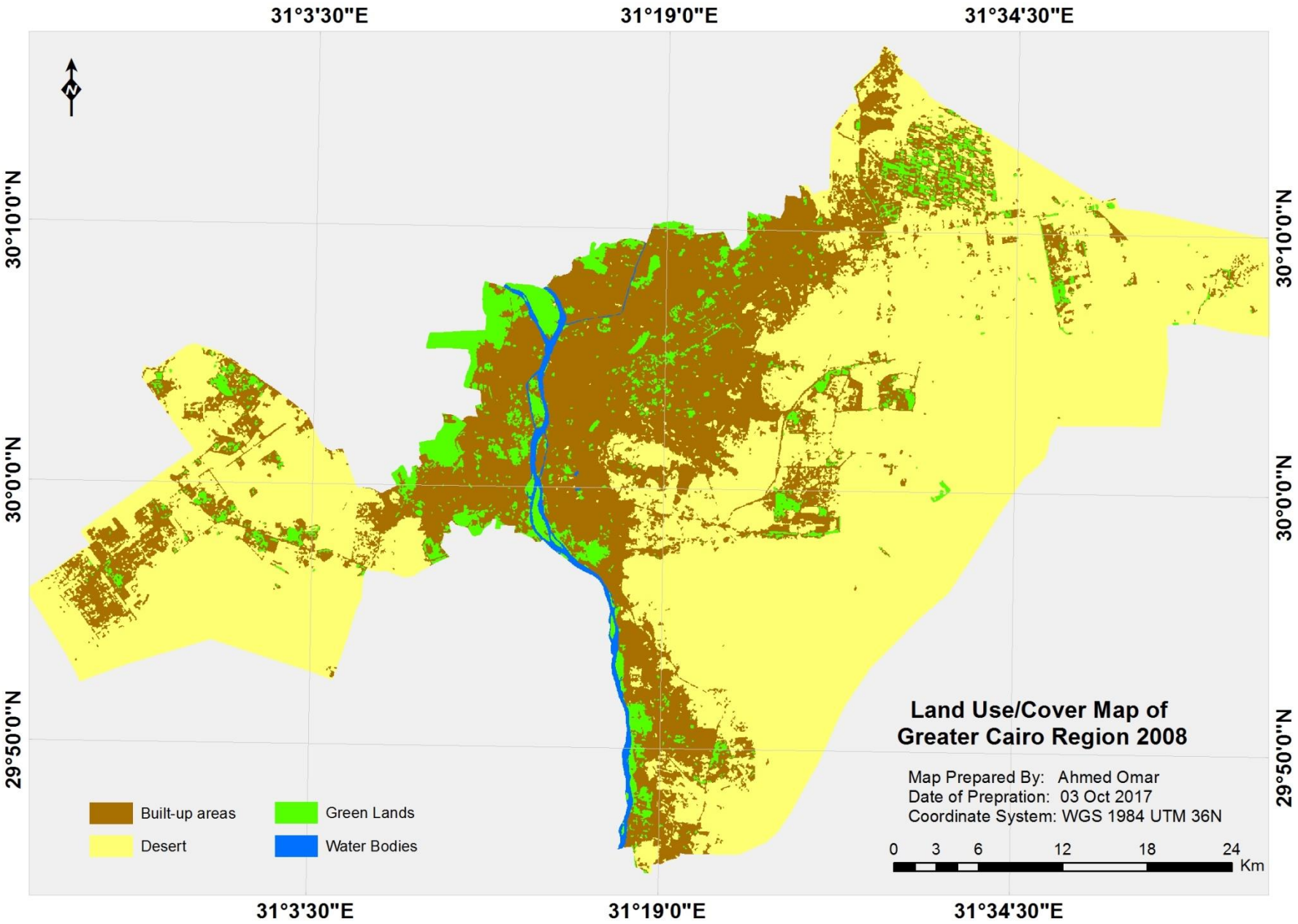

Map17: Greater Cairo Region Land Use Land Cover 2008.

Land use/cover map 2016 is generated by classification of Landsat 8 (OLI) 2016. This map is processed by supervised classification, Built-up areas with an area 921.2 Km^2, and Green Lands with an area 112.6 Km^2. And Desert is on the east with an area 939.1 Km^2 (Table 23) (Map 18).

Class	2016 (Area / Km2)	Percentage
Built-up areas	921.2	46.2 %
Green Lands	112.6	5.7 %
Deserts	939.1	47.2 %
Water Bodies	18.8	0.9 %
Total	1991.7	100 %

Table23: Land Use/Cover Categories in Greater Cairo (2016)

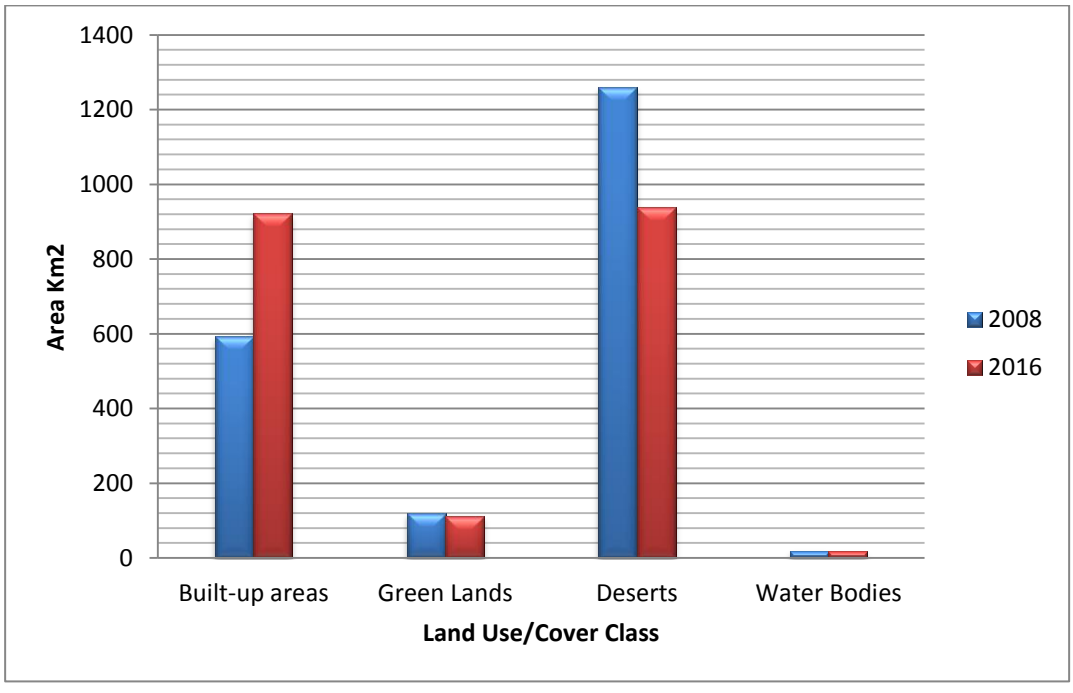

Figure33: Chart of Land Use/Cover change in Greater Cairo (2008-2016).

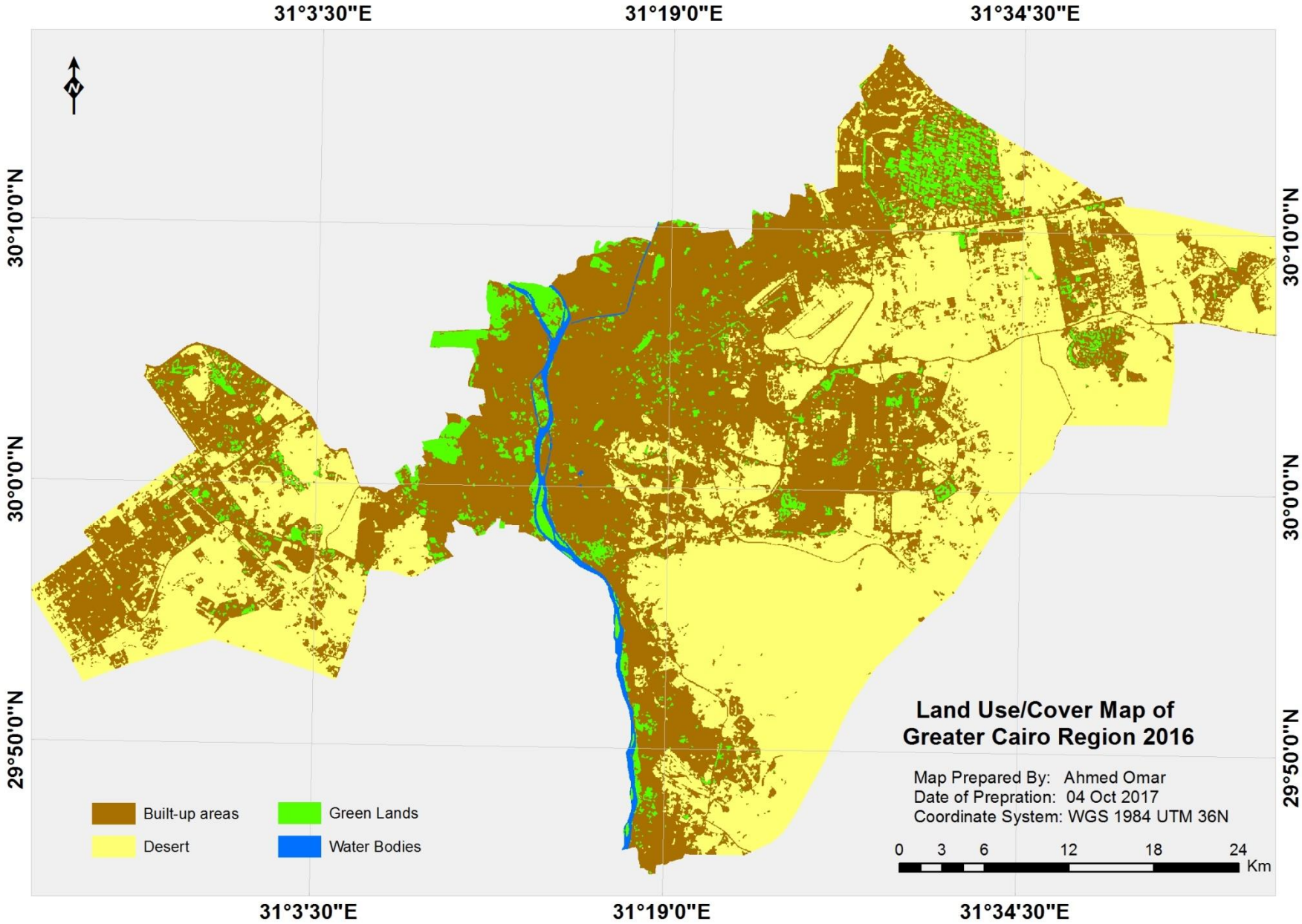

Map18: Greater Cairo Region Land Use Land Cover 2016.

3.3 Land Use/Cover Change Detection

In terms of quantitative changes, the area of study saw significant changes in the pre-defined land use cover classes.

(1) Built-up areas

This category has the most significant change in the area of study. The total area of the built-up areas category increased by (5%) between 1984 and 1992, this means a high rate of annual growth (0.63%), (Table 24). And increased by (5.4%) between 1992 and 2000, this means a high rate of annual growth (0.68%), (Table 25). And increased by (7%) between 2000 and 2008, this means a high rate of annual growth (0.88%), (Table 26). And increased by (16.5%) between 2008 and 2016, this means a high rate of annual growth (2.1%), (Table 27). Most of urban development (97.8%) in the desert areas in the eastern and northeastern of study area and the west part which represents 6th of October City and Sheikh Zayed City. (Map13).

Class Name	Size of Change (Km^2) (1984 - 1992)	Percentage of Change (1984 - 1992)	Annual Change (Km^2)	Annual Change (Percentage)
Built-up areas	100	5	12.5	0.63
Green Lands	-7.3	-0.4	-0.9	-0.05
Deserts	-91.1	-4.6	-11.4	-0.57
Water Bodies	-1.6	-0.08	-0.2	-0.01

Table24: Characteristics of Land Use/Cover change in Greater Cairo (1984 - 1992).

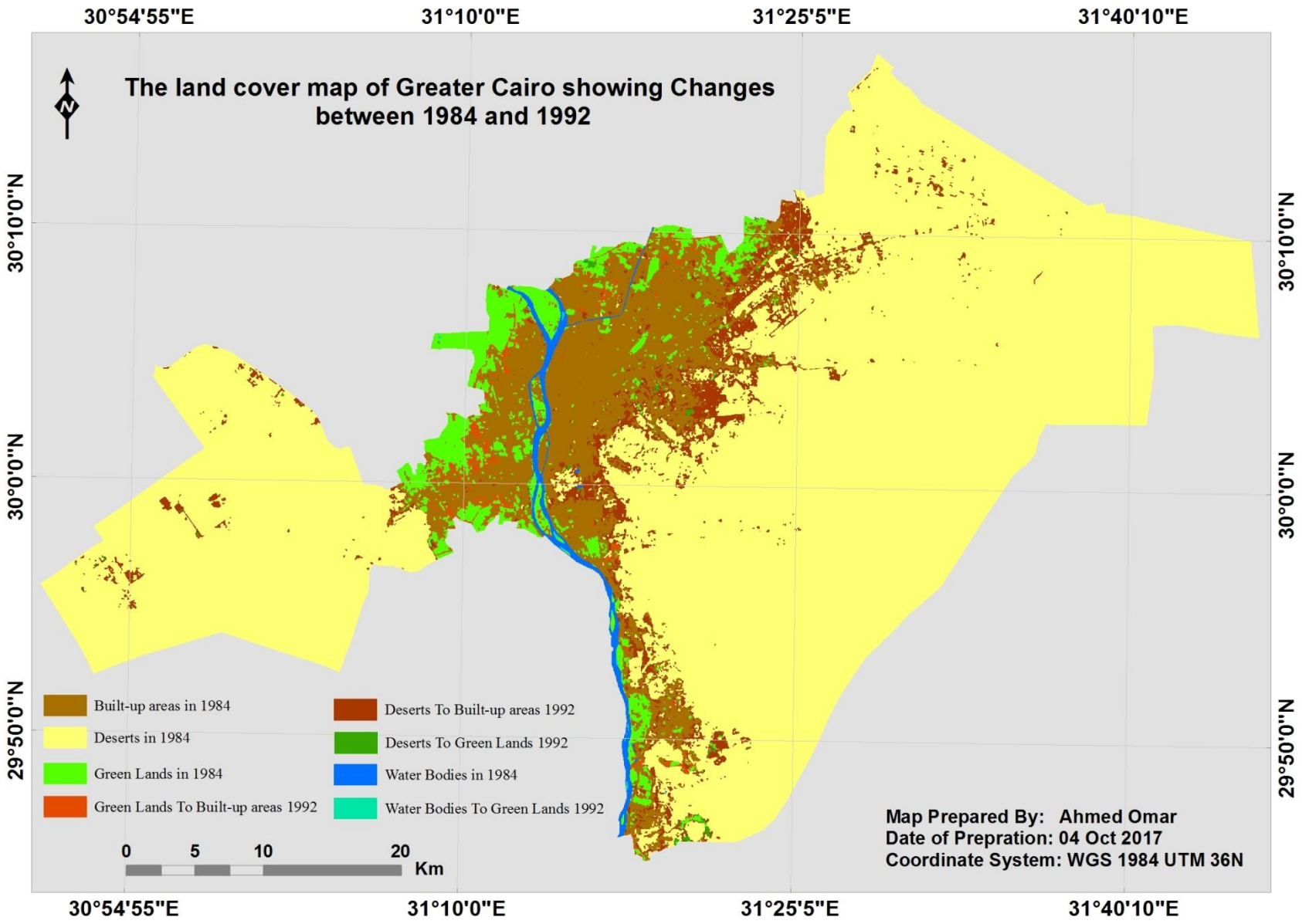

Map19: Change Detection Map showing Changes between 1984 and 1992.

Class Name	Size of Change (Km^2) (1992 - 2000)	Percentage of Change (1992 - 2000)	Annual Change (Km^2)	Annual Change (Percentage)
Built-up areas	108.1	5.4	13.5	0.68
Green Lands	28.7	1.4	3.6	0.18
Deserts	-135.8	-6.8	-17	-0.85
Water Bodies	-1	-0.05	-0.13	-0.006

Table25: Characteristics of Land Use/Cover change in Greater Cairo (1992 - 2000).

(2) Green Lands

Green lands class represented about (5.6%) of the total land use in the area of study in 1984 (Table 19) and (5.2 %) in 1992 (Table 20). This means almost (0.4%) decrease in its share in total. And represented about (6.7%) of the total land use in the area of study in 2000 (Table 21) and (6 %) in 2008 (Table 22). This means almost (0.7%) decrease in its share in total. And represented about (6 %) of the total land use in the area of study in 2008 (Table 22) and (5.7 %) in 2016 (Table 23). This means almost (0.3%) decrease in its share in total. Green lands category lost about (0.4 %) from its area between 1984 and 1992 (0.05 % annually) (Table 24). And increase about (1.4 %) in its area between 1992 and 2000 (0.18 % annually) (Table 25). And lost about (0.65 %) from its area between 2000 and 2008 (0.08 % annually) (Table 26). And lost about (0.37 %) from its area between 2008 and 2016 (0.05 % annually) (Table 27).

Class Name	Size of Change (Km^2) (2000 - 2008)	Percentage of Change (2000 - 2008)	Annual Change (Km^2)	Annual Change (Percentage)
Built-up areas	140.2	7	17.5	0.88
Green Lands	-12.9	-0.65	-1.6	-0.08
Deserts	-127	-6.4	-15.9	-0.80
Water Bodies	-0.3	-0.02	-0.04	-0.002

Table26: Characteristics of Land Use/Cover change in Greater Cairo (2000 - 2008).

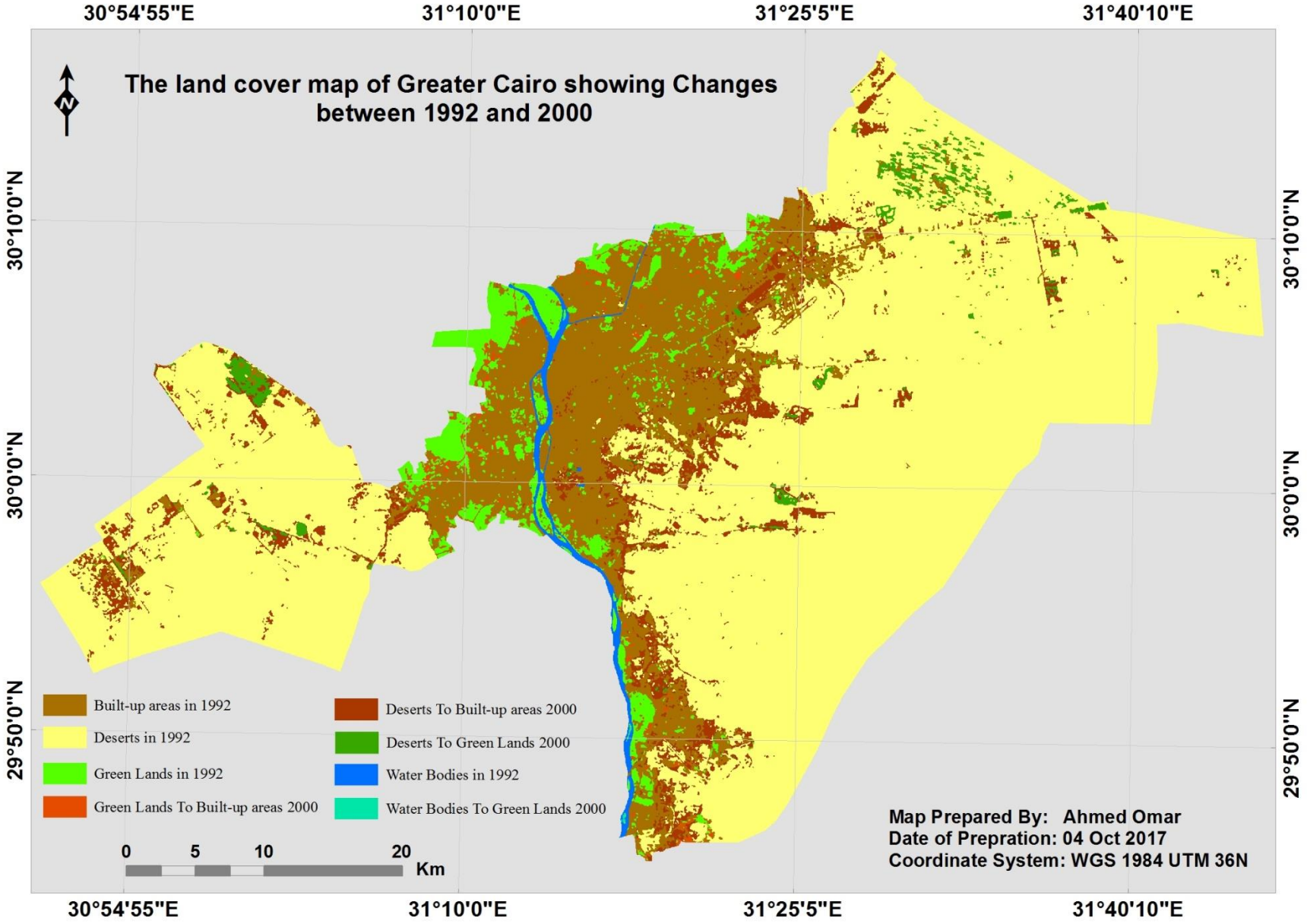

Map20: Change Detection Map showing Changes between 1992 and 2000.

(3) Desert

This category has the first most significant change in the area of study. The total area of the desert category decreased by (4.6%) between 1984 and 1992, (Table 24). And decreased by (6.8%) between 1992 and 2000, (Table 25). And decreased by (6.4%) between 2000 and 2008, (Table 26). And decreased by (16.1%) between 2008 and 2016, (Table 27). It was expected that the built-up areas category would gain the biggest share of lands from this category; however, the analysis of this category confirms that (33.9%) of the lost lands from this category was used for urban development.

(4) Water bodies

Water bodies decreased by (0.08%) between 1984 and 1992 (Table 24). And decreased by (0.05%) between 1992 and 2000 (Table 25). And decreased by (0.02%) between 2000 and 2008 (Table 26). And decreased by (0.01%) between 2008 and 2016 (Table 27). However, this change does not affect the whole share of the water bodies class as a part of the total land use in Grater Cairo Region, where its share was (1.1%) in 1984 (Table 19), and became (1.1%) in 1992 (Table 20). and became (1%) in 2000 (Table 21). and became (0.95 %) in 2008 (Table 22). and became (0.94%) in 2016 (Table 23). Most of the changes have been happening within the Nile River. The decrease water surface was may be attributed to the increase of the area of Nile river islands.

Class Name	Size of Change (Km^2) (2008 - 2016)	Percentage of Change (2008 - 2016)	Annual Change (Km^2)	Annual Change (Percentage)
Built-up areas	328.3	16.5	41	2.1
Green Lands	-7.4	-0.37	-0.9	-0.05
Deserts	-320.7	-16.1	-40	-2
Water Bodies	-0.2	-0.01	-0.03	-0.002

Table27: Characteristics of Land Use/Cover change in Greater Cairo (2008 - 2016).

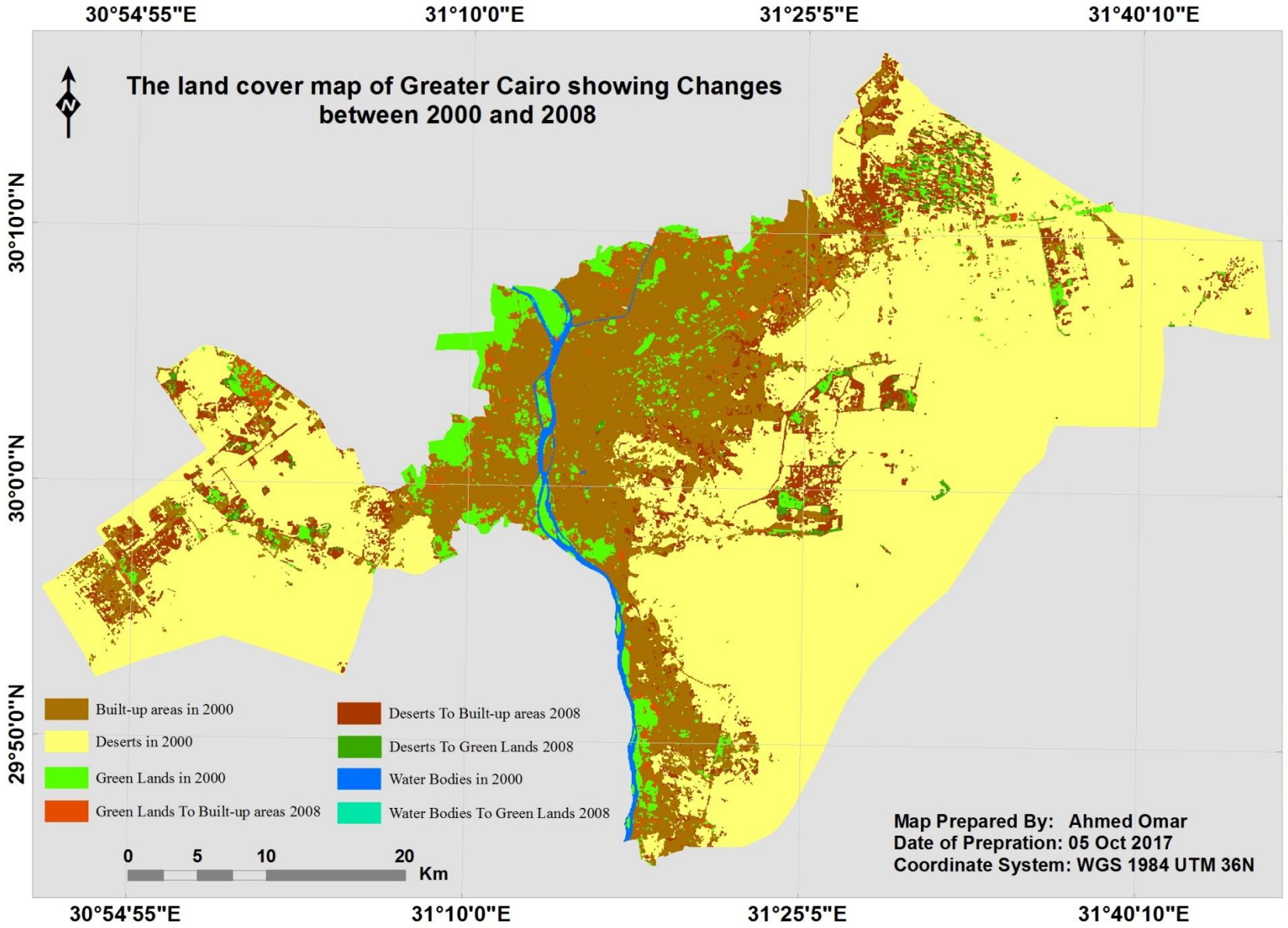

Map21: Change Detection Map showing Changes between 2000 and 2008.

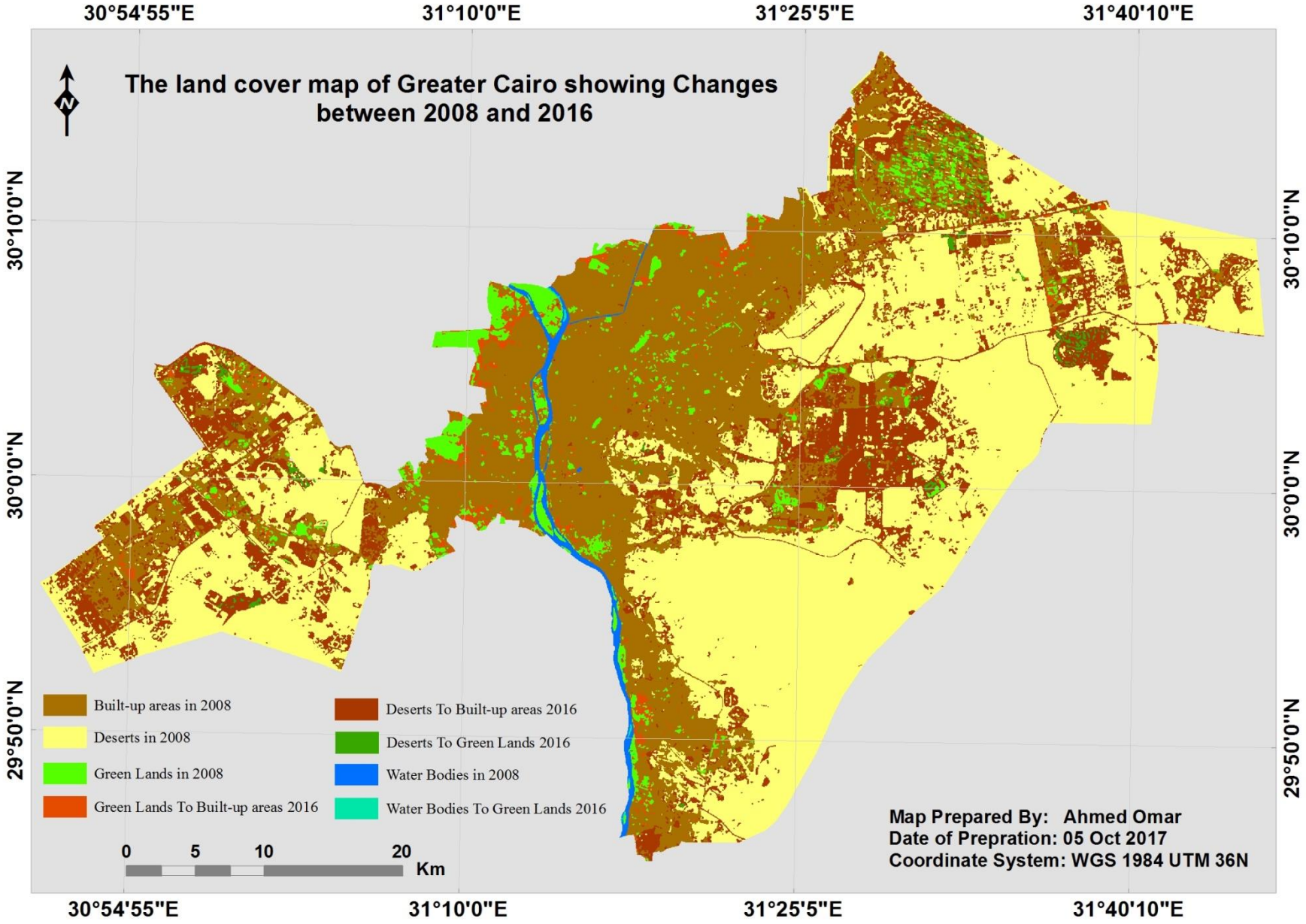

Map22: Change Detection Map showing Changes between 2008 and 2016.

3.3.1 Transition Matrix

The transition matrix records change that each land cover category to the other category. This matrix is produced by statistical analysis for Land cover change detection result. For the matrix table presented below (Table 28), the rows represent the newer land cover categories (Land Cover 1992) and the column represents the older categories (Land Cover 1984). (Table 29), the rows represent the newer land cover categories (Land Cover 2000) and the column represents the older categories (Land Cover 1992).

		Land Cover 1984				
		Built-up areas	**Green Lands**	**Deserts**	**Water Bodies**	**Class Total**
Land Cover 1992	**Built-up areas**	244.6	21.8	78.2	0	344.6
	Green Lands	0	89.7	12.9	1.6	104.2
	Deserts	0	0	1522.6	0	1522.6
	Water Bodies	0	0	0	20.3	20.3
	Class Total	244.6	111.5	1613.7	21.9	1991.7

Table28: Land Cover Changes: Transition Matrix of year 1984 to 1992. Areas are in km2.

		Land Cover 1992				
		Built-up areas	**Green Lands**	**Deserts**	**Water Bodies**	**Class Total**
Land Cover 2000	**Built-up areas**	344.6	14.5	93.6	0	452.7
	Green Lands	0	89.7	42.2	1	132.9
	Deserts	0	0	1386.8	0	1386.8
	Water Bodies	0	0	0	19.3	19.3
	Class Total	344.6	104.2	1522.6	20.3	1991.7

Table29: Land Cover Changes: Transition Matrix of year 1992 to 2000. Areas are in km2.

For the matrix table presented below (Table 30), the rows represent the newer land cover categories (Land Cover 2008) and the column represents the older categories (Land Cover 2000). (Table 30), the rows represent the newer land cover categories (Land Cover 2016) and the column represents the older categories (Land Cover 2008).

		Land Cover 2000				
		Built-up areas	**Green Lands**	**Deserts**	**Water Bodies**	**Class Total**
Land Cover 2008	**Built-up areas**	452.7	24.6	115.6	0	592.9
	Green Lands	0	108.3	11.4	0.3	120
	Deserts	0	0	1259.8	0	1259.8
	Water Bodies	0	0	0	19	19
	Class Total	452.7	132.9	1386.8	19.3	1991.7

Table30: Land Cover Changes: Transition Matrix of year 2000 to 2008. Areas are in km2.

		Land Cover 2008				
		Built-up areas	**Green Lands**	**Deserts**	**Water Bodies**	**Class Total**
Land Cover 2016	**Built-up areas**	592.9	45.8	282.5	0	921.2
	Green Lands	0	74.2	38.2	0.2	112.6
	Deserts	0	0	939.1	0	939.1
	Water Bodies	0	0	0	18.8	18.8
	Class Total	592.9	120	1259.8	19	1991.7

Table31: Land Cover Changes: Transition Matrix of year 2008 to 2016. Areas are in km2.

Chapter-4

4. Conclusions

The area of study witnessed a remarkable urban growth between 1984 and 2016. The land cover maps resulted from the supervised classification is shown in (Map 17), which shows a tremendous expansion of Built-up areas toward the east, northeast and west. Built-up areas are estimated at (244.6 km^2) in 1984. Between 1984 and 1992, (100 km^2) of new Built-up areas have been added to Greater Cairo totaling (344.6 km^2) of urban area in 1992. The rate of urbanization was (12.5 km^2/year) during the 8 years of study (Table 24), this figure (344.6 km^2) represents the sum of the original urban land in 1992. Built-up areas are estimated at (344.6 km^2) in 1992. Between 1992 and 2000, (108.1 km^2) of new Built-up areas have been added to Greater Cairo totaling (452.7 km^2) of urban area in 2000. The rate of urbanization was (13.5 km^2/year) during the 8 years of study (Table 25), this figure (452.7 km^2) represents the sum of the original urban land in 2000. Built-up areas are estimated at (452.7 km^2) in 2000. Between 2000 and 2008, (140.2 km^2) of new Built-up areas have been added to Greater Cairo totaling (592.9 km^2) of urban area in 2008. The rate of urbanization was (17.5 km^2/year) during the 8 years of study (Table 26), this figure (592.9 km^2) represents the sum of the original urban land in 2008. Built-up areas are estimated at (592.9 km^2) in 2008. Between 2008 and 2016, (328.3 km^2) of new Built-up areas have been added to Greater Cairo totaling (921.2 km^2) of urban area in 2016. The rate of urbanization was (41 km^2/year) during the 8 years of

study (Table 27), this figure (921.2 km^2) represents the sum of the original urban land in 2016.

Green Lands around Greater Cairo are estimated at (111.5 km^2) in 1984. Between 1984 and 1992, decreased Green Lands (7.3 km^2). Between 1992 and 2000, increased Green Lands (28.7 km^2). Between 2000 and 2008, decreased Green Lands (12.9 km^2). Between 2008 and 2019, decreased Green Lands (7.4 km^2). And the newly urbanized desert areas (78.2 km^2) between 1984 and 1992, (93.6 km^2) between 1992 and 2000, (115.6 km^2) between 2000 and 2008, (282.5 km^2) between 2008 and 2016.

The tradeoff between the Green Lands, desert, and Built-up areas are shown in (Tables 24, 25, 26 and 27) and (Maps 19, 20, 21 and 22). The present study reveals a total increase of Built-up areas from (244.6 km2) to (921.2 km2) with a total increase of (676.6 km2) in 32 years (1984-2016). The present study reveals that urban expansion is observed to be mostly toward north (upon agricultural lands) and toward east, northeast and west (desert). The loss of agricultural lands between 1984 to 2016 along the boundaries of Greater Cairo re-presents a significant threat to this non-renewable resource as agricultural land of Egypt is restricted to the Nile Valley and its delta. Factors driving urban sprawl include demography, regional topography, socio-economic factors and policies.

References

Acharya, Tinku, Ray, K. Ajoy, 2005, Image Processing: Principle and applications. New Jersey: John Wiley and Sons.

Arvind C., Pandy, Nathawat, M.S., 2006. Land Use Land Cover Mapping Through Digital Image Processing of Satellite Data – A case study from Panchkula, Ambala and Yamunanagar Districts, Haryana State, India.

Ayad, H. M., Saad Allah, D. M. & Abd Elazeem, H. S. 2013. Investigating urban growth scenarios in Wadi El Natrun area, Egypt, using the UPlan land use allocation model. *Journal of Land Use Science,* 8**,** pp. 304-320.

Campbell, B. James., 2002, Introduction to Remote Sensing. 3rd ed. London: Taylor and Francis.

Clark, D. 1982. Urban Geography: An Introductory Guide. London, Croom Helm.

Deer, P. J. 1995. Digital Change Detection Techniques: Civilian and Military Applications. International Symposium on Spectral Sensing Research (ISSSR), Melbourne, Victoria.

Furtado, Jose. Joaquim. Cai, Zhihua. Xiaobo, Liu. 2010. Digital image processing: supervised classification using genetic algorithm in matlab toolbox. China University of Geosciences. Report and Opinion. Vol. 2, Issue 6, pp. 53-60.

Irny, S.I. and Rose, A.A. (2005) "Designing a Strategic Information Systems Planning Methodology for Malaysian Institutes of Higher Learning (isp- ipta), Issues in Information System, Volume VI, No. 1, 2005.

Gibson and Power, 2000. Introductory Remote Sensing: digital Image Processing and Applications Routledge, London (2000), pp. 190-210.

Gordon, S., 1980. Utilizing Landsat imagery to monitor land use change: A case study of Ohio. Remote Sensing of Environment, 9, pp. 189-196.

Jensen, R.J. 1995. Introductory digital image processing. Prentice Hall, Upper Saddle River.

Jensen, J. R. 1996. Introductory Digital Image Processing: A Remote Sensing Perspective. Upper Saddle River, N. J., Prentice Hall.

Lillesand, T.M. & Kiefer, R.W. 1994. "Remote Sensing and Image Interpretation" John Wiley & Sons New York, 3, p. 750.

Lu, D., Mausel P., Brondiozio, E. and Moran, E. 2004. Change detection techniques. International Journal of Remote Sensing, 25, pp. 2365-2407.

Maktav, D. & Erbek, F. S. 2005. Analysis of urban growth using multi-temporal satellite data in Istanbul, Turkey. International Journal of Remote Sensing*,* 26**,** pp. 797-810.

Mas, J. -F. 1999. "Monitoring Land-Cover Changes: A Comparison of Change Detection Techniques. “International Journal of Remote Sensing 20(I): 139-52.

Pham, H. M. & Yamaguchi, Y. 2011. Urban growth and change analysis using remote sensing and spatial metrics from 1975 to 2003 for Hanoi, Vietnam. *International Journal of Remote Sensing,* 32**,** pp. 1901-1915.

Riordan, C. J. 1980. Non-Urban to Urban Land Cover Change Using Landsat Data. Summary Report of the Colorado Agricultural Research Experiment Station. Fort Collins, Colorado, Colorado Agricultural research Experiment Station.

Scaramuzza, P., Micijevic, E., & Chander, G. (2004). SLC gap-filled products phase one methodology. Landsat Technical Notes. Schowengerdt, R.A., Remote sensing–Models and methods for image processing, 2nd edn, (Academic Press, 1997).

Schowengerdt, A. Robert., 2007, Remote Sensing: Models and Methods for Image Processing. 3rd ed. London: Academic Press.

Singh, A. 1986. Change Detection in the Tropical Forest Environment of Northeastern India Using Landsat. In Remote Sensing and Tropical Land Management, by M. J. Eden and J. T. Parry. Chichester, John Wiley & Son: 237-54.

Stow. 1999. Reducing the effects of misregistration on pixel-level change detection. International Journal of Remote Sensing, 20, pp. 2477-2483.

United Nations Fund for Population Activities. Urbanization: A Majority in Cities. Available online: http://www.unfpa.org/pds/urbanization.htm

World Health Organization. Urbanization: Urban Population Growth. Available online:http://www.who.int/gho/urban_health/situation_trends/urban_population_growth_text/en/

YAGOUB, M. M. 2004. Monitoring of urban growth of a desert city through remote sensing: Al-Ain, UAE, between 1976 and 2000. International Journal of Remote Sensing, 25, pp. 1063-1076.